SENSITIVITY OF PERMAFROST TERRAIN IN A HIGH ARCTIC POLAR DESERT: AN EVALUATION OF RESPONSE TO DISTURBANCE NEAR EUREKA, ELLESMERE ISLAND, NUNAVUT

by

NICOLE J. COUTURE

Geography Department, McGill University, Montreal
August 2000

A thesis submitted to the Faculty of Graduate Studies and Research
in partial fulfilment of the requirements of the degree of
Master of Science

0-612-70405-X

ABSTRACT

A first approximation of ground ice volume for the area surrounding Eureka, Nunavut, indicates that it comprises 30.8% of the upper 5.9 m of permafrost. Volume depends on the type of ice examined, ranging from 1.8 to 69.0% in different regions of the study area. Excess ice makes up 17.7% of the total volume of frozen materials in the study area. Melt of ground ice in the past has produced thermokarst features which include ground subsidence of up to 3.2 m, formation of tundra ponds, degradation of ice wedges, thaw slumps greater than 50 m across, gullying, and numerous active layer detachment slides. With a doubling of atmospheric carbon dioxide, the rise in mean annual temperatures for the area is projected to be 4.9 to 6.6°C, which would lengthen the thaw season and increase thaw depths by up to 70 cm. The expected geomorphic changes to the landscape are discussed.

RÉSUMÉ

Pour la région avoisinante Eureka au Nunavut, une première approximation du volume de glace au sol révèle une proportion de 30.8% dans les 5.9 premiers mètres du pergélisol. Le volume de glace dépend du type de glace examiné et varie de 1.8 à 69.0%. La glace en excès constitue 17.7% du volume total de matériel glacé. La fonte de la glace au sol dans le passé a permis l'affaissement du sol jusqu'à 3.2 mètres, la formation de lacs thermokarstiques, la dégradation des fentes de gel, des glissements régressifs dûs au gel de plus de 50 mètres, des ravinements, et plusieurs décollements de la couche active. Avec l'accroissement du dioxide de carbone dans l'atmosphère, les prévisions indiquent une augmentation potentielle de la température moyenne annuelle de 4.9 à 6.6°C pour la région étudiée. Cette hausse de la température allongerait la saison de dégel et augmenterait les profondeurs de dégel à près de 70 cm. Les changements géomorphologiques attendus au paysage sont discutés.

ACKNOWLEDGEMENTS

Throughout the research, fieldwork and writing of this thesis, numerous people and organizations have helped me, and I would like to acknowledge their assistance. Foremost among them is my supervisor, Dr. Wayne Pollard. I would like to express my incredible appreciation to him for his teachings, enthusiasm, ideas, direction, and patience. He has been instrumental in helping me to both understand and appreciate the science and beauty of the Arctic landscape.

Funding for fieldwork was provided by the Department of Indian Affairs and Northern Development (Northern Scientific Training Program), the Atmospheric Environment Service (AES Research Support Opportunity), the Natural Science and Engineering Research Council of Canada (grant to W. Pollard), and would have been impossible without the generous support of the Polar Continental Shelf Project. Additional funds were provided through grants from the Quebec government's Fonds pour la formation des chercheurs et l'aide à la recherche (FCAR), the McGill Centre for Climate and Global Change Research, and the Royal Canadian Geographic Society.

I would also like to express appreciation to Doug Hodgson and Mark Nixon for their insightful discussions at various stages in this project and for survey data. Steve Robinson, Margo Burgess and Marianne Douglas helped out with comments and suggestions. Comments by J.A. Hyatt and an anonymous reviewer on an early article are gratefully acknowledged. Bea Alt, David Atkinson and Michael Nahir generously supplied meteorological and ground temperature data. Lyne Daigle of the National Research Council of Canada and Dan Riseborough were instrumental in my understanding of thermal conductivity probes. Sasha Anderson, John Brownstein, Steve Brunette, Neal Michelutti, and Greg Hawkins provided capable and cheerful field assistance.

The AES weather station staff and the personnel of Operation Hurricane in Eureka were always helpful and made fieldwork a joy and often an adventure. Of course, my time in Eureka would not have been the same without Derek Mueller and Jessie Turner who always helped out with discussions, ideas, field assistance, but especially great friendship and good times. Steve Robinson deserves special mention for providing the same down south, as do Chris Omelon, and Dale Anderson. To all the rest of my fellow grad students in the McGill Geography department: thanks for the encouragement and empathy you gave me during my time there, as well as the Friday nights! I would also like to thank all the staff of the McGill Geography Department who helped out in so many ways along the way.

My greatest thanks, however, have to go to my mother who was always there with whatever I needed. I am deeply grateful for her love, as well as her moral, emotional, and financial support, and of course her dog-sitting services. Thanks for everything, Mom.

Finally, I'd like to thank all those who cared enough to ask "So...ya done yet?" It is with great joy and enthusiasm that I can now answer "Yes!!!"

TABLE OF CONTENTS

LIST OF FIGURES

LIST OF TABLES

CHAPTER 1 - INTRODUCTION

1.1 Overview

The polar landscape is shaped by a number of interacting physical processes and permafrost plays an important geomorphic role. The study of permafrost is vital not only for learning more about the geomorphology of the polar regions, but for other practical and theoretical reasons as well. Engineers have long recognized the necessity of understanding the sometimes unstable permafrost that underlies the structures they build. Additionally, the extent and characteristics of permafrost can help investigators reconstruct glacial and sea level histories. More recently, researchers into climate change are discovering how global warming is affecting permafrost, and investigating how this landscape element can aid in their comprehension of past and future climate changes.

The Arctic is not a uniform environment and shows wide variation in climate and terrain. This study will examine how one landscape type -- a polar desert in the high Arctic -- is affected by the thaw of permafrost. In other permafrost regions, terrain response to changes in the surface temperature or other surface conditions has been more extensively studied and is much better understood, for example in the western Arctic where studies have been driven by the disturbances related to highway construction and oil and gas exploration. By contrast, a polar desert region is much colder and drier, and one cannot assume that the geomorphic response of the landscape will be similar to what has been seen in the western Arctic. The aim of this study is therefore to document the nature of the permafrost near Eureka, on Ellesmere Island in the Canadian Arctic Archipelago and to see how it has responded to disturbance in order to assess how sensitive the terrain might be to future changes.

1.2 Background

1.2.1 Permafrost and ground ice

Permafrost is "ground that remains at or below 0°C for at least two consecutive years" (International Permafrost Association 1998). It forms when summer heat does not penetrate deeply enough to warm all the ground that was frozen the previous winter. Permafrost underlies approximately one quarter of the earth's landmass and over 50% of Canada (Caron et al. 1995). Its distribution depends primarily on climate, but it is also affected by local variables such as vegetation, snow cover, topography, and soil and rock type. Permafrost is often divided into three broad zones: continuous, widespread discontinuous, and sporadic discontinuous (Figure 1). In the continuous zone, permafrost can be several hundreds of metres thick and is found everywhere throughout the zone except beneath large bodies of water. In the discontinuous zone, it is usually thinner and is interrupted by unfrozen areas: in the sporadic zone, permafrost can be as thin as a few decimetres and is found only in small pockets. Additional categories of zonation are alpine permafrost (found at high altitudes in temperate regions) and subsea permafrost (located on continental shelves bordering the Arctic Ocean).

The existence of permafrost involves a balance between cold temperatures propagating downwards from the ground surface and geothermal heat rising from the Earth's interior. The upper layer that thaws each summer is termed the active layer. Its thickness can range from 10-20 cm in areas of the high Arctic to well over 1 m in the sub-Arctic. Since temperatures below the active layer never rise above 0°C, the top of the permafrost table is generally considered to coincide with the base of this layer. Variations in the mean monthly temperatures throughout the year will change the temperatures in the upper portion of the permafrost, but these effects are attenuated with depth. The base of the permafrost itself is located at that point where geothermal heat raises the mean annual ground temperature above 0°C. These concepts are illustrated in Figure 2.

The definition of permafrost is dependent on the temperature of the ground only, not the presence of ice. Permafrost may be dry, consisting only of soil or rock, but this is rare (Bockheim and Tarnocai 1998), and moisture is generally present, usually as ice (although permafrost often also contains a small amount of water whose freezing point has been depressed below ambient temperatures). Ice within permafrost occurs when water freezes within the sediment (intra-sedimental ice), or when surface ice is buried. The term ground ice has been used to refer to both types, although the International Permafrost Association

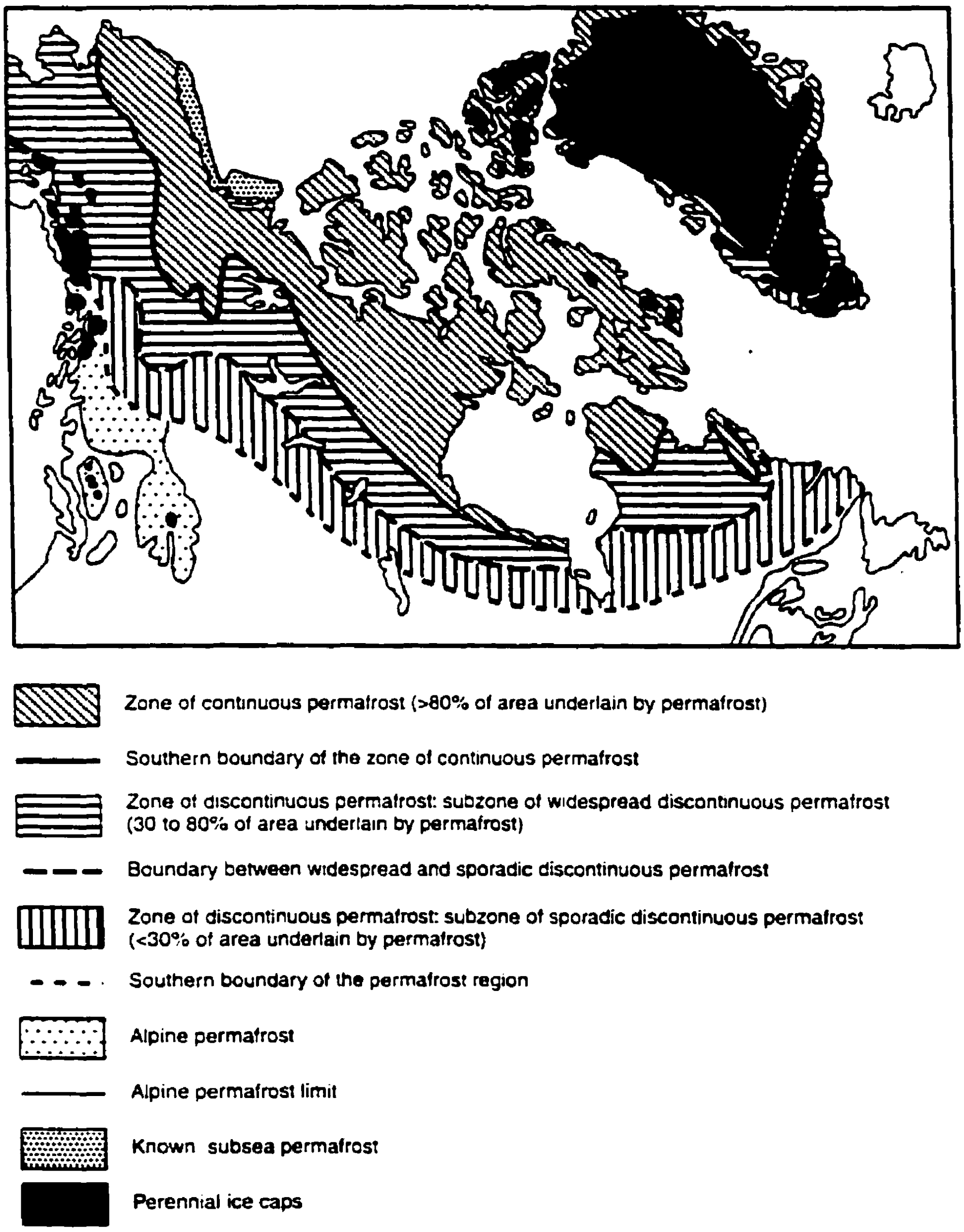

Figure 1. Distribution and zonation of permafrost in Canada (from ACGR 1988).

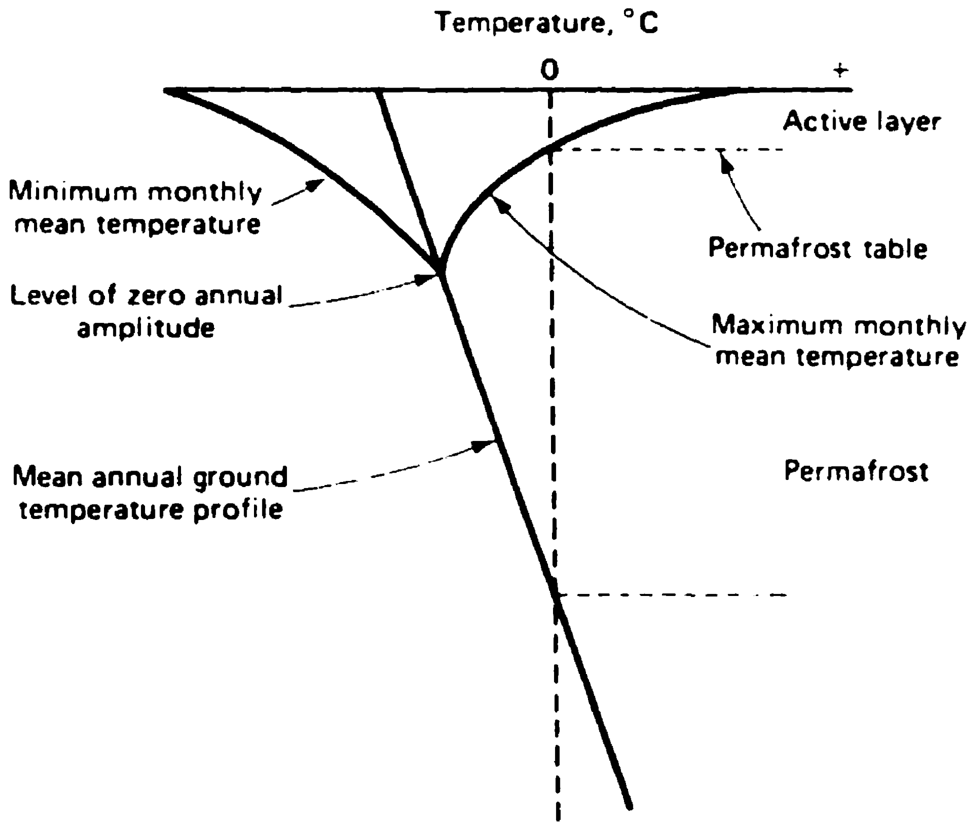

Figure 2. Idealized ground temperature profile in permafrost terrain (from Andersland and Anderson 1978).

now excludes buried ice from its definition (International Permafrost Association 1998). Intra-sedimental ice is further divided into syngenetic ice -- which forms at the same time that surficial materials are being deposited -- and epigenetic ice -- which aggrades into existing deposits. Although a number of classifications of ground ice have been developed -- notably by Russian researchers (e.g. Shumskiy and Vtyurin 1963) -- a genetic classification of intra-sedimental ice commonly used in North America is the one developed by Mackay (1972) (Figure 3). It shows the diversity of ways in which ground ice originates, as well as the various forms that it can take. Note that this classification excludes buried ice. The more common forms of ground ice include pore ice (within the soil voids), segregated ice (lenses of ice that form when cryotic suction draws water to the freezing front), ice veins, ice wedges, and massive ice bodies.

Ice wedges are one of the more visible geomorphic features associated with permafrost and are widespread in regions of perennially frozen ground. They are initiated when thermal contraction cracks develop in permafrost areas (Leffingwell 1915). Surface meltwater trickles down into the thermal contraction crack and freezes to form an ice veinlet. Over the years, the cracks often occur at the same place, and the veinlets build up to form an ice wedge (Figure 4). In a theoretical analysis of the stresses occurring in frozen ground, Lachenbruch related the thermal contraction cracking to rapid drops in air temperature (Lachenbruch 1962). However, exhaustive field experiments by Mackay (1974, 1988, 1992) that documented the timing, frequency, direction, geometry, and magnitude of ice wedge cracking have demonstrated that the mechanics of the process are quite complex. The size of ice wedges is related to the age of the wedge and the availability of water. In regions of Siberia, ice wedges can grow to several tens of metres wide (French 1996). North American ice wedges are generally smaller, usually 1.5-2 m wide and approximately 4.5-6 m high (Brown 1967, Mackay 1974, Harry et al. 1985). Ice wedges tend to be roughly triangular in shape, although changes in environmental conditions can result in a different geometry (Mackay 1990). Seasonal thawing at the top of an ice wedge often results in a trough running along its length. This feature is especially evident above the larger wedges and, in plan view, these troughs form a network of polygons on the tundra (Figure 5). The size of

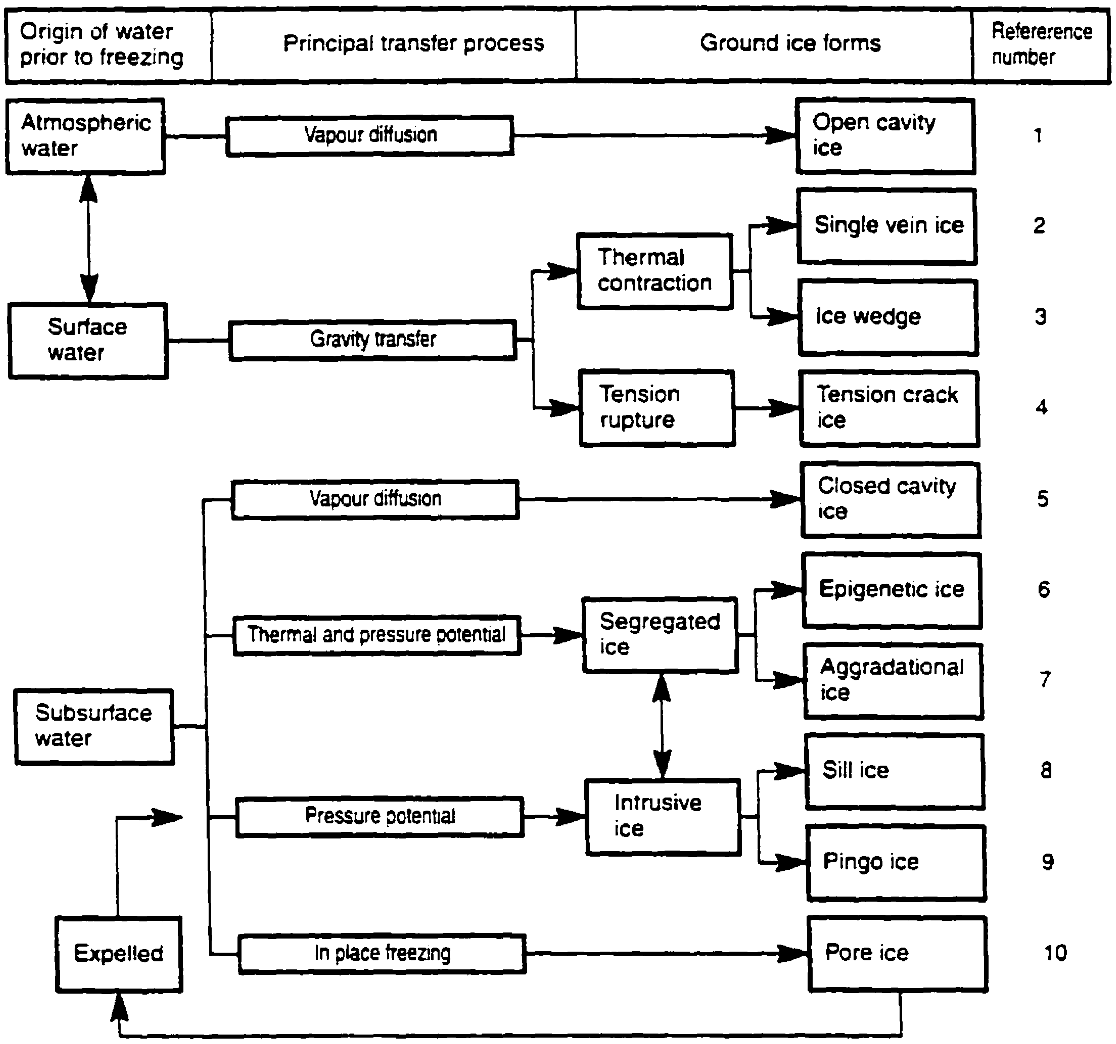

Figure 3. A genetic classification of ground ice (from French 1996).

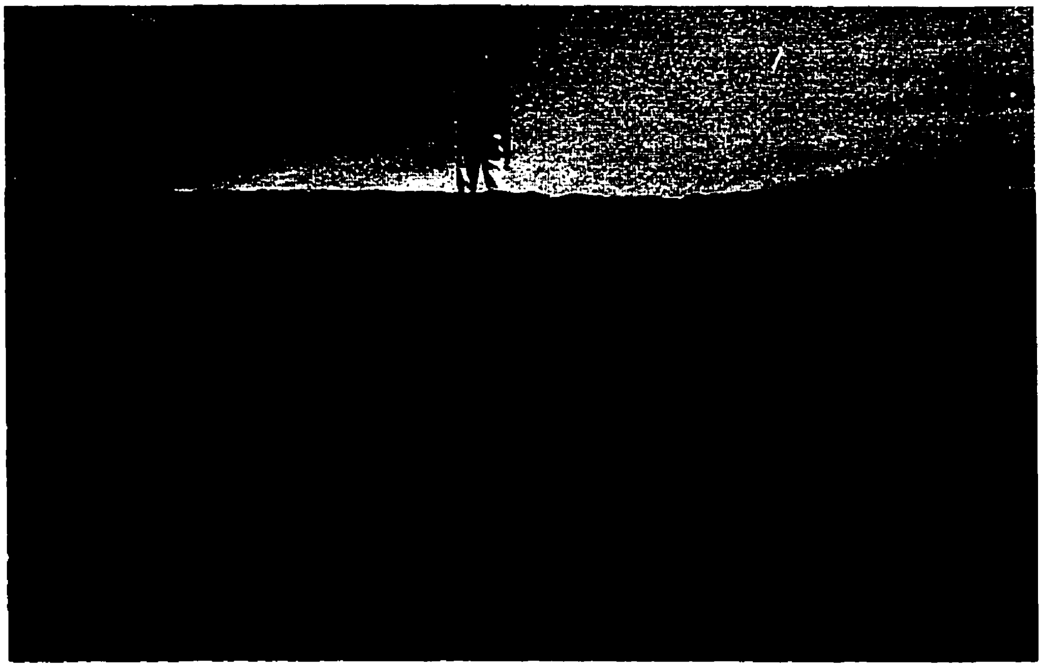

Figure 4. Natural exposure of an ice wedge, Fosheim Peninsula, Ellesmere Island, Nunavut.

Figure 5. Polygons on the tundra are delineated by troughs running along the top of ice wedges. The polygons shown here are approximately 30 m across.

the polygons is related to the soil in which the wedges form and the soil's response to thermal stress.

Massive ice takes the form of large tabular bodies having an ice content greater than 250% (ice to dry soil on a weight basis) (International Permafrost Association 1998). Buried surface ice such as glacier ice or snowbank ice fits within this definition, but massive ice can also form by ice segregation at the freezing front, by the intrusion of water under pressure, or by a combination of both processes. Massive ice beds (Figure 6) can cover hundreds of square metres and be tens of metres thick. They are found in many areas of Canada including the Yukon coastal plain (Harry et al. 1988, Pollard and Dallimore 1988, Pollard 1990), the Mackenzie Delta area (Mackay and Dallimore 1992, Rampton 1988), and the Arctic Islands (French et al. 1986, Pollard 1991). The origin of massive ice provides important information about a region's glacial and climatic history. For instance, positive

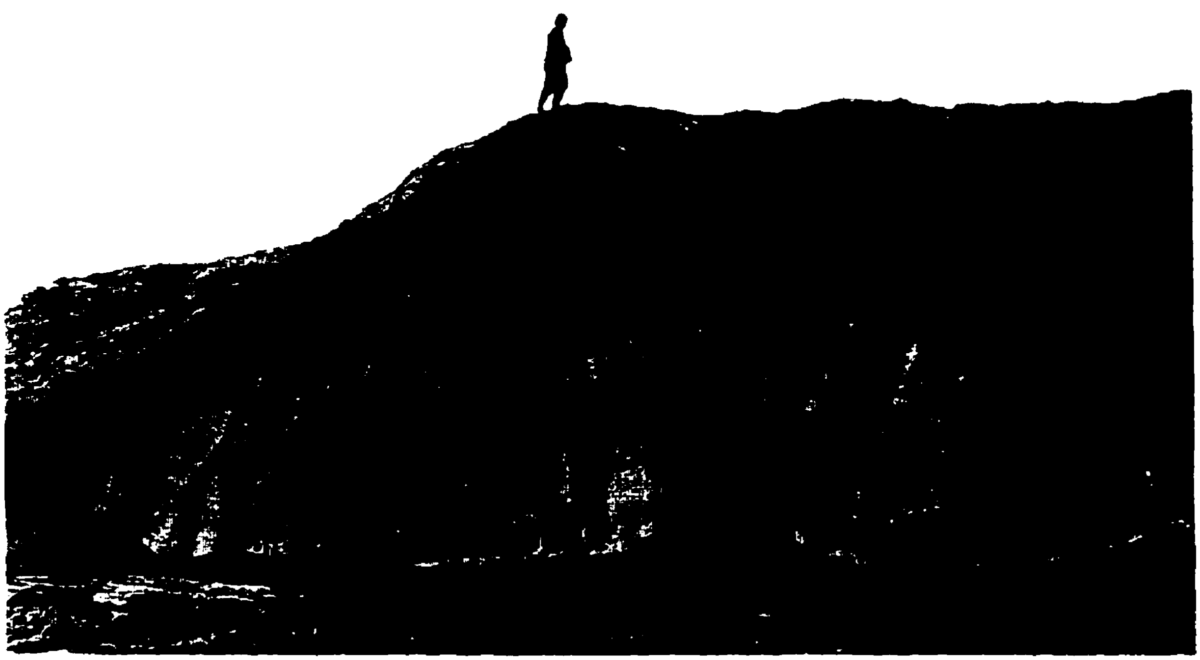

Figure 6. Bed of massive segregated ice on the Fosheim Peninsula. This exposure is approximately 4 m high by 25 m wide.

identification of massive ice as glacier ice can prove a theory about the limits of glaciation. A good deal of the research on these ice bodies has therefore focussed on whether they are of glacial or segregated origin (French and Harry 1990, Rampton 1988, Mackay and Dallimore 1992, Mackay 1971, Fujino et al. 1988). Until bodies of massive ice are exposed, detecting them can be problematic. However, their presence has been shown to be associated with certain geomorphic features such as scars from thaw slumping (Mackay 1963), involuted hills (Rampton 1974), and marine deposits in terrace-like structures (Pollard in press). A knowledge of surficial geology can also help in locating bodies of massive segregated ice since Mackay (1973) has shown that such ice is most commonly found at the interface where fine-grained sediments overlie coarse-grained ones. Geophysical techniques such as ground penetrating radar have also been used to delineate massive ice beds (Robinson et al. 1993), although the usefulness of these techniques can be limited by soil properties and conditions (Scott et al. 1990).

Determining the location and volume of all ground ice types within permafrost is of value in reconstructing geomorphic history and in assessing the sensitivity of terrain to anthropogenic or natural thermal disturbance. In the western Arctic, several studies (Brown 1967, Pollard and French 1980, Harry et al. 1985) have documented ground ice volumes. In one case, ice accounted for up to 70% by volume of the upper portions of permafrost (French et al. 1986). Research into ground ice volumes in the eastern Arctic is limited. Hodgson and Nixon (1998) reported values of 53% by volume on the Fosheim Peninsula, but their work concentrated on areas that they suspected of being ice-rich. Of greater importance than the total volume of ground ice, however, is the volume of excess ice within permafrost. Excess ice is defined as "ice in excess of the fraction which would be retained in the soil voids upon thawing" (Pihlainen and Johnston 1963). It is significant in that it provides an indication of how much ground subsidence can be expected upon melting of the permafrost. Ground ice contents are typically higher near the ground surface (Pollard and French 1980), with excess ice commonly found just below the active layer (Mackay 1970).

1.2.2 Thermokarst

The geomorphic changes to the ground surface caused by the melting of ground ice are collectively known as thermokarst. Thermokarst is generally initiated in one of two ways: the active layer increases in thickness, or part of it is removed. Either way, the top of the underlying permafrost becomes subject to melting. A number of the natural and anthropogenic surface changes that can lead to the development of thermokarst are illustrated in Figure 7.

If excess ice is present in a soil, thermokarst will begin with simple ground subsidence, as the ground surface lowers in proportion to the volume of excess ice that has melted. The thermokarst then perpetuates itself, however, since the lowered surface means that the new top of permafrost is now subject to melting. This results in a new cycle of subsidence. An example of this process is shown in Figure 8. It can sometimes take many years before the ground stabilizes. For instance, one long-term study showed that the active layer continued to deepen for 20 years following a forest fire (Mackay 1995). Ground subsidence is not spatially uniform, being greater in zones that are more ice-rich, such as those with ice wedges or bodies of massive ice. Additionally, microclimatic variables like vegetation or drainage will influence where the melting will be greatest. Thermokarst depressions often serve as collectors for snow in winter or for water in summer. Both these factors contribute to a further warming of the underlying permafrost, since they retard the penetration of cold air temperatures into the ground.

Distinct from simple ground subsidence is another form of thermokarst known as thermal erosion. In this case, it is running water that causes ground ice to melt rather than changes to the active layer. Thermal erosion generally takes place along rivers or coasts, but it can occur wherever water runs along a slope. Often, thermal erosion and ground subsidence both play a part in the development of thermokarst features.

Thermokarst processes produce a number of characteristic landforms. This may be a simple depression of the ground surface resulting from subsidence, but often more distinct forms

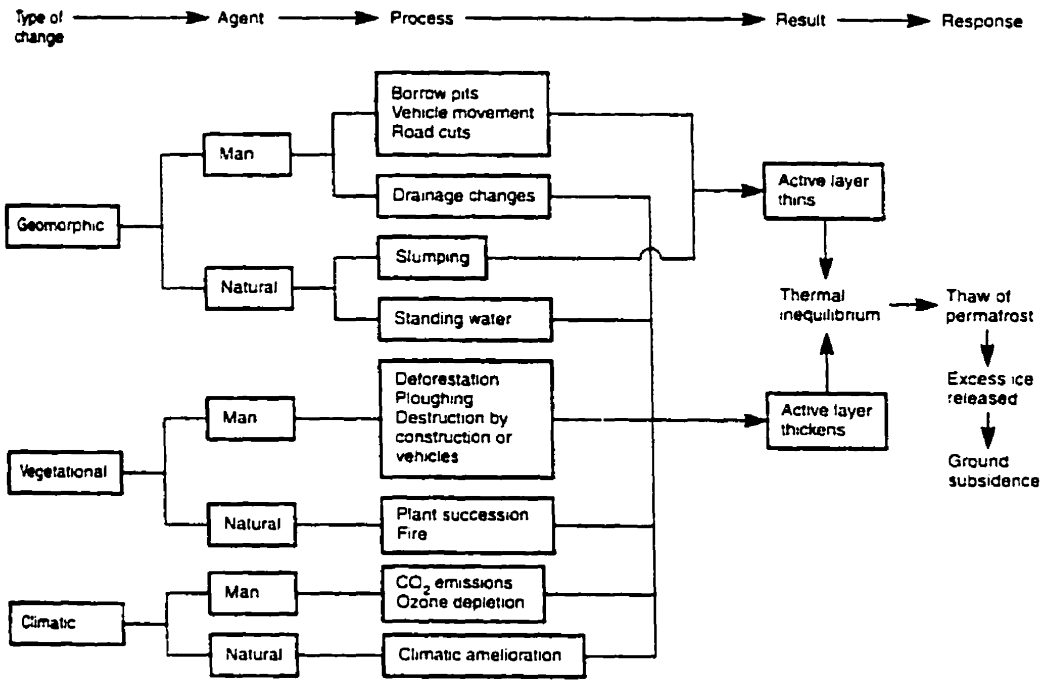

Figure 7. Diagram illustrating how geomorphic, vegetational and climatic changes may lead to permafrost degradation (from French, 1996).

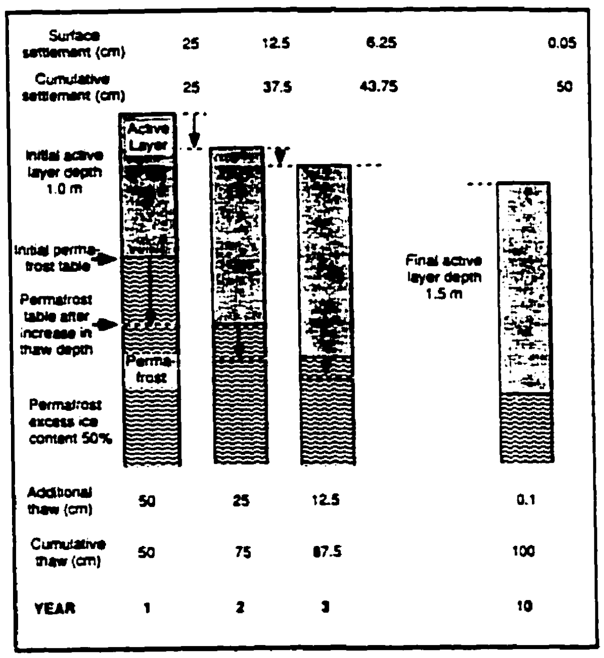

Figure 8. Ground subsidence in response to an increase in the thickness of the active layer in permafrost with an excess ice content of 50%. The active layer increases from 1.0 to 1.5 and in so doing, 1.0 m of permafrost is thawed and the surface settles by 0.5 m (from Woo et al., 1992).

develop. For example, the troughs above ice wedges often act as water collectors, especially where they intersect, and they may coalesce to form a beaded drainage pattern which is characterized by "short straight sections separated by angular bends" (Washburn 1973) (Figure 9). The water-filled depressions are also often the start of thaw lakes, which grow as surrounding ground ice thaws (Burn 1992). As thermokarst preferentially develops along the ice wedges, the polygon centres are isolated, resulting in "thermokarst mounds". Their local topographic relief can be up to 6 m, although 1.5 m is more common in North America (French 1975). In parts of Russia, this preferential melting along ice wedge troughs is the start of a process which results in broad depressions called "alasses" that can be as large as 25 km^2 (French 1996). Thermal erosion can result in the development of significant gullying. Very little research has been done on gullied surfaces and the contribution of gullying to the further development of thermokarst.

Thermokarst often involves slope failures. One type of failure, termed a retrogressive thaw slump, is initiated when a particularly ice-rich soil or a massive ice body is exposed. The icy material in the headwall of the slump rapidly melts and the overlying soil collapses, leaving a crescent shaped scar. In Canada, retrogressive thaw slumps are seen throughout the western Arctic (Mackay 1963, Burn and Friele 1989, de Krom 1990, Harry et al. 1988) and the Arctic islands (Pollard 1991, Lamothe and St-Onge 1961, Lewkowicz 1987). The retreat rates of the headwalls of retrogressive thaw slumps are generally from 7-16 m a year (Burn and Lewkowicz 1990), but annual values up to 19.5 m have been recorded (de Krom 1990). In one case on Ellesmere Island, subsurface water from a thaw pond flowing into a thaw slump resulted in retreat of 25 m in 38 days (Edlund et al. 1989). Retrogressive thaw slumps eventually stabilize when the ice in the headwall has completely melted, or when sufficient overlying material falls on the ice-rich face to insulate it from further melt; in the latter case, subsequent exposure can re-activate the slump. Another type of slope failure involves only the active layer. This occurs when pore water pressures build up at the base of the active layer (McRoberts and Morgenstern 1974), usually as the result of rapid thaw or heavy rains. Shear strength drops and, with the top of permafrost acting as the failure plane, the active layer becomes detached and travels downslope, leaving long, shallow, ribbon-like scars.

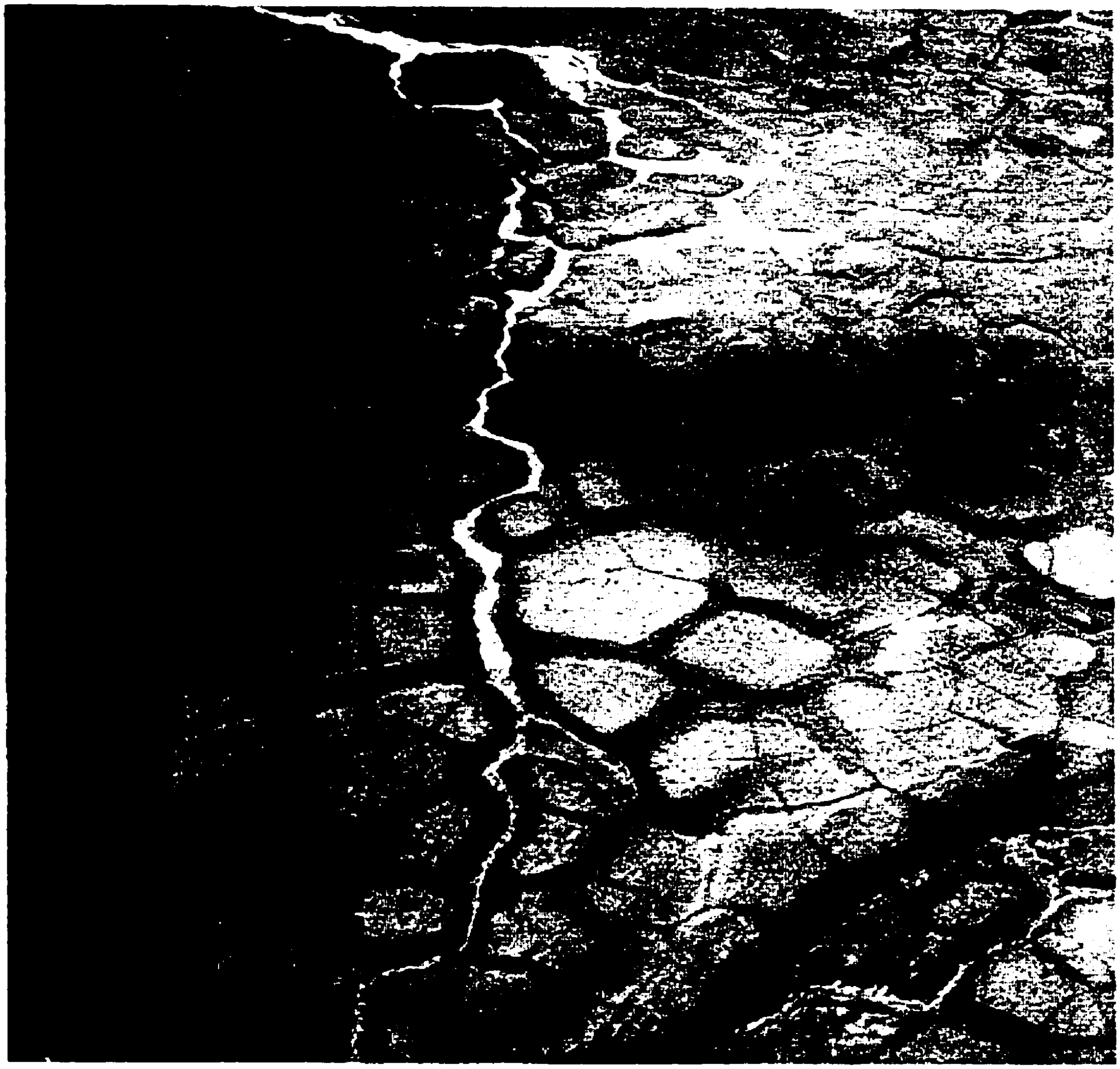

Figure 9. Beaded drainage pattern formed when water collects in coalescing ice wedge troughs. Note the larger ponds where troughs intersect.

These failures are referred to as active layer detachment slides when the material within the active layer is relatively rigid and dry, and as skinflows or earth flows when the active layer is saturated (Lewkowicz 1990). Both retrogressive thaw slumps and active layer failures are common throughout the Canadian Arctic. A form of slope failure that is limited to coastlines and riverbanks is block slumping. As a cliff is undercut by water, ice wedges often act as planes of weakness and large blocks of soil will tumble from the face.

1.2.3 Ground thermal regime

In order to understand how thermokarst will develop, it is necessary to understand the ground thermal regime in a permafrost area, that is, how temperature varies with depth. At any one location, geothermal heat is relatively constant, so active layer depth and permafrost thickness are therefore primarily functions of the surface temperature and the thermal properties of the soil or rock. The most important thermal property is thermal conductivity: a measure of the rate of heat transfer. Figure 10 shows how surface temperature and thermal conductivity can affect the thermal regime of the permafrost. As long as surface temperature and soil properties are stable, the permafrost remains in equilibrium. If they change, however, the temperature gradient will adjust accordingly. The active layer can be affected by changes in surface conditions within days or weeks, and therefore it tends to be the more important geomorphic variable. Temperature changes at the surface may also affect the upper portion of the permafrost, altering how much of it is subject to seasonal variations in temperature. In areas of deep, continuous permafrost, thermal changes at the ground surface can take thousands of years to propagate down through the ground and affect the base of the permafrost.

Ground surface temperatures are directly related to air temperatures, but they can be significantly affected by several microclimatic variables, with snow cover and vegetation being the most significant (Smith and Riseborough 1996). Snow insulates the ground so areas with thick and early snow cover remain warmer. One modelling study indicates that snow can increase the mean annual surface temperature by almost 12°C (Goodrich 1982). Vegetation shields the ground from incoming solar radiation, and therefore has a cooling

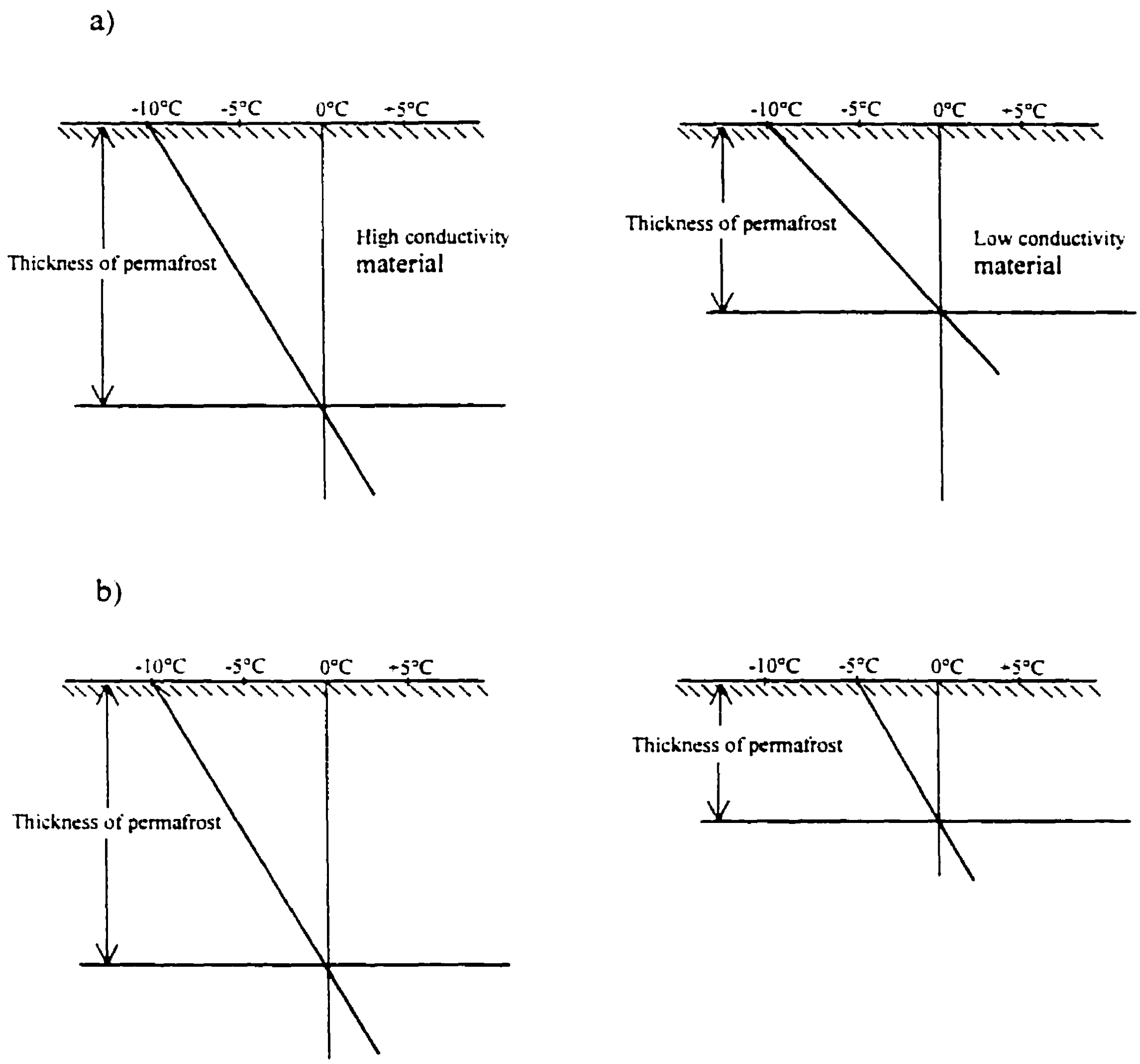

Figure 10. Changes to the ground thermal regime and resulting permafrost thickness a) when there is a difference in the thermal conductivity of the surficial material and b) when there are differences in the ground surface temperature.

effect in summer; this effect is enhanced in areas where peat is present, due to its high insulative value. Vegetation, however, also traps snow, which keeps heat from escaping in winter, so its influence on ground temperatures is not a straightforward one. A number of field studies have examined the influence of microclimatic variables on the ground thermal regime (Nicholson and Granberg 1973, Brown 1978, Mackay 1995), in one case indicating ground temperatures can vary by as much as 20°C (Smith 1975). In the high Arctic where precipitation is low and vegetative cover is minimal, the effects of microclimate are lessened (Brown 1974), and the properties of the soil take on more significance in regulating ground temperatures.

Heat can be transferred from the ground surface down through the soil by convection of water, but water movement is limited in permafrost environments. As a result, convection is usually negligible as a mechanism of heat transfer in permafrost, and heat conduction predominates (Lunardini 1998, Nixon 1975). In analyzing changes in the ground thermal regime and the penetration of thaw, a commonly used equation is the Stefan formula, which is based on heat conduction theory. The Stefan formula requires some simplifying assumptions which tend to overestimate the depth of thaw slightly, but in comparing it with other more complex solutions, several authors conclude that it nevertheless provides reasonable results (Nixon and McRoberts 1973, Johnston 1981). According to the formula, the depth of thaw is dependent on the square root of time, the thermal conductivity of the soil, and its volumetric latent heat of fusion.

The thermal conductivity of a soil is the rate at which it transfers heat. Thermal conductivity varies with the state of the soil, being higher in frozen than unfrozen soils, since the conductivity of ice is 2.2 W/m°C, about four times that of water. Soils with a higher moisture content will also have an increased thermal conductivity because the thermal conductivity of water is greater than that of air. Other factors which can influence a soil's thermal conductivity are its structure, temperature, solute content, and freezing history (Farouki 1981). A number of different methods exist for determining thermal conductivity and a detailed analysis of the benefits of each is given by Farouki (1981). One of the better methods for field observations uses a thermal conductivity probe that is inserted into the soil and then heated. A temperature sensor within the probe measures the rate of the rise in temperature, in effect giving a measure of how quickly the surrounding soil transfers heat away. Using the theory of a line heat source (see Weschler (1966) for a good summary), the soil's thermal conductivity is then determined from a plot of the temperature rise of the probe against the logarithm of time elapsed.

A soil's volumetric latent heat of fusion is the heat absorbed when the ice in the soil is converted to liquid water. Since the latent heat of water is a constant, the latent heat of the soil can be calculated from the total moisture content. However, it must be remembered that liquid water can exist below 0°C, so allowance must be made for the unfrozen water content when determining the volumetric latent heat of the soil. Another point to consider is that the Stefan formula assumes that all the ice present in the soil melts at 0°C, despite the fact that high pressures, solutes and other impurities can lower the freezing temperature of water. Nixon and McRoberts (1973) have shown, though, that any error introduced by this assumption is insignificant.

1.2.4 Terrain disturbance

Changes in the ground thermal regime often occur following surface disturbance. Much of the research on terrain disturbance in Canada and Alaska has been prompted by oil and gas exploration activities (e.g., Kurfurst 1973, van Everdingen 1979, Lawson et al. 1978, French 1981, Jorgenson 1997), although a number of investigations have concentrated on other types of anthropogenic as well as natural disturbances (e.g. Forbes 1996, Radforth 1972, French 1975, Mackay 1995). Good reviews of much of this research are provided by Lawson (1986), Heginbottom (1973), Kurfurst (1973), and in two reports by the Cold Regions Research and Engineering Laboratory (Brown and Grave 1979, Walker et al. 1987).

Regardless of the cause of surface disturbances, Lawson (1986) notes that they take one of four initial forms: 1) compaction of vegetation, 2) killing of vegetation, 3) removal of vegetation, and 4) removal of near-surface sediments. Another form of disturbance which should be considered is the compaction of not just the vegetation, but the soil itself (Heginbottom 1973).

The most common effect of disturbance on the ground thermal regime is an increase in the ground surface temperature. This is due to a decrease in the insulative value of the vegetation, or a decrease in its albedo, that is, its ability to reflect solar radiation (Kurfurst 1973). Removal of surficial sediment does not necessarily change the surface temperature, but it will obviously affect the temperature profile with depth, as previously frozen ground is now much closer to the surface. Another important effect of surface disturbance on the ground thermal regime is related to the soil's material properties: compaction of the ground and consolidation during subsidence will alter the bulk density of the soil (Halvorson et al. 1998), changing its porosity and thermal conductivity (Farouki 1981). Disturbances can also cause indirect changes to ground temperatures when drainage is altered or when water pools in the ruts and thermokarst depressions formed by a disturbance.

A number of factors influence the level and extent of any disturbance. Mackay (1970) notes that the most important one is the amount and distribution of various types of ground ice. Soils that are ice-rich contain more excess ice, resulting in greater melt following disturbance. Furthermore, if the disturbance exposes beds of massive ice or ice wedges, rapid geomorphic change can occur. The resulting changes in relief and drainage often perpetuate the effects of the initial disturbance. Sediment type has also been found to be significant in assessing susceptibility to disturbance, since coarse-grained materials are less subject to erosion and mechanical failure than finer-grained ones (Lawson 1986). Areas of higher relief are more likely to experience gullying and removal of thawed material, leading to further instability. In flatter areas, the initial disturbance may be limited to thaw subsidence, but this subsidence can nevertheless generate significant relief over time. Disturbance can be greatly minimized by restricting anthropogenic activities to periods of the year when the active layer is frozen. Nevertheless, the effects of winter disturbance can sometimes persist for many years (Emers and Jorgenson 1997), particularly in areas where snow cover is low and does not protect the underlying ground (Felix and Raynolds 1989).

Recovery from disturbance can only begin once the terrain achieves stability. Two kinds of stability must come about: physical and thermal. Physical stability occurs when subsidence and slope movement cease; only once that has happened can the ground reach a new thermal stability. Vegetation will recolonize the area, although not necessarily with the same species as were there originally (Walker, 1987). Recovery rates will vary widely depending on the extent of the disturbance and the nature of the site, but it can take up to 30-50 years for a retrogressive thaw slump to stabilize (French 1996).

1.2.5 Climate change and permafrost

Anthropogenic disturbance of permafrost is limited to specific areas. Much more widespread disturbance, however, can be expected if ground surface temperatures rise as a result of global warming caused by an increase in atmospheric carbon dioxide (CO_2). In the last century, global temperatures have increased by approximately 0.5°C. General circulation models (GCM's) used to model future climates show that there will be further temperatures increases of 1 to 4.5°C by the year 2100 (IPCC 1996). Warming is projected to be two to three times greater in the polar regions due to a number of feedback mechanisms, including changes in the surface albedo and the extent of sea ice (Walsh 1995). It should be noted, however, that climate models are less accurate at higher latitudes, and can show deviations from observed temperatures of up to 10°C (Walsh and Crane 1992). This is due to a paucity of baseline data and an incomplete understanding of the feedback mechanisms. According to the climate models, temperature increases in the canadian Arctic are predicted to be from 3 to 10°C, and will be greatest in late autumn and winter (Maxwell 1997). Precipitation is also expected to rise, particularly in the winter.

Research into how permafrost can be expected to respond to changing climate often focusses on the areal extent of permafrost degradation. Anisimov and Nelson (1997) predicted that the area in the northern hemisphere underlain by permafrost would be reduced by up to 22% under a climate associated with a doubling of atmospheric CO_2. In Canada, the boundary between the continuous and discontinuous zone could shift north by hundreds of kilometres

(Maxwell 1997). Woo et al. (1992) suggest that up to half of the permafrost in the discontinuous zone could disappear, although another study which accounts for factors which affect permafrost response to warming suggests that as much as 70% of the discontinuous zone is vulnerable to loss (Smith and Burgess 1999). The vertical distribution of permafrost and its thermal regime will be altered by surface warming as well. As the permafrost warms, it will melt from the top, increasing the depth of the active layer; but melt will also occur at the bottom as well, decreasing the total permafrost thickness. How quickly this occurs will vary with site conditions, nevertheless, some studies give an indication of the magnitude of change and the times involved. For example, Kane et al. (1991) showed that a 4°C warming at the surface would increase the active layer depth 50 cm to 97 cm over a 50 year period. Lunardini (1996) showed that with a 2.5°C temperature increase, the total change in the thickness of a relatively warm permafrost layer would be 18 m over 55 years. Over 185 years, this would increase to 25 m.

1.3 Research goals and organization of the thesis

Most of the research on climate change in the Arctic has focussed on atmospheric, oceanic, or glacial systems. There has been much less research into how a warming climate will affect permafrost and ground ice, and what changes this will bring about in the geomorphology of the landscape. In Canada, the work that has been done on the response of permafrost has been centred in the Yukon and the Northwest Territories, while virtually none has been done in Nunavut. To fill this gap, the primary objective of this thesis is therefore to evaluate how the terrain in Nunavut's high Arctic polar desert will respond geomorphically to a warming climate. This will be tested by making the assumption that the landscape response to anthropogenic disturbances and to particularly warm periods in the recent past can serve as analogues for global warming. The following specific research goals have been identified:

1. Quantify the different types of ground ice present in the area near Eureka, on Ellesmere Island in the Canadian Arctic Archipelago,
2. assess the forms of thermokarst which have developed in the past in response to

anthropogenic and natural disturbances,

3. measure the ground thermal regime at a number of study sites,
4. model how the area's permafrost will respond to warmer climate scenarios.

Chapter 2 describes the physical setting of the study area and provides a more detailed analysis of the region's permafrost. The methods used to measure the ground ice, thermokarst, and ground thermal regimes in the study area are provided in Chapter 3. This chapter also lays out the model used to determine the change in climate that can be expected for the area, as well as a model of thaw that will be used to assess the landscape response to global warming. Analyses of ground ice volumes, thermokarst activity, and thermal regimes are included in Chapter 4, while Chapter 5 examines the responses to climate warming, based on the output of the two models. A discussion of the study's findings is contained in the final chapter, along with conclusions drawn.

CHAPTER 2 - STUDY AREA

2.1 Introduction

The study area is located on Ellesmere Island in the Canadian Arctic Archipelago. More specifically, it focuses on Eureka (80°00'N, 85°55'W), a site on the Fosheim Peninsula, in the west central portion of the island (Figure 11). Anthropogenic activity in the area has been ongoing for the last half century. A weather station run by the Canadian Meteorological Centre (CMC) was established at Eureka in 1947 and has been in continuous operation ever since. The airstrip built to enable re-supply of the weather station has drawn a number of other players to the site as well. Since the 1960's, the Polar Continental Shelf Project (PCSP) has operated an outpost for the support of scientific research, and a number of northern airlines have used Eureka as a base of operations or as a refueling stop. During the 1970's, activity centred around the search for oil and gas. Since the start of the 1980's, the Department of National Defence (DND) has maintained a summer presence there in order to service communications equipment, and in the early 1990's, a private facility for atmospheric research was built. The infrastructure in Eureka consists primarily of the airstrip, a scattering of buildings, a limited number of roads, communications and power lines, and fuel depots (Figure 12). All of these areas see heavy vehicular traffic. Gravel is spread regularly on the roads and airstrip, and they are graded in summer and ploughed in winter. There is little or no vegetation in the immediate vicinity of the roads and buildings. Activity declines with distance from these areas, although people regularly travel across the tundra on foot, by all terrain vehicle, or occasionally by truck.

Eureka's former airstrip is located approximately 5 km northeast of the settlement. It was originally built in 1947 to service the weather station, but was abandoned in 1951 because of drifting snow in winter and problems created by thawing permafrost in summer (Gadja 1949). Airstrip construction involved grading and rolling of the ground surface as well as removal of the vegetation. The airstrip is still clearly visible on aerial photographs taken in 1998 (Figure 13). Another site of anthropogenic activity is an abandoned oil well, Panarctic's Gemini E-10 well, located 35 km east of Eureka (79°59'N, 84°04'W) (Figure 14).

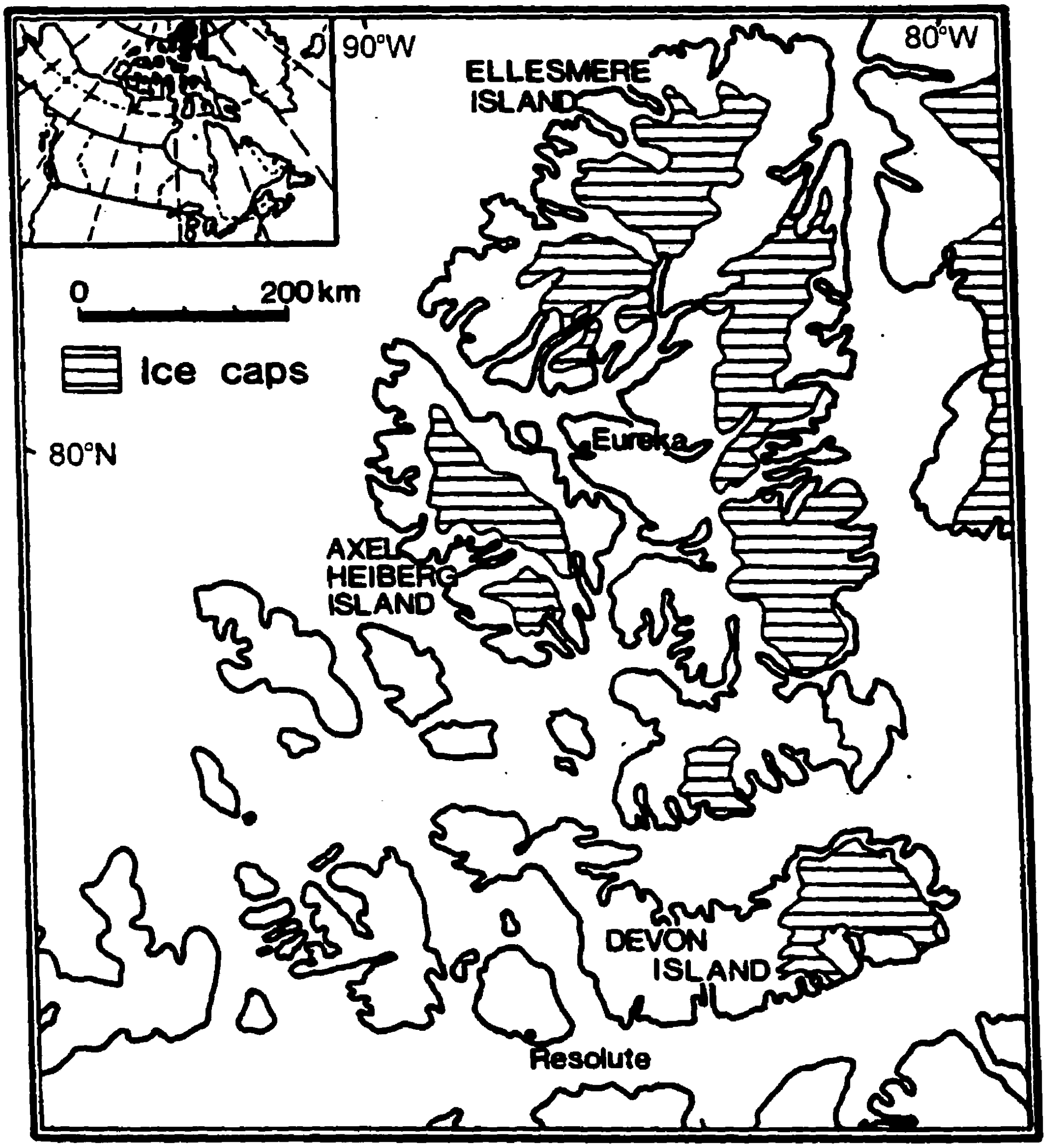

Figure 11. Eureka on the Fosheim Peninsula, Ellesmere Island, Nunavut.

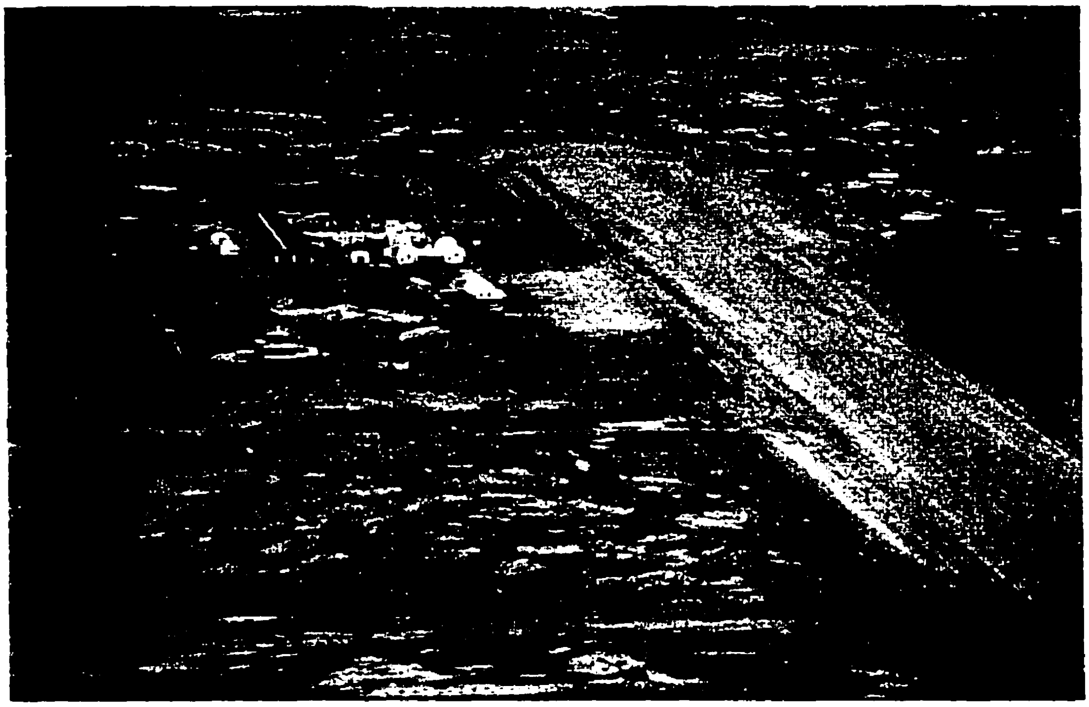

Figure 12. Infrastructure at Eureka. Note the current airstrip, buildings, roads beyond the buildings, and the fuel depot to the right of the airstrip.

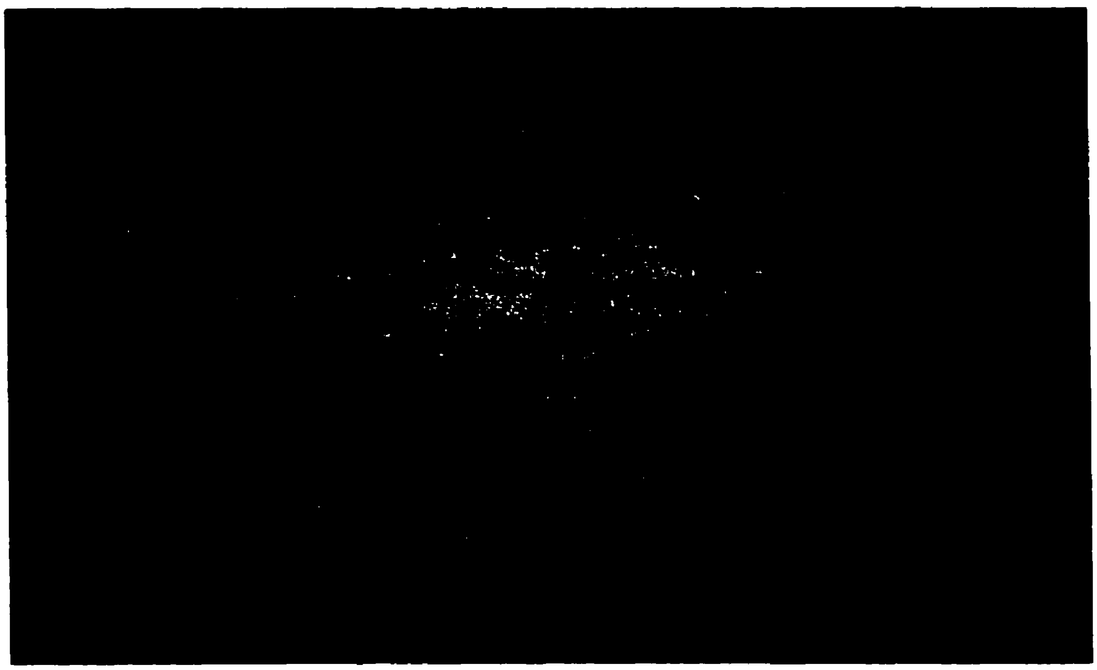

Figure 13. Eureka's former airstrip is still visible from the air. The strip was built in 1947 and was abandoned in 1951.

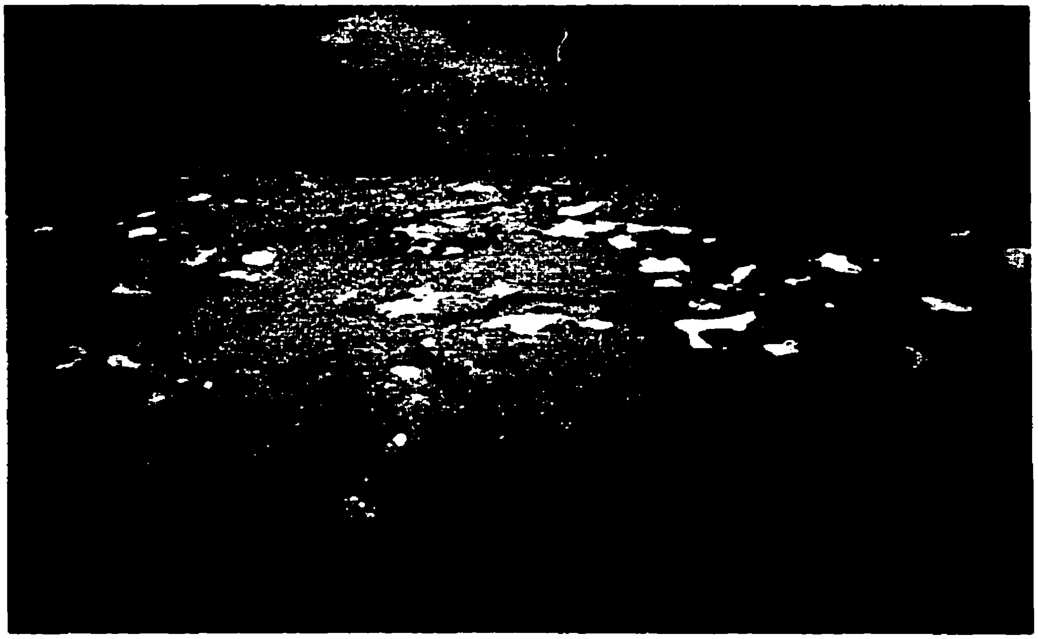

Figure 14. Aerial photograph showing Panarctic's Gemini E-10 wellsite. The location of the wellhead is indicated by the X. Note the road in the foreground on the left. The disturbed terrain around the wellhead is the result of the drilling activities and the existence of a surface sump.

Figure 15. One of the steep ridges characterizing the Eureka area. The lower, lighter coloured part of the ridge is blanketed with marine sediments, while the upper, darker coloured part is mantled by weathered bedrock.

Exploratory drilling operations began in October 1972 and were suspended in March 1973 (Panarctic Oils Ltd. 1973). In addition to the drilling activities themselves, disturbance of the area was caused by the construction of a road and an airstrip, and the storage of drilling fluids in a surface sump adjacent to the wellhead.

2.2 Physiography and surficial materials

The Fosheim Peninsula, together with portions of neighbouring Axel Heiberg Island, consists primarily of broad, rolling lowlands surrounded by mountains rising to 2200 metres above sea level (m.a.s.l.). Several steep north-south running ridges within this intermontane region rise above 500 m.a.s.l. (Figure 15). Poorly consolidated rocks of the Eureka Sound Group underlie the area (Ricketts 1986). Reconstruction of the last glaciation of the region suggests that it was limited to ice caps on regional uplands and cirque glaciers (Bell 1996). In the early Holocene, about one third of the peninsula was inundated (Figure 16) and the marine limit has been placed approximately 150 m above its current position (Hodgson 1985). Below marine limit, a fine- or medium-grained marine sediment blankets the terrain, at times forming thick deposits (Hodgson et al. 1991). Outcrops of intact bedrock -- primarily sandstone, siltstone and shale -- occur on the local ridges and at other points above marine limit, although in general, most of the area above the 150 m contour is mantled by weathered bedrock (Bell 1992, Hodgson et al. 1991). Many short rivers and gullies dissect the terrain throughout the study area. The area is relatively lush compared to others parts of the high Arctic, with the most common vegetation types being arctic willow (*Salix arctica*) and mountain avens (*Dryas integrifolia*) (Edlund and Alt 1989).

2.3 Climate

The climate of the Fosheim Peninsula is influenced to a large degree by the surrounding mountains, which limit the influx of cold air from the Arctic Ocean (Edlund and Alt 1989). The mean annual temperature at the Eureka weather station is -19.6°C. February is the coldest month with a mean temperature of -38.2°C, while July is the warmest, with a mean temperature of 5.6°C. Summer temperatures are exceptionally warm for this latitude (Edlund

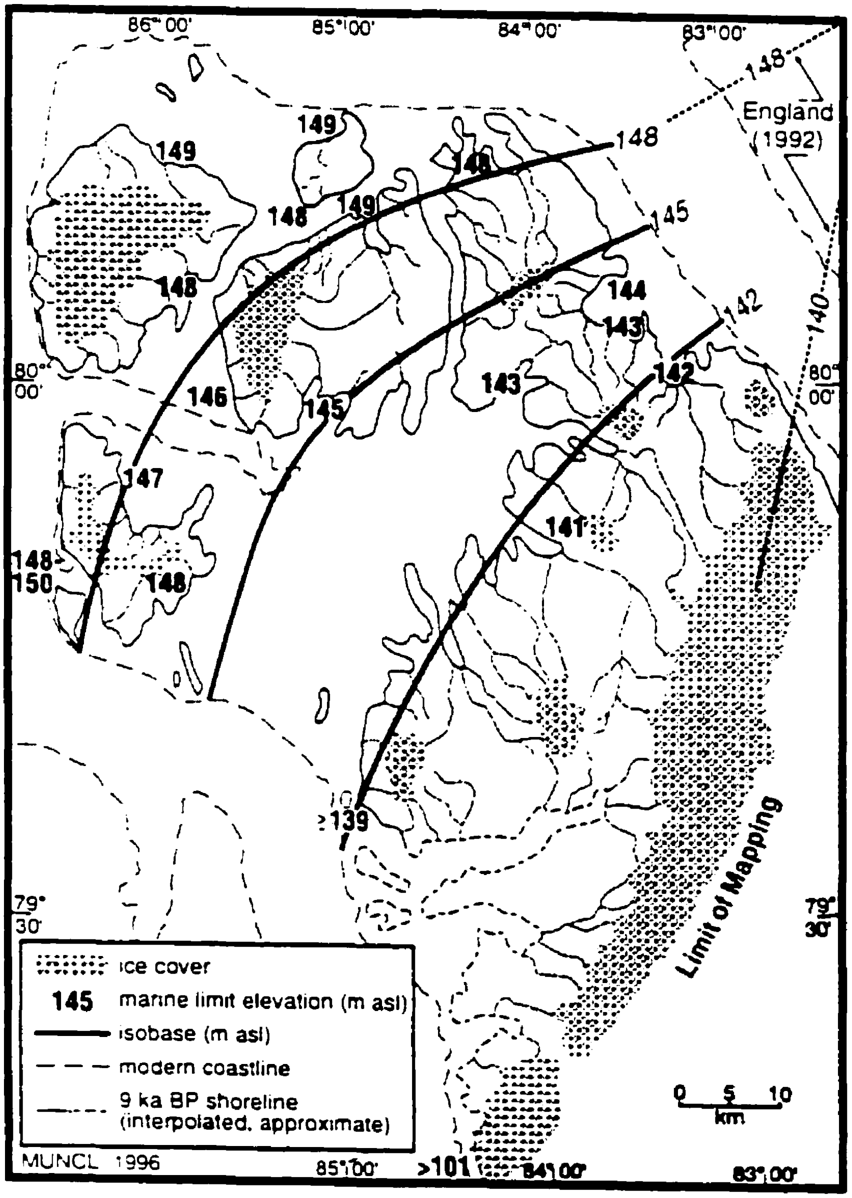

Figure 16. Map showing the Holocene marine limit on the Fosheim Peninsula (from Bell 1996).

et al. 1989), and have ranged as high as 19.4°C. There is generally a temperature inversion at the Eureka weather station which is located at 10 m.a.s.l., so temperatures increase sharply at approximately 50 m.a.s.l. Additionally, a number of investigations suggest that the location of the Eureka weather station on Slidre Fiord causes its temperature observations to be cooler than ones further inland. One example comes from a long term monitoring station set up as part of a global change study by the Geological Survey of Canada (GSC) at Hot Weather Creek, 25 km east of Eureka. Summer temperatures at Hot Weather Creek are consistently higher than at the Eureka weather station (Edlund et al. 1989, Young et al. 1997). From 1988 to 1994, the mean July temperature at Hot Weather Creek was 9.4°C, fully 5.0°C warmer than Eureka during that same period. Only two years of sporadic meteorological data are available for the Gemini well site, which is 7 km east of Hot Weather Creek. What data is available, however, agrees well with information from Hot Weather Creek, showing only a 0.5°C difference between the two sites in summer.

Mean annual precipitation at Eureka is only 68.0 mm, making it one of the driest areas in Canada. Only one quarter of this precipitation falls as rain (Environment Canada 1998); the rest falls as snow. Much of this snow is redistributed by the winds and accumulates in hollows, so that snow cover is often low, if not virtually nil in some places. Snowmelt and runoff generally begin in late May or early June, although a significant amount of the snow also sublimates before then (Woo and Young 1997).

2.4 Permafrost

Ellesmere Island is located well within the zone of continuous permafrost and so permafrost is found everywhere except beneath large bodies of water. A measurement of permafrost thickness made at a borehole at the Gemini wellsite shows it to be 502 m thick (Judge et al. 1981). This site is quite close to the Holocene marine limit and was one of the first areas exposed to sub-aerial temperatures as the sea level lowered. Since this area has been exposed for a longer time than others, this value for permafrost thickness is probably close to the maximum for the Fosheim Peninsula. Throughout the region, the active layer -- the ground that thaws seasonally -- is relatively thin, and probing in a variety of terrains indicates a mean active layer thickness of 57 cm; depending on local microclimatic conditions, however, the base of the active layer can be as shallow as 30-40 cm. An investigation by the Geological Survey of Canada using data from shallow cores determined that ground ice of all types constitutes 53% by volume of the area's surficial materials (Hodgson and Nixon 1998). It should be noted, however, that this study focussed on areas suspected of being ice-rich.

Various forms of ground ice appear throughout the study area. Pore ice and thin lenses of segregated ice are found in abundance, although they are limited in areas of mantled bedrock above marine limit. Ice wedges are ubiquitous over much of the peninsula. The wedges occur in all surficial materials and have been recorded to depths of 8 m and widths of 5 m (Hodgson et al. 1991), although smaller dimensions are more usual. They vary in density, depending primarily on soil type. The polygons formed by the troughs that occur at the tops of the wedges range from 10 to 25 m in diameter (Lewkowicz and Duguay 1999). Beds of massive ice appear to be relatively common, based on the number of retrogressive thaw slump scars identified on aerial photographs. In addition, massive ice has been detected by direct observation (e.g. Edlund et al. 1989, Hodgson et al. 1991, Pollard 1991, Robinson and Pollard 1998), and the use of ground penetrating radar (Barry 1992, Robinson 1994). Many of these massive ice beds are considered to be of segregational origin, forming when water is drawn by cryotic suction to the freezing front (Pollard and Bell 1998). The occurrence of massive ice has been closely linked with fine-grained marine sediments, especially where they form flat to gently dipping terraces in otherwise irregular terrain (Pollard 1991, Pollard and Bell 1998). Thermokarst features include the retrogressive thaw slumps caused by the melting of massive ice. Robinson recorded headwall retreats of 8-14 m/year at high angle retrogressive thaw slumps near Hot Weather Creek (Robinson in press). Active layer detachment slides are common occurrences, particularly during warm summers (Edlund et al. 1989, Lewkowicz 1992). In fact, Lewkowicz notes that the number of active layer detachment slides on the Fosheim Peninsula is anomalously high compared to other regions in the Canadian high Arctic (Lewkowicz 1992).

2.5 Study sites

In order to quantify ground ice on the Fosheim Peninsula, measurement of regional ground ice volumes was conducted in an area of 1887 km^2, centred on Eureka (Figure 17). This area was selected because it is one for which ground ice data is available and because it encompasses representative subsurface units for the region. Additionally, two disturbed sites were selected for a systematic examination of thermokarst development and ground thermal regimes. The first site is the old airstrip 5 km northeast of Eureka. The airstrip lies on a plateau at 116 m.a.s.l. which consists of sandy clayey silt of marine origin over poorly consolidated clayey shale (Hodgson and Nixon 1998). The second site is Panarctic's abandoned oil well -- Gemini E-10 -- 35 km east of Eureka. The site is 126 m.a.s.l. and is on thick silt and sand marine-deltaic sediments (Hodgson and Nixon 1998). In addition to these two primary study sites, supplemental data was collected at a number of locations in the immediate vicinity of Eureka. Preliminary fieldwork at Eureka was conducted from July 2 to July 27, 1997, with the main body of work taking place from June 29 to August 27, 1998. The Gemini site was visited twice: from June 30 to July 3, 1998 and again on August 12, 1998.

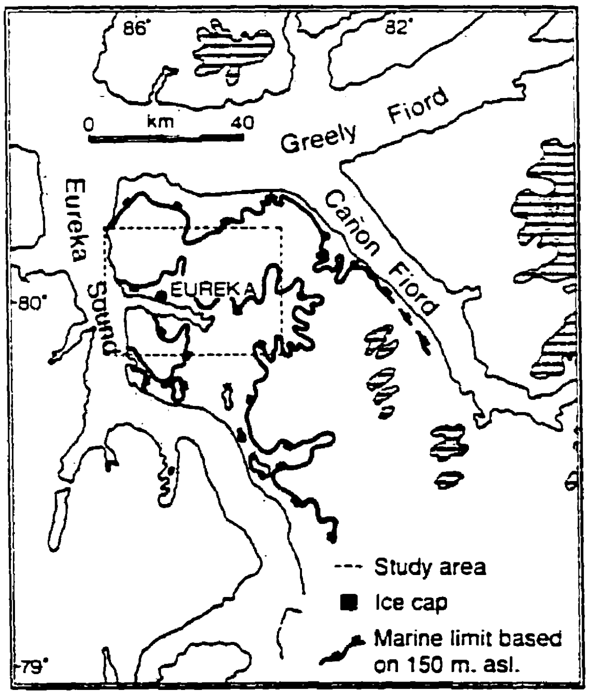

Figure 17. Map delineating the study area around Eureka in which ground ice volumes were measured.

CHAPTER 3 - METHODOLOGY

3.1 Introduction

In order to assess the sensitivity of permafrost terrain in the Eureka area, a combination of fieldwork, archival data collection and laboratory analysis was used. One of the objectives of this thesis is to quantify ground ice in the study area. Knowing the volume of the different types of ground ice is important in order to assess what forms of thermokarst to expect if the ground ice were to melt. To meet this goal, a first approximation of ground ice volume for the region was conducted using topographic maps, aerial photographs and field measurements. The methods used are given in section 3.2. A second objective is to assess the forms of thermokarst that have developed in response to past disturbances. Since past thermokarst is the result of melting ground ice (regardless of whether the trigger for melt was a warm climatic period or an anthropogenic disturbance), the melting of ground ice as a result of climate warming is likely to produce the same geomorphic features. Existing thermokarst features were therefore surveyed in the field and measured from air photos, and details are provided in section 3.4. Another objective is to measure the ground thermal regimes at the study sites. This was achieved by taking direct field measurements of ground temperatures, active layer thicknesses and thermal conductivity. Measuring the ground thermal regime helps determine whether it changes as a result of disturbance and provides the information necessary to determine how deeply heat from warmer predicted air temperatures will penetrate into the ground. The techniques used to measure the elements relating to the round thermal regime are provided in Section 3.3. The final objective of this study is to model how permafrost will respond to a warmer climate. A two-step approach is used here. First, the predicted temperature increases for the Eureka area are established by using a climate model and supplementing it with baseline climate data from the Eureka weather station. The climate model and the baseline data are described in Section 3.5. The second step is to use the predicted air temperatures and the elements of the ground thermal regime as inputs for a model of thaw depths. This model of thaw is based on Stefan's formula. It and the parameters it uses are more fully described in section 3.6. Once all of these elements are collected -- amount of ground ice, thermokarst features, predicted air temperatures, and predicted thaw -- it becomes possible to draw conclusions about how climate change will affect this permafrost landscape.

3.2 Ground ice volume

The total volume of ground ice is calculated by estimating the areal extent of various types of ice-rich terrain in the study area. Four different subsurface units are considered: 1) those with pore ice, thin segregated ice lenses and a high density of ice wedges, 2) those with pore ice, thin segregated ice lenses and a low density of ice wedges, 3) regions underlain by massive ice, and 4) regions above marine limit that are mantled by weathered bedrock. The area of each type of subsurface unit is then multiplied by a percentage of ice content by volume that is established for the unit. Excess ice values are also calculated for each subsurface unit. Since excess ice values represent the water that cannot be contained within the soil pores and which would run off after thaw, they provide an indication of how much ground subsidence can be expected when ground ice melts, and they help in determining what geomorphic response to expect.

3.2.1 Extent of Permafrost

This study considers the top 6.5 m of soil because this was the lower limit of most of the sample data, and also because the immediate effects of surface disturbance are unlikely to penetrate to much greater depths. The total area of the study region and the areas of the different subsurface units were measured using a digital planimeter and 1:50,000 scale maps from the National Topographic Series (NTS 49G/14, 49G/15, 49G/16, 340B/3 and 340B/4). Several areas were considered to contain no ground ice and were therefore excluded. For instance, the assumption was made that fiords, large lakes and rivers are either deeper than 6.5 m, or that unfrozen zones (termed "taliks") exist beneath them to at least this depth. Although some ground ice has been shown to exist in the sediments of shallow Arctic lakes (Burn 1990), this assumption has little effect on the study's overall results since shallow water bodies cover only 1% of the study area. Another area excluded from the calculations is the steep slopes of ridges where bedrock is intact or is covered by extremely coarse, angular colluvium which field observations show contains negligible ground ice. Robinson and Pollard (1998) describe an occurrence of ground ice in bedrock, but note that it is a rare occurrence and occurs at considerable depth (>20 m).

3.2.2 Pore and Segregated Ice

Much of the ice in frozen sediment occurs as pore ice and as thin lenses, usually of segregated origin (Figure 18). For this study, data on pore ice and thin ice lenses are derived from cores drilled by the Geological Survey of Canada between 1972 and 1974, and from samples gathered from sediments above natural exposures of massive ice during field work in 1994 and 1995. A mean ice content value was calculated and was considered to be representative for areas in the study region below the Holocene marine limit, except where massive ice is present (discussed below). Ice contents for areas above marine limit mantled by weathered bedrock are averages based on published values.

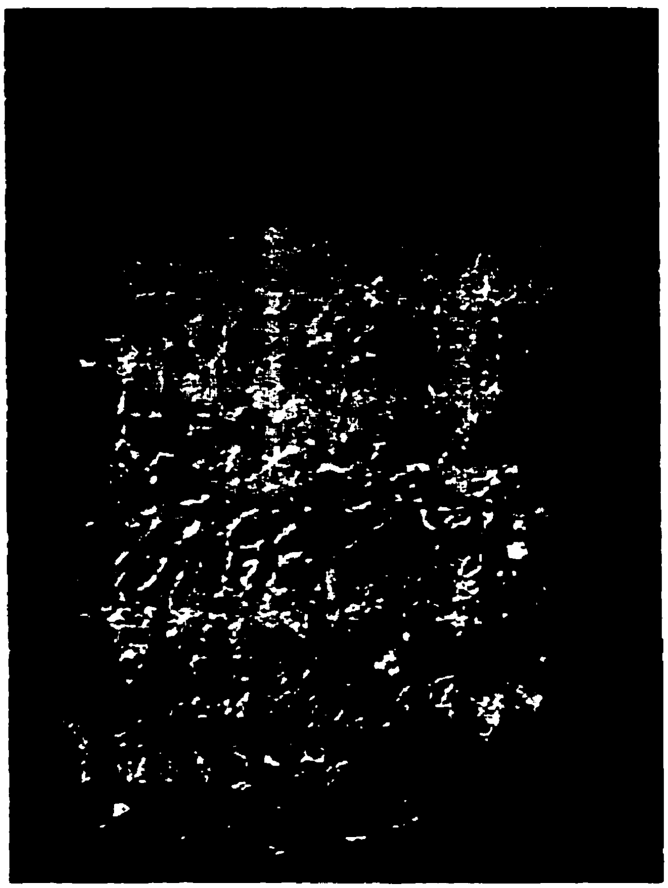

Figure 18. Pore ice and thin segregated ice lenses.

3.2.3 Ice Wedge Ice

Ice wedges form when water repeatedly trickles into thermal contraction cracks in the ground and refreezes. On the Fosheim Peninsula, they are most abundant within fine-grained sediment below marine limit. For the purposes of this study, the wedges are considered to consist of pure ice. A single average dimension for ice wedges was derived from more than 100 measurements of naturally exposed ice wedges on the Fosheim Peninsula between 1992 and 1995. If ice wedges are assumed to be roughly triangular in cross-section, then the percentage of wedge ice in a volume of frozen ground is calculated as:

$$[1] \qquad V_w = \frac{0.5 \cdot \bar{w} \cdot \bar{d} \cdot L}{d_s \cdot A} \times 100$$

where V_w = percentage volume of wedge ice

$\bar{w}$ = mean wedge width

$\bar{d}$ = mean wedge depth

L = total length of ice wedge troughs in a sample site

d_s = depth of the sample site

A = area of the sample site

Based on field observations and examination of air photographs, estimation of the volume of ice wedges is divided into two steps. First the percentage volumes are determined for sample sites of high and low density wedges, then these percentages are extrapolated to the larger study area. The troughs that run along the tops of the wedges are generally quite visible on air photographs. The total length of ice wedges and the area for each sample site are therefore measured from large-scale air photographs, and the percentage volume of wedge ice for each site is calculated using Equation [1]. Areas of high density ice wedge polygons are then estimated from small scale air photographs of the entire study region. Given the ubiquitousness of ice wedges, the remaining area below marine limit is assumed to be covered by low density ice wedges.

3.2.4 Massive Ice

Using measurements from samples taken at natural exposures of massive ice on the Fosheim Peninsula, a mean volumetric ice content was calculated for shallow (<6 m) massive ice. The depth to the top of massive ice beds is variable, so a mean depth is calculated based on published values. Using the ice content for sediment above massive ice calculated earlier and the measured volumetric ice content of massive ice itself, volumetric ice content for the top 5.9 m of permafrost in areas underlain by shallow massive ice is calculated. As mentioned earlier, the distribution of such ice has been closely linked with fine-grained marine sediments, especially where they form terrace structures. Air photos of three areas below marine limit were examined (National Air Photo Library A16676-53, A16734-61, A27038-24) for such terraces and the area they cover is assumed to correspond to that of massive ice beds.

3.2.5 Excess ice

Values for excess ice depend on total ice content and the porosity of the soil. Using mean values of soil porosity (33% for gravel, 38% for sand, 44% for silt, and 50% for clay), excess ice values for each subsurface unit were calculated using the equation:

$$PEI = \frac{(PIV/1.09) - 100e + PIVe}{(PIV/1.09) - 100e + PIVe + 100 - PIV} \qquad [1]$$

where PEI = percentage of excess ice

PIV = percentage ice volume

e = porosity

3.3 Survey of thermokarst features

During the 1998 field season, topographic surveys were carried out at the two primary study sites -- the abandoned airstrip at Eureka and the Gemini E-10 well site. A Sokkia B3C engineer's level was used to determine the amount of ground subsidence compared to the surrounding terrain, and to establish the areal extent of thermokarst features. Survey readings were made at any break in slope, or when features such as ice wedge troughs were encountered. At the abandoned Eureka airstrip, a 1973 survey made by the Geological Survey of Canada was replicated, using notes and charts of the survey points provided by the GSC. A comparison of air photographs from 1973 with the 1998 field observations showed virtually no change in the pattern of ice wedge troughs, so these features were also used to ensure that the survey lines matched the 1973 ones. At the Gemini well site, three lines ranging from 62 to 100 m long were surveyed across the airstrip. Four additional lines radiating out from the wellhead were also surveyed. These were at 90° from one another and ranged from 113 to 172 m in length. Less detailed surveys were also conducted at four other disturbed sites where thermokarst activity was evident. Qualitative observations of general thermokarst conditions in the larger study area were also made.

3.4 Ground thermal regimes

In order to understand how ground thermal regimes might change following disturbance, measurements of several thermal parameters were made at disturbed sites as well as at nearby undisturbed locations, which were generally within a few metres of one another. Soil samples were also taken to provide other relevant data. Samples were weighed in the field and, upon the return to the university, were analyzed for moisture content, grain size, specific gravity and bulk density. Although data were collected from several different areas, the focus was once again on the two primary sites.

3.4.1 Ground temperatures

Ground temperatures were measured at regular intervals throughout the summer of 1998 using a temperature probe. Recordings were made at the surface, at depths of 5, 10, 20, 25, and 30 cm, and thereafter at 10 cm intervals until the base of the active layer was reached. Additionally, a Brancker XL-800 data logger was set up at the abandoned airstrip site to make continuous measurements from July 11 to August 23 (Figure 19). It recorded air and surface temperatures, as well as ground temperatures in two areas (on the strip and off the strip) at depths of 10, 25 and 50 cm. Technical problems caused loss of data on three of the eight channels shortly after installation, but two of the channels were repaired and resumed recording on July 17. At the Gemini site, three "Onset StowAway" data loggers were

Figure 19. Study site at the abandoned Eureka airstrip. A Brancker data logger recorded air and ground temperatures at various depths. The area to the left is the disturbed surface of the strip, while the area to the right is in undisturbed terrain.

Figure 20. Thermal conductivity probe inserted horizontally into soil. The probe is heated and its temperature measured over time. How quickly the temperature of the probe rises is an indication of how quickly the soil transmits heat away.

installed on July 1 at the surface, and at depths of 25 and 38 cm (the base of the active layer on that date). These were removed on August 12.

3.4.2 Active layer

The development of the active layer over the 1998 summer season was monitored by periodically measuring its thickness. At all sites, this was determined by probing with a steel rod until refusal. Generally, five measurements were made and averaged. In order to examine the spatial variability of the active layer, several transects were set up. At the abandoned Eureka airstrip, three transects were made along lines corresponding to cross-sections in the 1973 GSC survey. One measurement of active layer depth was made every 5 m. At the Gemini well, one measurement of the active layer was made every 2 m along the survey lines across the airstrip, and every 5 m along the survey lines radiating from the wellhead.

There is a Circumpolar Active Layer Monitoring (CALM) site just south of the abandoned airstrip at Eureka and, in 1998, the author collected data from the site for the monitoring program. This involved taking measurements of the active layer at what was believed to be its maximum thickness for the season. Two probings of active layer thickness were made at 100 points in a 1 km^2 grid. These data are used to supplement the data collected at the abandoned airstrip. Measurements were made between August 6 and 13, 1998. The CALM site also has a frost tube, a water-filled tube anchored in the permafrost which contains a bead marker. The bead is checked the year after it is put in place and provides a measure of the actual depth to which the thaw progressed the previous fall. When the Eureka CALM site's frost tube was checked in the spring of 1999, it indicated that the 1998 thaw had progressed 2 cm deeper than when the measurements at the grid points were made in August 1998.

3.4.3 Thermal conductivity

The thermal conductivity of active layer soils was measured with a conductivity probe that was constructed based on information provided by Wechsler (1966) and by Slusarchuk and

Foulger (1973). The probe is a stainless steel sheath with a heater running its length and a thermistor placed at the halfway point. Power is supplied to the heater by a 12V gel cell battery. A multimeter measures the resistance of the thermistor, which is then converted to a temperature. When the battery is connected to the probe, heat is conducted through the probe to the surrounding soil. The temperature of the probe is measured at regular intervals. How quickly the probe temperature rises provides an indication of the ability of the surrounding soil to conduct heat away, in other words, it is a measure of the soil's thermal conductivity. The actual thermal conductivity is determined by the equation:

[2] $$k = \frac{q}{4\pi (T_2 - T_1)} \ln \left(\frac{t_2}{t_1} \right)$$

where k = soil thermal conductivity

q = heat flux per unit length of probe

T_1, T_2 = temperature at times 1 and 2

t_1, t_2 = times 1 and 2

At the study sites, soil thermal conductivity was measured by inserting the probe horizontally into the wall of a pit at a depth of either 15 cm or 25 cm (Figure 20). The probe was allowed to equilibrate to the soil temperature for 20 minutes, after which the test was started. The battery was connected to the heater and the probe temperature was recorded every 30 seconds. Although the temperature rise of the probe generally leveled off after approximately 10 minutes, the total test times ranged from 15 to 20 minutes.

3.5 Climate warming

To determine how permafrost in the Eureka area will respond to a warmer climate, it is first necessary to estimate the predicted warming for the region. Data on future climate warming are based on projections from the Canadian Centre for Climate Modelling and Analysis (CCCMA). Two scenarios are examined. The first uses output from the Canadian Global

Coupled Model (CGCMI) which has both an atmospheric and an oceanic component (Boer et al. 2000). Monthly data is available for the period 1900 to 2100, as is daily data for a number of different time windows. Six of the model's grid cells which overlap the Fosheim Peninsula (79.78N-83.48N, 82.50W-90.00W) have mean monthly values which agree reasonably well with observed temperatures at Eureka between 1975 and 1995 (Figure 21). Mean daily temperatures from these cells were compared with those from the period 2040-2060 (corresponding to a doubling of CO_2 relative to 1975-1995). The temperature differences between the two periods were then added to actual mean values from the Eureka weather station record to arrive at an estimate of future Eureka temperatures. The model's grid cells are large (3.75° latitude by 3.75° longitude) and the number of cells used is small so it may not provide the best representation of a future climate. A second climate scenario is therefore examined. The values used are regional temperature increases based on the CCCMA's second generation general circulation model, which consists of the atmospheric component only of CGCMI (Figure 22). Once again, these values are added to actual mean

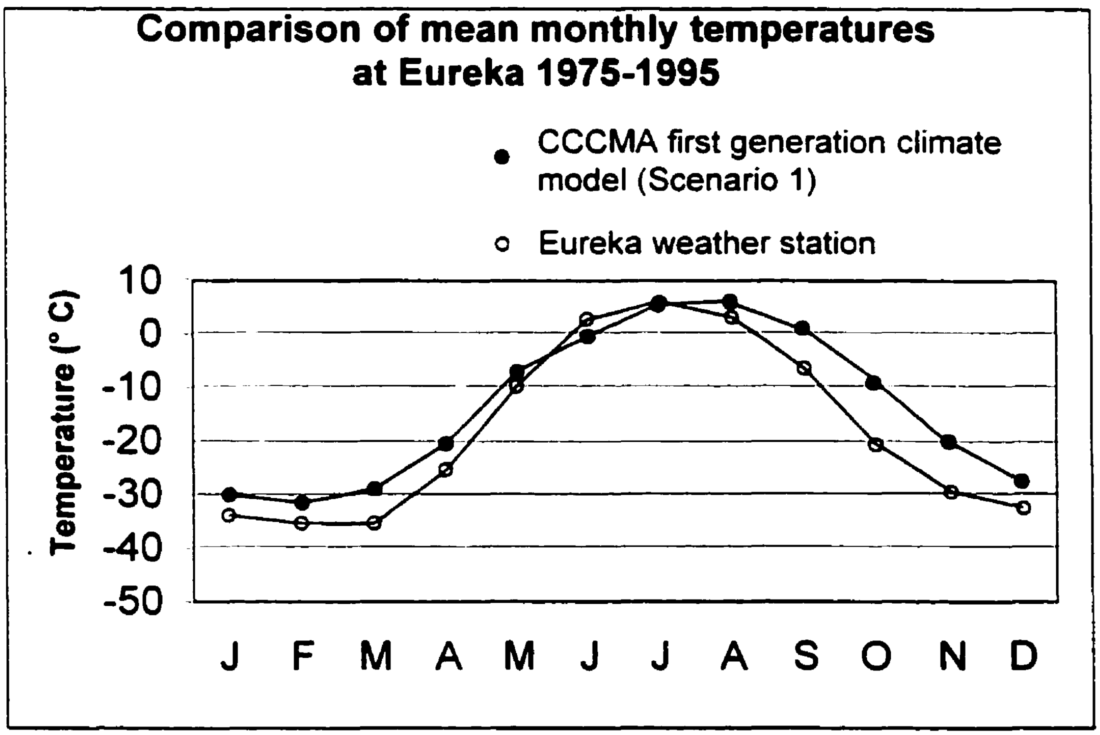

Figure 21. Comparison of temperatures from the CCCMA first generation general circulation model (Scenario 1) and actual values measured at the Eureka weather station between 1975 and 1995.

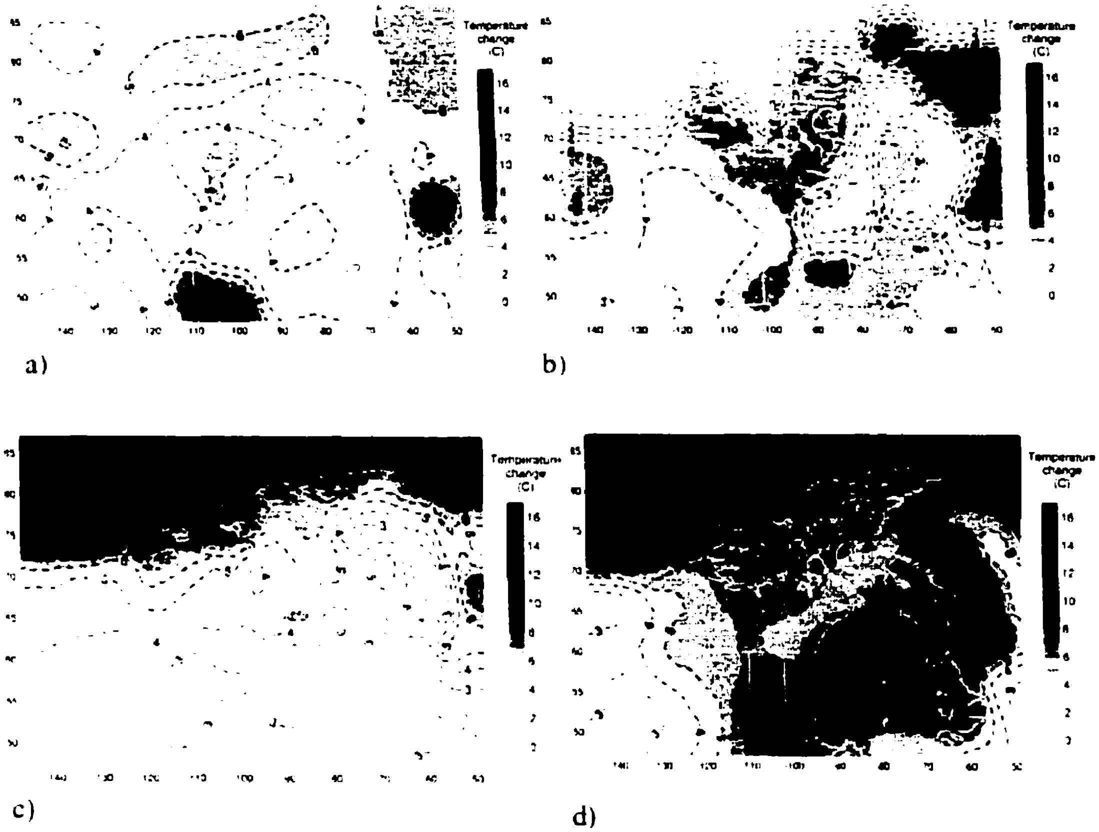

Figure 22. Projected change in mean temperatures based on the CCC GCM (1992) for a doubling of atmospheric CO_2 for a) spring, b) summer, c) autumn, and d) winter (from Maxwell 1997).

values from the weather station to estimate future temperatures.

3.6 Model of thaw

Having predicted what air temperatures can be expected in the Eureka area under climate warming, the next step is to see how these increased temperatures will affect the depth of thaw. The Stefan formula is used to calculate this depths. The formula is as follows:

$$[3] \qquad z = (2k_u T_s t / L)^{1/2},$$

where z = depth of thaw (m)

k_u = thermal conductivity of the unfrozen soil (W m^{-1} °C^{-1})

T_s = step change in surface temperature (°C)

t = time (s)

L = soil's volumetric latent heat of fusion (J m^{-3}).

In reality, a ground surface will not experience a step change in temperature over a thaw season, so T_s and t are replaced by the total number of thawing degree days (°C days) in the season. Thawing degree days provide a measure of the magnitude and duration of conditions above freezing. For instance, if the mean daily air temperature is 4°C for 3 days, the total number of thawing degree days for that period would be 12. The predicted air temperatures from the climate model described in the previous section provide the information needed to establish the number of thawing degree days. The other variables in Equation 3 are thermal properties of the soil and they will be constant for a given soil at a given time. The equation can now be re-written as:

$$[4] \qquad z = b\,(TDD)^{1/2},$$

where b = thermal constant

TDD = number of thawing degree days in the thaw season

Thermal constants for the soils in the study area are derived from data on thaw depths and thawing degree days that were measured during the 1998 season.

CHAPTER 4 - RESULTS: NATURE OF GROUND ICE AND PERMAFROST CONDITIONS

4.1 Introduction

In order to assess how sensitive permafrost terrain is to changes in surface conditions and how it will respond to those changes, three elements must be examined: the volume and stratigraphic distribution of ground ice, the type and extent of thermokarst features which can develop, and the nature of the ground thermal regime. This chapter examines the nature and range of these variables in the Eureka area. Section 4.2 documents the percentages of ground ice volumes in different types of subsurface units in the overall study area, including both the total volume of ground ice and the volume of excess ice. In section 4.3, existing thermokarst is measured to provide an indication of the magnitude of the features that can develop when ground ice thaws, and the rate at which this occurs. Section 4.4 examines the various elements that comprise the ground thermal regime and uses values from the 1998 season to arrive at thermal constants that are used in predictions of future thaw depths.

4.2 Ground ice volumes

In this section, mean volumes of ground ice are calculated for the four different types of subsurface units found in the Eureka area. The calculations are based on sample data collected from archives, previously published sources and air photo analysis. The level of confidence in the methods of collection ranges from high for samples from natural exposures, to medium for borehole samples, to low for those based on air photo analysis. The sample sites and methods of collection are shown in Figure 23. In considering ground ice contents, a caveat to consider is that ground ice has high spatial variability. Ice contents are dependent on a number of factors that can differ over short distances. For instance, the drainage and soil or rock type can govern the initial supply of water available for freezing, or relief and aspect can influence the snow cover and hence the ground temperatures. These and other site-specific factors will determine what the exact ground ice content will be at any one spot, so the values calculated here are based on averages for each subsurface unit.

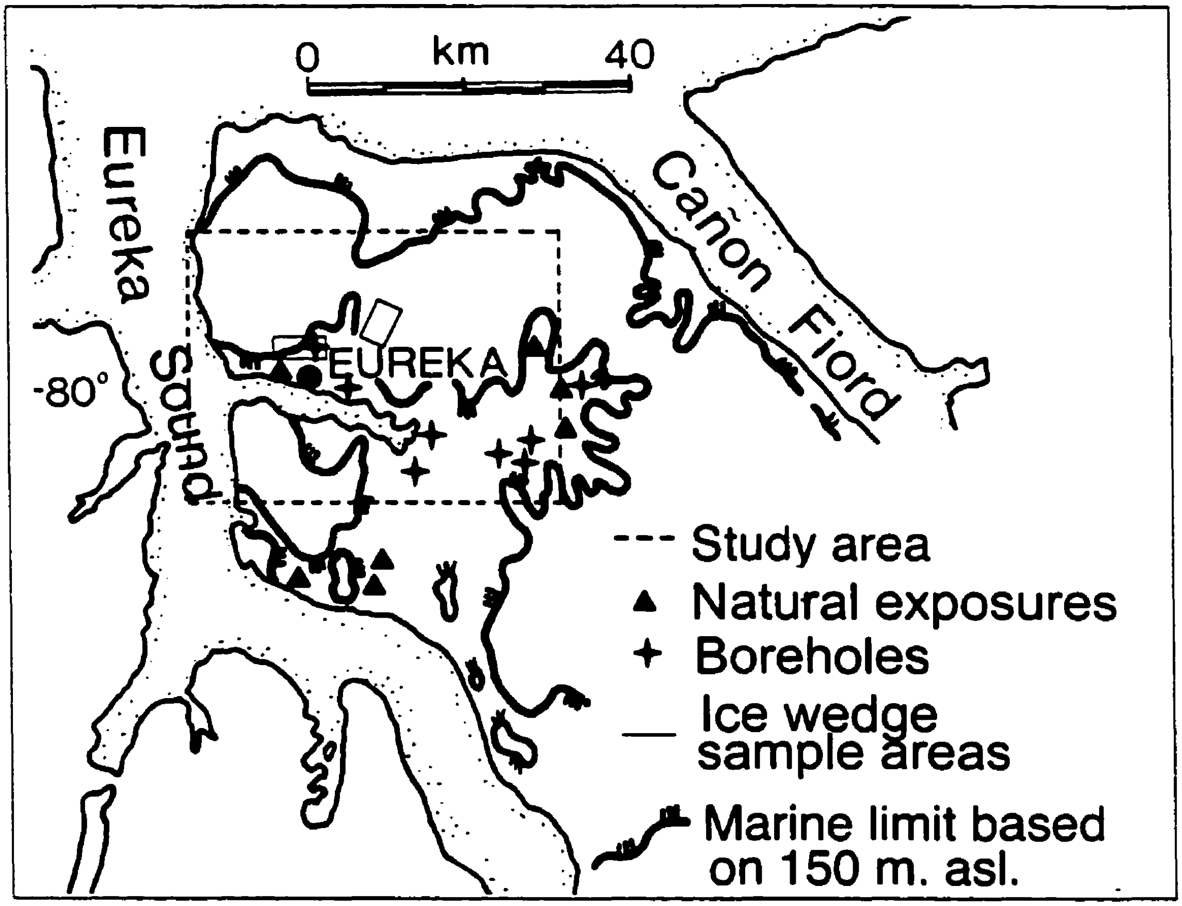

Figure 23. Map of study area showing sampling sites for natural exposures of massive ice and borehole drilling sites. Sample areas where ice wedge lengths were measured are also indicated. See text for additional details.

By definition, the active layer freezes and thaws each year, redistributing water and ice throughout the annual cycle. As a result, since the estimates of ground ice volume concern only the volume of perennially frozen materials, the average active layer thickness of 0.6 m for the Eureka area is subtracted from the selected 6.5 m depth so that the thickness of materials actually used in calculations is 5.9 m. Zones beneath large water bodies and steep bedrock slopes were assumed to have no ground ice or to contain amounts that are insignificant for the purposes of this study. Once they were excluded from the initial 1887 km^2, the total area where ground ice might occur was 1456.8 km^2. Since the thickness of frozen ground examined is 5.9 m, the total volume of frozen materials in the study area is therefore 8.6 km^3.

To begin with, the volumetric ice content due to pore and thin segregated lenses was calculated for areas below marine limit. Soil moisture measurements from natural exposures and boreholes at 35 sites yielded 72 values of gravimetric ice content. Although a number of visual estimates of ice content were made as well, they are not used here because visual estimation often understates the volume of ice in a sample (Pollard and French 1980). In order to obtain a better estimate of the subsidence that can be expected from the thaw of pore ice and thin segregated ice lenses, the moisture contents were converted to volumetric ice content values using the method developed by Pollard and French (1980). The volumetric ice contents thus obtained are plotted against depth (Figure 24) and polynomials up to the 6th order were tested for goodness-of-fit, generating a maximum value of $r^2 = 0.1265$. Since this does not provide a strong indication of correlation between ice content and depth, the samples' mean volume of 48.6% was assumed to adequately represent the entire profile. The scatter of the data points about the mean (standard deviation = 17.0) reflects the expected spatial variability of ground ice.

In areas above marine limit that are mantled by weathered bedrock, Pollard (in press) reports ice contents of 3-10%. Hodgson et al. (1991) estimate the ice content to be 5-50% within 1-1.5 m of the ground surface, and to be much lower or non-existent further down in the profile. For the purposes of this study, Hodgson et al.'s mean value of 27.5% is used for the

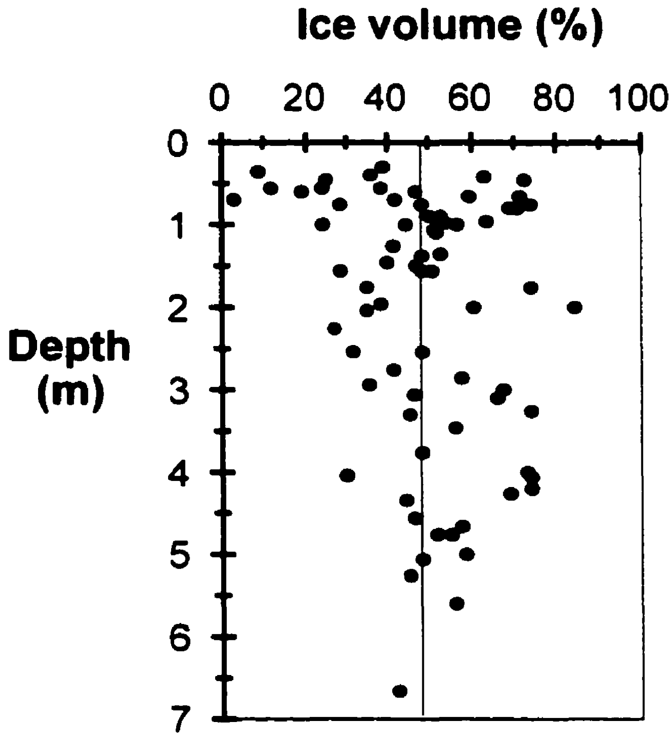

Figure 24. Ground ice volume vs depth in areas of pore ice and thin segregated ice lenses. The mean value of 48.6% is shown.

Figure 25. Natural exposure of massive ice in the headwall of a retrogressive thaw slump near Eureka. Approximately 3-6 m of sediment overlies this bed of massive ice which is approximately 2 m high and 15 m across.

top 1.5 m of the soil profile, and Pollard's mean value of 6.5% is used below 1.5 m.

On the Fosheim Peninsula, the mean depth of ice wedges is 323 cm (SD=87) and the mean wedge width is 146 cm (SD=56), giving a depth-to-width ratio of 2.2:1. This ratio is similar to ones found by Harry et al. (1985) in the Yukon Coastal Plain (2.6:1) and by Brown (1967) in Alaska (2:1). Two sample sites near Eureka were selected for measurement of ice wedge lengths from air photographs, one with a high density of ice wedges (NAPL A30860-173, scale 1:1860) and the other with a lower density (NAPL 30860-164, scale 1:1984). Using Equation [1], the percentage ice volumes were calculated to be 3.5% in areas of high density wedges and 1.8% where the density of wedges was low.

Measurements from samples taken at 73 natural exposures of massive ice on the Fosheim Peninsula between 1990 and 1995 indicate a mean ice content of 88.5% (SD=13.5%) for shallow (<6 m) massive ice. The top of massive ice beds as reported by Hodgson and Nixon (1998), Pollard (1991) and Robinson (1994) typically varies between 1 and 6 m on the Fosheim Peninsula (Figure 25), so the mean depth of 3.5 m is used. Using the ice content for sediment above massive ice calculated earlier and the volumetric ice content of massive ice itself, the top 5.9 m of permafrost in areas underlain by shallow massive ice is calculated to contain 69.0% ice by volume.

Areal coverage and the percentage of ground ice volume for the different subsurface units are summarized in Table 1. The highest ice volume (69.0%) is, as expected, in areas underlain by shallow massive ice. Pore ice and thin segregated ice lenses comprise 48.6% by volume of frozen materials below marine limit, while in areas of bedrock mantle above marine limit, they account for 9.7%. The lowest ice volume is associated with wedge ice; it accounts for 3.5% of the volume of frozen ground in areas of high density wedges, and 1.8% of volume in areas of low density. Ground ice in all its forms comprises 30.8% of the upper 5.9 m of permafrost in the study region. This is lower than the value of 53% found by Hodgson and Nixon (1998), but they intentionally sampled in areas known to have high ground ice contents.

Table 1. Absolute value and percentage of ground ice, by subsurface unit.

	Area (km^2)	Frozen materials (km^3)	Ice volume (km^3)	Ice content (%)
Massive ice	44.0	0.23	0.179	69.0
Pore/segregated ice lenses	702.1	4.14	1.970	48.6
Bedrock mantle	710.7	4.19	0.407	9.7
Ice wedges				
High density	138.3 [1]	0.82 [1]	0.028	3.5
Low density	563.8 [1]	3.32 [1]	0.060	1.8
Total	1456.8	8.56	2.644	----

[1] Not included in total since ice wedges and pore/segregated ice lenses occur in same subsurface units.

Table 2 Percentage by ground ice type, and amount of excess ice.

	Ice volume (km^3)	Percentage of total ice (%)	Excess ice (% of subsurface unit)
Massive ice	0.179	6.8	61.1
Pore/segregated ice lenses	1.970	74.5	29.9
Bedrock mantle	0.407	15.4	0.0
Ice wedges			
High density	0.028	1.0	33.0 [1]
Low density	0.060	2.3	31.5 [1]
Total	2.644	100.0	----

[1] Includes the 29.9% due to pore ice and segregated ice lenses since they occur in the same subsurface units as ice wedges.

The contribution of the different ice types to the total ice volume is shown in Table 2. Pore ice and thin segregated ice lenses above and below marine limit comprise 89.9% of the total, while massive ice accounts for 6.8%, and wedge ice for 3.3%. The values for excess ice represent how much volume would be lost if the ice were to melt, since the resulting water is that which is in excess of what can be contained in the soil voids. In areas of pore ice and thin segregated ice lenses only, the value for excess ice is 29.9%. This value is in the medium range for excess ice. Although thaw of the entire soil column is unlikely, if all 5.9 m of the permafrost under consideration were to thaw, this would mean that the ground surface could subside by up to 1.8 m. When both low and high density ice wedge polygons are considered along with the pore and segregated ice lenses, excess ice accounts for 31.5 to 33% of the frozen materials over the entire subsurface unit. Greater subsidence would occur due to the higher excess ice content of the subsurface unit, however it would be concentrated over the ice wedges themselves. Although ice wedges normally contain some sediment which washes into the thermal contraction cracks when water trickles into them, they are assumed to be pure ice for the purposes of this approximation of ground ice volume. It would be speculative to estimate the exact amount of subsidence that would occur over the wedges, although theoretically, it could be as much as the entire depth under consideration: 5.9 m. In subsurface units where massive ice is present, excess ice values are high, with 61.1% of the ice being considered excess. This represents a potential ground subsidence of 3.6 m. If the excess ice values for each of the different subsurface units are weighted by area, excess ice comprises 57.2% of the total ice volume, or 17.7% of the total volume of frozen materials in the study area.

4.3 Thermokarst

The values for excess ice mentioned above provide an indication of the theoretical potential for ground subsidence. The geomorphologic response to a disturbance, however, is not limited to simple subsidence. An examination of past thermokarst activity at both the primary study sites and other, secondary sites offers a more complete view of what kind of terrain response to expect.

Figure 26. Vegetation surrounding a tundra pond on the old Eureka airstrip.

4.3.1 Abandoned airstrip at Eureka

Close to a half century after the abandonment of the airstrip at Eureka, it still shows evidence of the disturbance caused by its construction and use. It is clearly distinguishable on air photographs (see Figure 13), primarily due to differences in ice wedge troughs and vegetation on and off the airstrip. Depressions above ice-wedge troughs on the strip are wider than in the adjacent, undisturbed terrain and are often water-filled. The immediate area surrounding these depressions is generally quite lush (Figure 26), consisting mainly of grasses, including cottongrass (*Eriophorum spp.*). Other plant species -- primarily Arctic willow (*Salix arctica*) and mountain avens (*Dryas integrifolia*) -- are found both on and off the strip, but coverage tends to be about 30% sparser in the disturbed areas.

Three profiles of the old airstrip at Eureka were surveyed in 1998, replicating those made by the Geological Survey of Canada in 1973 (Hodgson and Nixon 1998) (Figure 27). Much of the observed response to disturbance involves widespread simple subsidence due to the melting of ground ice. The 1973 survey found that the ground surface on the strip itself had

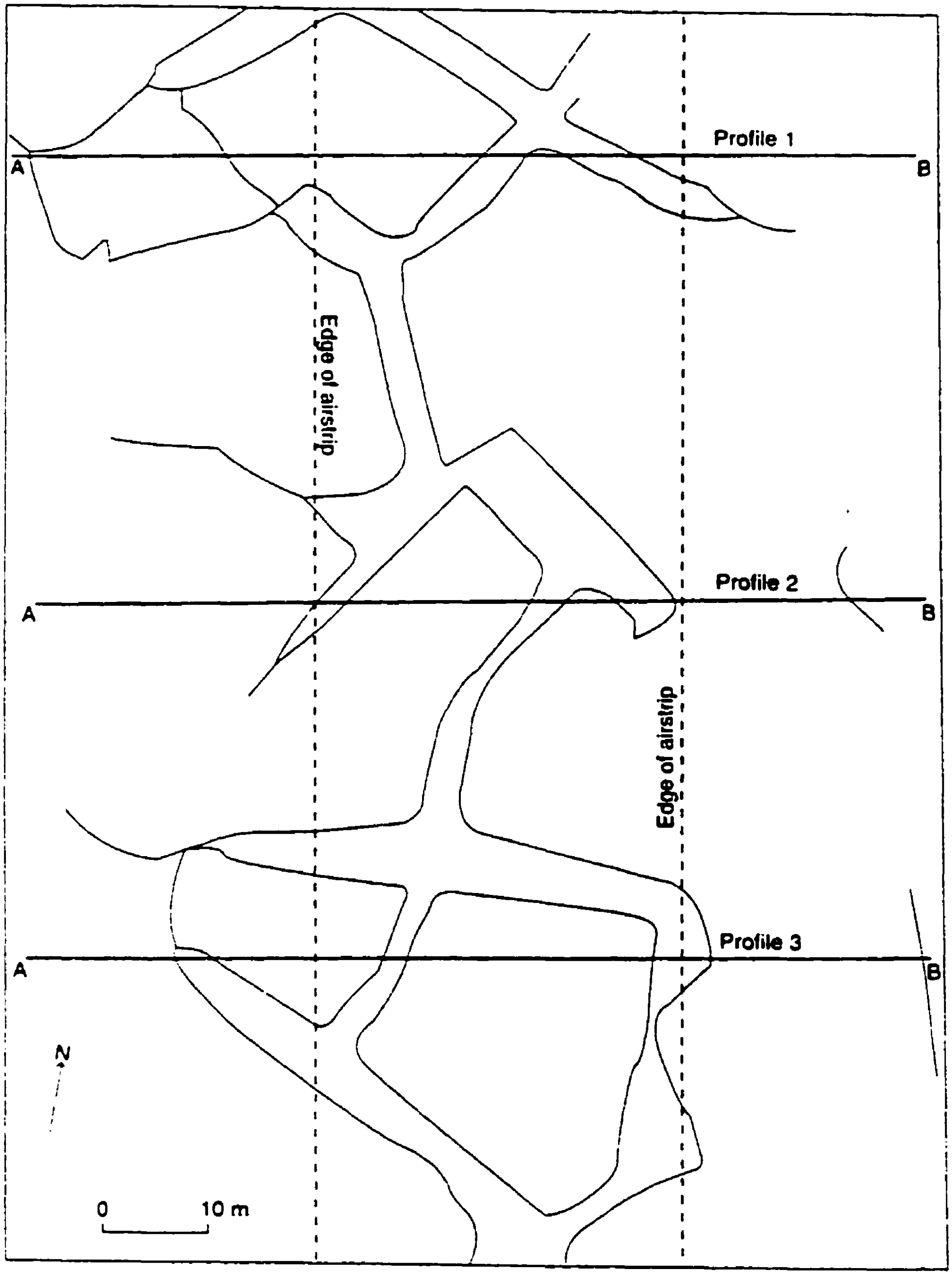

Figure 27a. Plan of the south end of the abandoned Eureka airstrip showing the location of the surveyed profiles (from Hodgson and Nixon 1998).

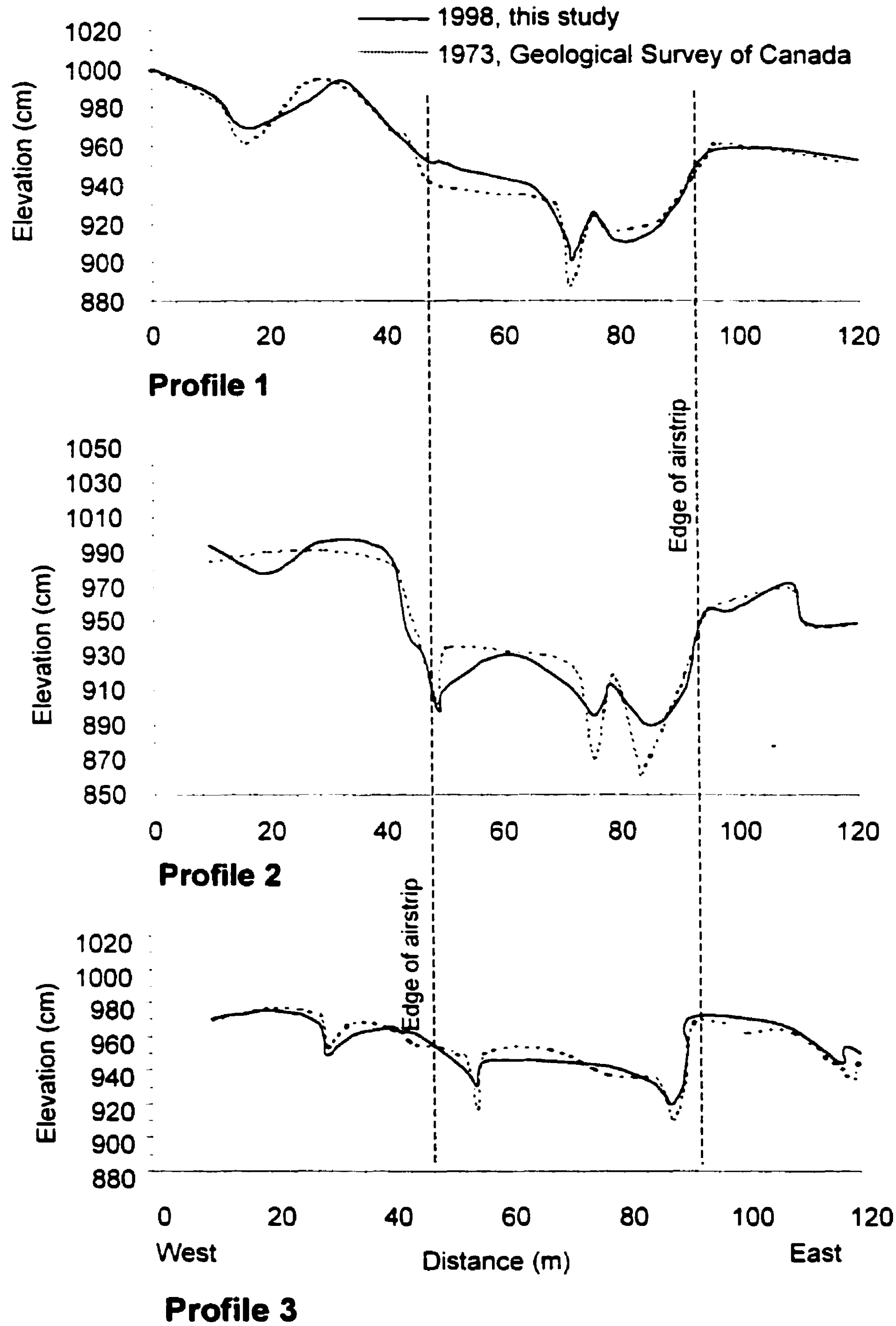

Figure 27b. Profiles across the abandoned Eureka airstrip showing changes in surface elevation between 1973 and 1998.

subsided from 10 to 60 cm below adjacent undisturbed terrain (Hodgson and Nixon 1998). Since the excess ice content in areas which contain only pore ice and segregated lenses is calculated to be 29.9%, this suggests that between 33 and 201 cm of the original permafrost thawed in the period between the initial disturbance in 1947 and the 1973 survey. Differences in the amount of subsidence may be explained by site-specific features that affect the amount of heat being transferred into the ground, such as differences in water or snow accumulation. However, since 29.9% is an average ground ice value for the entire subsurface unit, the differences in subsidence may also be due to differences in the actual ground ice contents along the surveyed profiles.

Subsidence above ice wedges measured up to 120 cm in the 1973 survey. This is to be expected given the high excess ice content of ice wedges. However, if the maximum thaw was indeed 201 cm and the ice content of the wedges is 100% as this study assumes, then 201 cm of subsidence should have occurred, rather than only 120 cm. At first glance, this appears to confirm the notion that ice wedges do contain at least some sediment. One further element that must be taken into consideration in examining subsidence above ice wedges is brought up by the results of the airstrip survey done in 1998. The observations indicate that, from 1973 to 1998, the airstrip surface had subsided up to 10 additional cm in some locations, most notably in the vicinity of ice wedges, but the depressions immediately above the wedges were shallower than they were in 1973 (Figure 27b). The initial relief created by the greater subsidence over the ice wedges appears to have caused a general reworking of adjacent materials down into the depressions above the wedges, resulting in a smoother profile than existed in 1973. It is possible that some of this reworking had already occurred before the 1973 survey, which is why the subsidence was only 120 cm. It is difficult say if this slope movement has ceased completely, but the smoothing of the profiles does indicate that the site is on its way to physical stability.

Active layer depths were measured along the survey profiles and at several nearby sites in both undisturbed and disturbed terrain. The mean active layer depth off the airstrip is 47.8 cm, which is significantly different from the mean of 53.5 cm on the airstrip. This difference in the depth of thaw appears to be due to the slightly higher moisture contents found in the disturbed terrain on the airstrip, since soils with higher moisture contents conduct heat better. This is supported by measurements with the thermal conductivity probe, which show that the disturbed terrain on the airstrip had a thermal conductivity of 1.66 W/m °C, which is over three times higher than the 0.49 W/m °C recorded in undisturbed terrain.

Between 1947 and 1998, there was no major changes in the climate of the Eureka area, so the melt of the permafrost appears to be due to the removal of part of the active layer and to an increase in the soil thermal regime, which itself results from the interplay of several variables. The rolling and compaction of the airstrip during construction would have compressed the soil, increasing its thermal conductivity. These activities, together with any grading or scraping of the surface would have killed or removed the vegetation, which normally shields the ground surface from warm summer air temperatures. The albedo of the surface presumably increased as well, meaning that more solar radiation was absorbed. Finally, water most probably played a dual role following the start of permafrost thaw. As the permafrost began to melt, the moisture content of the active layer directly above it would have risen, once again increasing the soil's thermal conductivity. Additionally, when the ground started to subside, water began to pond in ice wedge troughs and most likely in other topographic lows. This would have increased the mean annual surface temperature of the soil at the bottom of the ponds.

4.3.2 Gemini E-10 well site

Exploratory drilling work was conducted at Panarctic's Gemini E-10 well site during the winter of 1972-73. The effects of the disturbance are most evident in the area surrounding the wellhead, in what appears to have been the area used as a sump for the drilling fluids. At this particular well site, the fluids were dumped onto the ground surface and were contained by snow dams. In March 1973, the drilling fluid leaked into a nearby stream and thaw of ground ice is suspected as having contributed to the failure of the sump (Hodgson and Nixon 1998). During fieldwork in 1998, three profiles were surveyed across the airstrip and adjacent road, and four more radiating out from the wellhead (Figure 28). The most

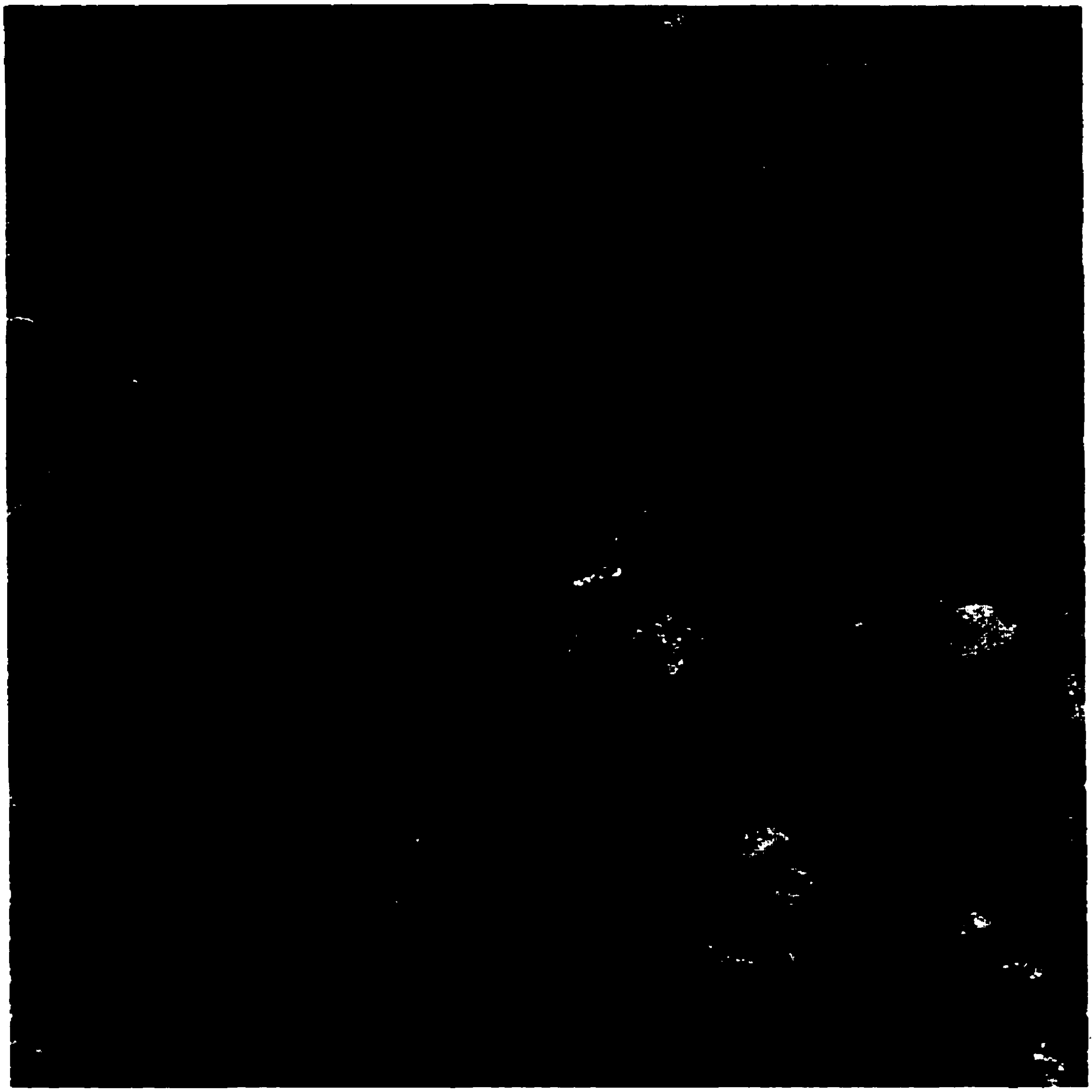

Figure 28. Aerial photo of Gemini wellsite showing location of survey lines.

Figure 29. One of the many depressions near the wellhead at the Gemini wellsite. This depression was likely caused by the melting of permafrost with an ice content greater than 30%.

obvious thermokarst features are large depressions surrounding the wellhead ranging from approximately 7 to 80 m wide, many of which contain standing water (Figure 29). Subsidence within these depressions is from 15 cm to 3.15 m. Using the excess ice content calculated for areas containing pore ice and segregated ice lenses of 29.9%, this corresponds to thaw of between 50 cm and 10.5 m of permafrost. Much of this thaw would be for similar reasons to those mentioned for the Eureka airstrip: removal of sediment and vegetation, and changes in the ground thermal regime. The surface sump obviously played a role in altering the thermal regime, since the most obvious thermokarst features are in the area where the sump appears to have been located. Thermal conductivities at the Gemini site were 3.0 W/m °C for the disturbed site and 4.7 W/m °C for the undisturbed site. The difference in thermal conductivity between undisturbed and disturbed areas is not as great as at the Eureka site, therefore changes to the moisture content of the soil and the ponding of water appear to have been of greater importance than thermal conductivity itself in effecting change at the Gemini wellsite. Nevertheless, it is unlikely that disturbance caused enough changes in the vegetation or albedo at the ground surface, or in the thermal conductivity or moisture content of the soil column to have thaw penetrate more than 10 m. This suggests that the ground ice content for the areas where the deepest depressions are found was locally much higher than 29.9%. Active layer depths within the broader depressions are generally greater (although not significantly) than for undisturbed terrain, which has an average active layer depth of 62 cm in August. However, the active layer can be as deep as 1.22 m in the depressions with standing water. Some of the narrower, dry depressions have the shallowest active layers of any terrain at the Gemini site (46 cm in August), possibly due to the persistence of snow within them in the spring which would insulate them from warmer summer air temperatures.

Disturbance along the airstrip profiles is less dramatic. The soils on the strip contain more sand and gravel than those surrounding the wellhead and since they are therefore better drained, they likely have a lower ground ice content. Overall ground subsidence is approximately 10 cm on the airstrip compared to the surrounding undisturbed terrain. This increases by a further 5 to 10 cm above ice wedges on the airstrip itself and in the wheel ruts of the road beside the airstrip where compaction and changes to the albedo and vegetation were greater. Active layer depths are fairly constant across the profiles with a mean depth of 52 cm in August. The one exception to this is the area surrounding a pond at the west end of profile 2, where the active layer deepens to 77 cm in August.

4.3.3 Other thermokarst sites

In addition to the two primary study sites -- the abandoned Eureka airstrip and the Gemini well site -- less detailed observations of thermokarst features were made at a number of other locations in the Eureka area. Some of these features are obviously the result of anthropogenic activities, some of natural processes, while others appear to be caused by a combination of the two types of disturbance.

The most intense land use in Eureka occurs on the airstrip, the roads, and in the areas surrounding the various buildings, all of which see heavy vehicular traffic. This results in compaction of the soil, killing of vegetation and changes to the surface albedo, all of which can raise the ground thermal regime substantially. An illustration of how dramatically soil temperatures can be affected is provided by an example from August 21 when a disturbed site next to the weather station had a ground surface temperature that was 10.8°C warmer than at the abandoned airstrip, despite the fact that the air temperature was 1.1°C cooler. The active layer at this site was difficult to measure due to the presence of gravel and cobbles, but other, similarly disturbed sites close to Eureka had active layers greater than 1 m. This is twice the mean thickness of 53.5 cm found at the disturbed location on the abandoned airstrip. Thaw of 1 m in an area with a mean excess ice content of 29.9% would result in an initial ground subsidence of 29.9 cm, while subsidence could be up to 1 m above ice wedges with an excess ice content of 100%. These are only initial values and even more of the permafrost would thaw in subsequent years, since the lowering of the ground surface means that the top of the permafrost would again be subject to thaw. It is difficult to assess the extent of thermokarst in these most highly disturbed areas near Eureka since any depressions or surface irregularities in high traffic areas are regularly filled with sand and gravel. However, a number of formerly disturbed areas that are no longer in use show the classic topography of thermokarst terrain, with numerous depressions (Figure 30). A survey of an old dumpsite just to the northwest of Eureka's current airstrip showed that these depressions can be up to 1.8 m deep. The natural drainage of such areas has been disrupted and runoff tends to be directed along ice wedge troughs, leading to thermal erosion of the wedges. Vegetative patterns, too, have been altered, as most of the disturbed area has very sparse vegetation except for in the immediate vicinity of tundra ponds, which are surrounded by thick grasses.

Another form of thermokarst seen near Eureka is gullying. One region where it is particularly evident is in the area south of the current airstrip on the slope leading down to Slidre Fiord (Figure 31). Much of the gullying here is due to thermal erosion as a result of natural drainage, however in certain places this is compounded by runoff from the water systems of buildings in Eureka. A majority of the gullies appear to originate along ice wedge troughs, although they do not continue to follow the troughs further downslope. Profiles

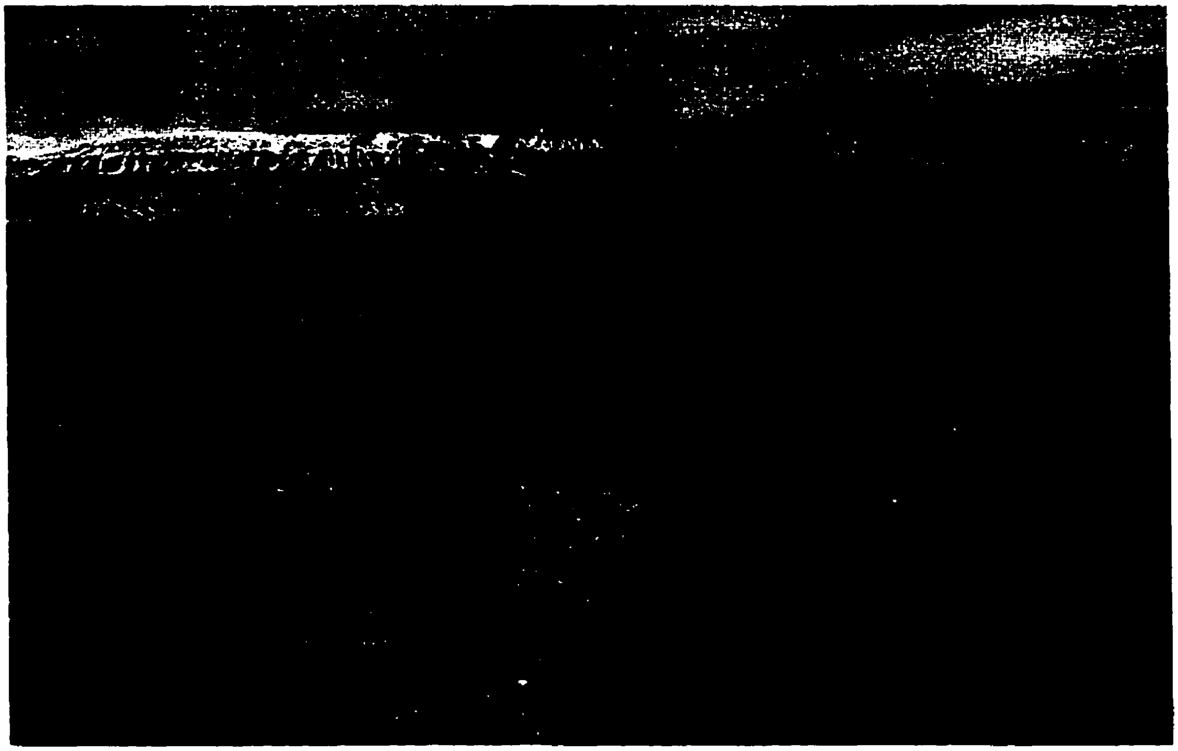

Figure 30. Thermokarst terrain to the northeast of Eureka's current airstrip.

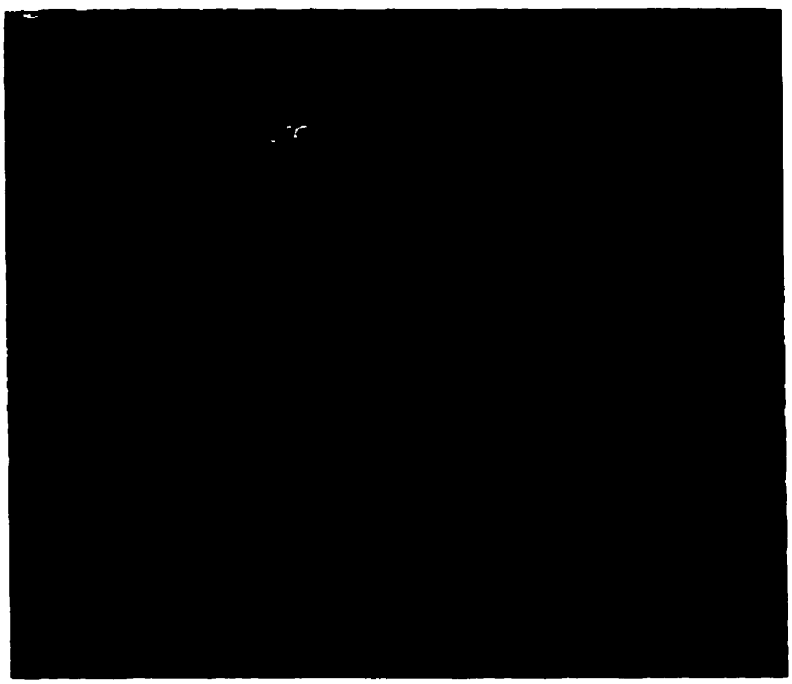

Figure 31. Significant gullying along the slope south of the Eureka airstrip. Many of the gullies originate along ice wedge troughs.

surveyed across the slope show that the gullies are approximately 1.5 to 2 m deep. Active layer depths are quite variable and ranged from 25 to 85 cm in the last week of July. The deepest active layers are near the outlet of the buildings' water systems where the moisture likely raises the soil thermal conductivities. The shallowest active layers tend to be in the centers of the gullies. This may be because, as at the Gemini wellsite, snow is more likely to accumulate in these depressions and to persist for a longer time in the spring.

Active layer detachment slides are common thermokarst features on the Fosheim Peninsula. The slides occur when pore water pressure builds up at the base of the active layer, usually when the top of the permafrost melts rapidly due to an especially warm period, or following heavy precipitation. Lewkowicz observed that the frequency of occurrence in the Eureka area ranges from 0.2 to 75 slides/year in the period 1959-1988 (Lewkowicz 1990). During the latter half of July 1998, at least two dozen active layer detachment slides were observed on slopes in the immediate Eureka area, primarily between the weather station and the airstrip, and to the southeast of the strip. The primary trigger for the active layer detachment slides appears to have been a sharp temperature increase in the third week of July. Most of these slides were approximately 8-15 m wide and 25-50 m long. Active layer detachment slides are significant in that the entire active layer is removed, subjecting the underlying permafrost to melt. How much of that permafrost melts depends on the time of the slide in relation to the end of the thaw season, however, at least 60 cm of thaw can be expected the following summer, given the average active layer depth for the area. If the mean excess ice content of 29.9% is assumed, this would engender subsidence of the ground surface of 18 cm, although this could be even greater if an ice wedge or massive ice is exposed by the active layer detachment slide. The occurrence of active layer detachment slides on any particular slope does not necessarily follow every warm spell or rainstorm, since slopes that have recently failed achieve a new equilibrium. Lewkowicz estimates that it takes at least 6 years, and more commonly 15 years, before a slope will fail again (Lewkowicz 1990).

Retrogressive thaw slumps develop when a particularly ice-rich zone or a body of massive ice is exposed and begins to thaw. As the ground ice melts, the overburden of soil slides down the icy headwall or collapses at its base and, as melt progresses, the headwall retreats, leaving a crescent-shaped scar. Such slumps occur regularly around Eureka and throughout the Fosheim Peninsula and over 150 stabilized slumps were identified by aerial reconnaissance in 1994 (Pollard in press). In 1998, only one retrogressive thaw slump was active in the immediate vicinity of Eureka. The slump, on the west side of a stream known as Sapper's Creek, was approximately 20 m wide and was located near the top of a 30 m high slope. It appears to have been initiated by the exposure of a 4-5 m thick body of massive ice halfway up the slope. The exposure was recent, as there was very little retreat of the headwall and most of the debris had accumulated in the stream at the base of the slope itself. Unfortunately, this slump was discovered near the end of the field season so its development could not be followed. Another retrogressive thaw slump, this one stabilized, is located just north of the current airstrip in Eureka. It is multi-lobed and so appears to result from the melt of more than one body of massive ice. The slump is approximately 5 m deep and affects an area 70 m wide and 40 m long. Previous research in the area shows that retrogressive thaw slumps can vary from 10 to >90 m in width and from 10 to 210 m in length (Barry 1992, Robinson 1993). In his 1993 study, Robinson found several individual slumps which covered more than 5000^{2}m and he noted that 12% of his 80 km^2 study area had been affected by thermokarst, primarily in the form of retrogressive thaw slumping (Robinson 1993).

4.4 Ground thermal regimes

During the 1998 field season, three soil properties relating to the ground thermal regime were measured at a number of sites: variations in ground temperatures with depth, active layer depths, and thermal conductivities. These properties provide an indication of how heat travels through the soil column, and it was hoped to use them to estimate how it might do so under the different surface conditions that would prevail under a warming climate. To gauge the expected changes to the landscape that would arise when permafrost melts, it is essential to know what the depth of seasonal thaw will be. Stefan's formula is used to estimate future thaw depths and, as explained in Section 3.6 (equation 4), two input variables are needed for Stefan's formula: the number of thawing degree days (TDD) at the ground surface and a thermal constant for the soils in questions. The following two sections describe how these variables are derived from the ground surface temperatures and the thaw depths recorded at Eureka. Soil thermal conductivity values are incorporated into the thermal constant used in the formula so the actual measured values were not used except to aid in interpretation of variations in thaw depths.

4.4.1 Thawing degree days in 1998

The first input variable needed for Stefan's formula is the number of thawing degree days (TDD) at the ground surface. The thaw season is considered to begin once temperatures rise above 0°C on four consecutive days, and is considered to end after three consecutive days below freezing. Unfortunately, the ground temperatures measured in 1998 at Eureka's abandoned airstrip and at the Gemini well site did not encompass the entire thaw season. To overcome this, the number of thawing degree days at the ground surface had to first be extrapolated from the Eureka weather station air temperature records.

Figure 32 shows the air temperatures measured at the Eureka weather station for the 1998 thaw season. The thaw season (for air temperatures) began on Julian day 151 (May 31) and ended on Julian day 250 (September 7). Table 3 provides an indication of how the 1998 temperatures compared with the average for the entire period of record at the weather station. In 1998, June, July, August and September were all warmer than the norm and, as a result, the thaw season was 19% longer than usual (100 days versus an average of 87 for 1948-1997), and there were 33% more thawing degree days than usual (486 TDD rather than the mean of 343 TDD).

Power laws were fitted to both sets of measured temperatures -- air temperature at the weather station and ground temperature at the study sites -- and Figure 33 shows that the correlation between the two sets of temperatures was high, producing an R^2 value of 0.85 for the abandoned airstrip and 0.83 for the Gemini site. The weather station temperatures were then input into the equations generated by the power laws to calculate ground surface temperatures for the two primary study sites for the entire thaw season. Figure 34 shows the air and ground temperatures for the sites from Julian day 151 (May 31) to Julian day 250

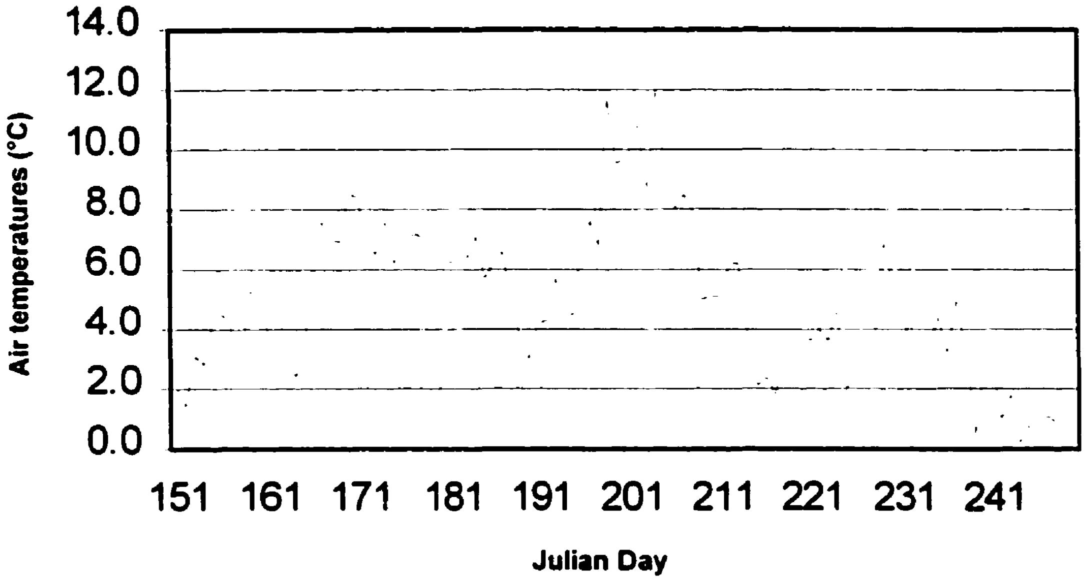

Figure 32. Air temperatures at the Eureka weather station during the 1998 thaw season which began on May 31 and ended September 7.

Table 3. 1998 temperatures at the Eureka weather station compared with the average temperatures for the entire period of record.

	1948-1997	1998
Mean May temp.	-10.6	-10.5
Mean June temp.	2.3	5.4
Mean July temp.	5.6	6.9
Mean Aug. temp.	3.0	3.4
Mean Sept. temp	-7.7	-0.8
Thawing degree days	343	486
Length of thaw season	87	100
Start of thaw season	Julian day 158 (June 7)	Julian day 151 (May 31)
End of thaw season	Julian day 244 (Sept. 1)	Julian day 250 (Sept. 7)

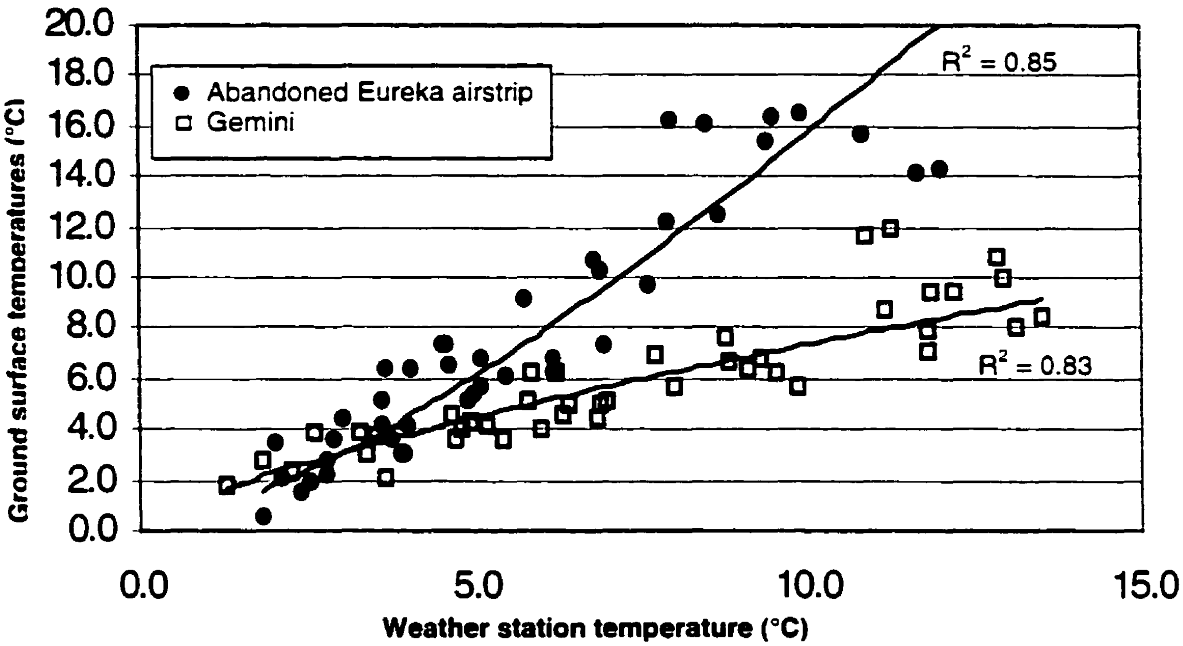

Figure 33. Correlation of of air temperatures at the Eureka weather station with ground surface temperatures at the two primary study sites.

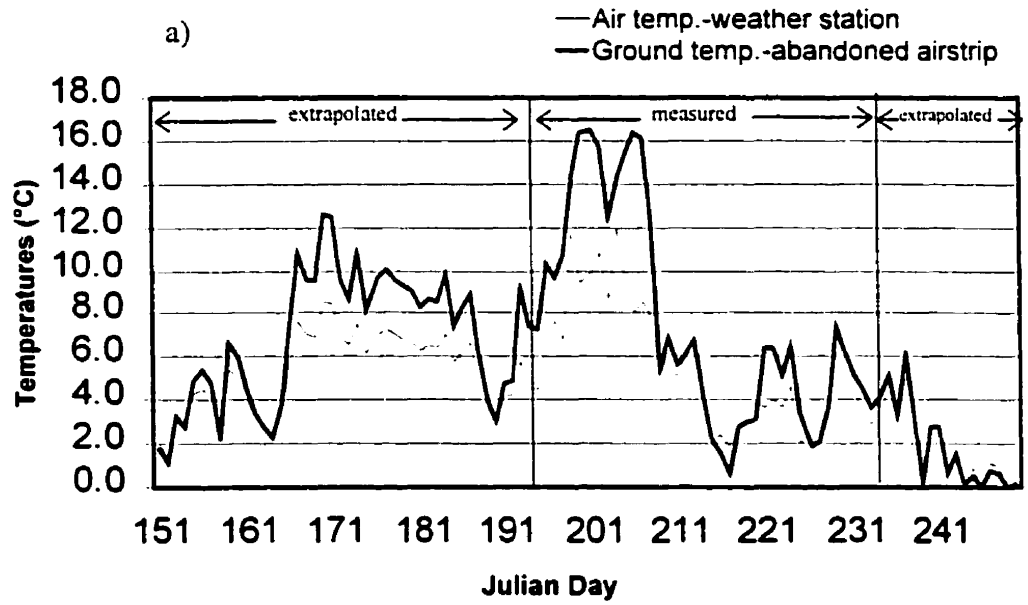

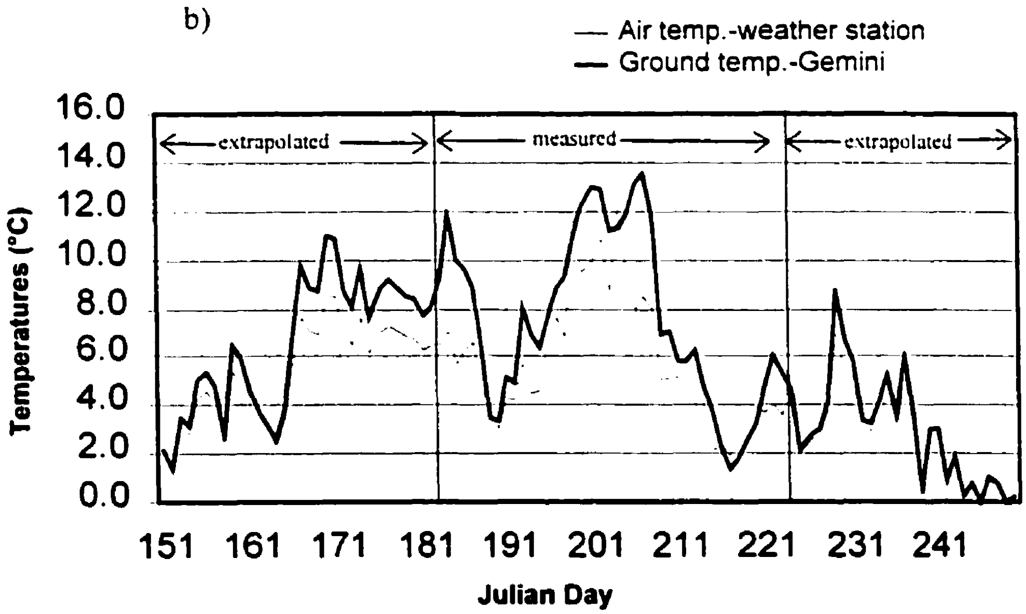

Figure 34. A comparison of air temperatures at the Eureka weather station with the ground surface temperature at a) the abandoned Eureka airstrip and b) the Gemini wellsite.

(September 7) and indicates what portion of the ground thaw season was measured and what portion was extrapolated from air temperatures. This method assumes that air and surface temperatures rise above freezing at the same time, even though ground temperatures are generally slightly warmer. As a result, thawing degree days at the ground surface may be slightly underestimated, but if one assumes that ground temperatures are on average 2°C warmer than air temperatures, then the error is less than 2% over the thaw season. Using these extrapolated ground surface temperatures, the total number of thawing degree days at the ground surface was calculated to be 633 TDD at the abandoned airstrip and 597 at Gemini, compared with 486 TDD at the Eureka weather station. The higher number of thawing degree days at the study sites is a reflection of the fact that ground temperatures are usually warmer than air temperatures, and that locations on the Fosheim Peninsula which are further inland than Eureka often see warmer temperatures.

4.4.2 Thermal constants

In order to use Stefan's formula to estimate the depth of thaw in a soil, the second input variable needed is a thermal constant for that soil. For each of the study sites, thermal constants are calculated from 1998 thaw depths and the number of cumulative thawing degree days for the date on which the measurements were taken. Table 4 shows thaw depths at different times of the season, the number of cumulative thawing degree days on that date, and thermal constants for a number of undisturbed and disturbed sites in the Eureka area, including the abandoned airstrip and the Gemini well site. In the spring of 1999, a frost tube at the Circumpolar Active Layer Monitoring site showed that the maximum thaw depth was 2 cm deeper than the final measurement taken there in 1998. This value was therefore added to the final 1998 measurement at all other sites to get an estimate of all other maximum thaw depths. Table 4 shows that in general, the more disturbed soils have higher thermal constants, reflecting the variations in moisture content, thermal conductivity, and bulk density of the soils. This is supported by the thermal conductivity measurements made with the probe, which showed that at the abandoned airstrip for instance, the disturbed site had a thermal conductivity of 1.66 W/m °C versus 0.49 W/m °C at the undisturbed site. At each individual study site, the thermal constant generally decreases throughout the season, by about 0.5.

Table 4. Thaw depths throughout the summer of 1998, including the number of cumulative thawing degree days on that date, and thermal constants for a number of undisturbed and disturbed sites in the Eureka area. See text for details.

Site	Thaw depth (cm)	TDD	Thermal constant	Condition
G1 (July 1)	45.0	208	3.1	Disturbed
G1 (Aug. 12)	64.0	522	2.8	
G1 (Sept. 7)	66.0 *	597	2.7	
G2 (July 1)	50.0	208	3.5	Undisturbed
E2 (July 11)	48.0	286	2.8	Undisturbed
E2 (July 17)	50.0	341	2.7	
E2 (July 31)	54.0	514	2.4	
E2 (Aug. 7)	53.5	535	2.3	
E2 (Aug. 13)	55.5	566	2.3	
E2 (Aug. 23)	54.5	610	2.2	
E2 (Sept. 7)	56.5 *	633	2.2	
Center (Aug. 7)	58.0	535	2.5	Slightly disturbed
Center (Aug. 13)	57.5	566	2.4	
Center (Aug. 23)	59.0	610	2.4	
Center (Sept. 7)	61.0 *	633	2.4	
E3 (July 11)	50.0	286	3.0	Disturbed
E3 (July 31)	65.0	514	2.9	
E3 (Aug. 7)	65.0	535	2.8	
E3 (Aug. 13)	64.0	566	2.7	
E3 (Aug. 23)	62.0	610	2.5	
E3 (Sept. 7)	64.0 *	633	2.5	
CALM (July 3)	40.0	239	2.6	Undisturbed
CALM (July 31)	53.5	514	2.4	
CALM (Aug. 7)	50.5	535	2.2	
CALM (Aug. 11)	51.0	556	2.2	
CALM (Aug. 13)	51.5	566	2.2	
CALM (Aug.23)	50.5	610	2.0	
CALM (Sept. 7)	52.5 #	633	2.1	
E1 (Aug. 19)	67.5	593	2.8	Disturbed
E1 (Sept. 7)	69.5 *	633	2.8	
E7 (Aug. 21)	83.0	601	3.4	Undisturbed
E7 (Sept. 7)	85.0 *	633	3.4	
E8 (Aug. 21)	105.0	601	4.3	Disturbed
E8 (Sept. 7)	107.0 *	633	4.3	
E9 (Aug. 22)	53.5	605	2.2	Undisturbed
E9 (Sept. 7)	55.0 *	633	2.2	
E10 (Aug. 22)	47.0	605	1.9	Disturbed
E10 (Sept. 7)	49.0 *	633	1.9	

* estimated value based on frost tube data
# measured from frost tube in spring 1999

This is indicative of a decrease in thermal conductivity as runoff and especially evaporation progressively lower the moisture content in the thawed layer. The end-of-the-season constants therefore represent an integration of the moisture content values over the entire season. They range in value from 1.9 to 4.3 and represent the differing properties of the various soil types in the Eureka area.

CHAPTER 5 - RESULTS: RESPONSES TO CLIMATE WARMING

5.1 Introduction

Chapter 4 provided data on the nature of ground ice and thermokarst conditions in the Eureka area. Based on that data, this chapter examines how the permafrost terrain in the Eureka area is likely to change as a result of increased air temperatures associated with global warming. A three step process is employed, which is depicted graphically in Figure 35. First of all, it is necessary to predict what temperatures can be expected for the area under global warming. This is done in section 5.2, where two possible climate change scenarios for the Eureka area are developed. These scenarios are based on current air temperatures for Eureka, which are then supplemented with data from the Canadian Centre for Climate Modelling and Analysis (CCCMA). The second step is to examine how much of the permafrost will thaw as a result of the predicted warming, and this is detailed in section 5.3. To begin with, the air temperatures for the two possible climate scenarios are translated into ground temperatures using the same power laws developed in section 4.4.1 to correlate the air temperatures at the Eureka weather station with the ground temperatures at the primary study sites. With the ground surface temperatures in hand, the number of thawing degree days at the surface that can be expected under the two climate scenarios can be calculated. These thawing degree days then become inputs for Stefan's formula. The other input for the formula is a soil thermal constant, and a range of thermal constants is used here to simulate the varying soil types and states that could be expected. The output of Stefan's formula is a number of different possible thaw depths for each of the two climate scenarios. The final step in predicting landscape response to warming is to predict what thermokarst activity will be induced by these increased thaw depths. This is developed in section 5.4 and is based on the ground ice volumes and thermokarst features characteristic of the Eureka area.

5.2 Predicted air temperatures

To predict air temperatures for the Eureka area under global warming, the output of two models from the Canadian Centre for Climate Modelling and Analysis (CCCMA) were used. One of the models (Scenario 1) likely provides more accurate results in that it includes both

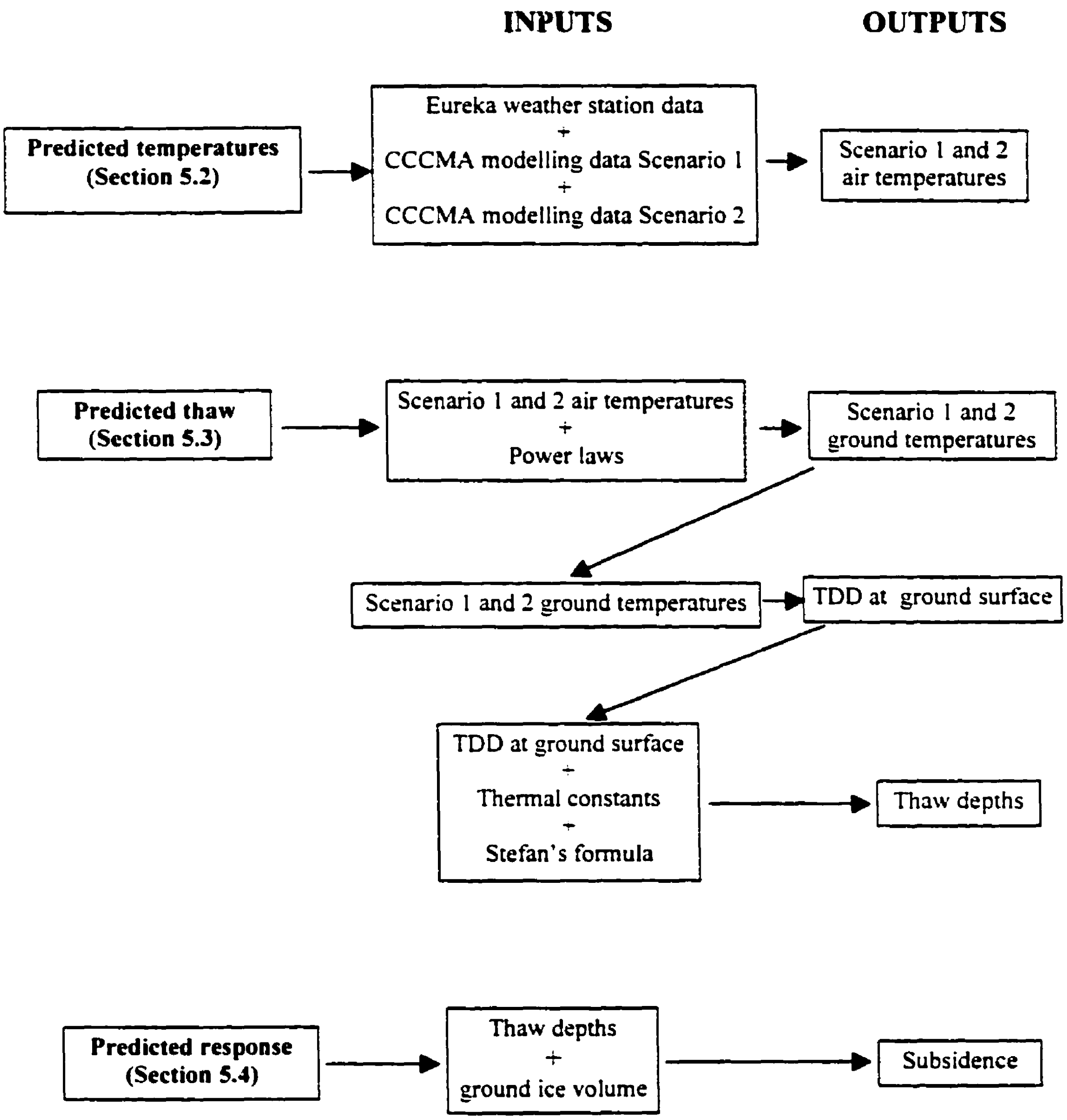

Figure 35. Three step process indicating how air temperatures are used to predict the response of permafrost terrain to warming.

Table 5. Predicted changes in mean monthly and annual air temperatures at the Eureka weather station under two different modelled climate warming scenarios.

	1948-1997 (°C)	Scenario 1 (°C)	Scenario 2 (°C)
January	-36.8	-31.6	-28.2
February	-38.2	-34.1	-29.6
March	-37.2	-32.8	-32.7
April	-27.5	-22.5	-22.9
May	-10.6	-8.2	-6.0
June	2.3	4.3	7.2
July	5.6	8.3	10.6
August	3.0	5.1	7.9
September	-7.7	-5.1	0.4
October	-22.0	-15.3	-14.1
November	-31.0	-21.0	-23.0
December	-34.9	-23.2	-26.2
Mean annual	-19.6	-14.7	-13.0
Thawing degree days	343	552	856
Length of thaw season	87	98	113
Start of thaw season	Julian day 158 (June 7)	Julian day 153 (June 2)	Julian day 150 (May 30)
End of thaw season	Julian day 244 (Sept. 1)	Julian 250 (Sept. 7)	Julian day 262 (Sept. 19)

an atmospheric and an oceanic component, however, its grid cells are large and only a small number of them can be considered representative of the Eureka area. For this reason, a second model was also examined (Scenario 2). It provides seasonal estimates of temperature increases for the region. The results for the period 2040-2060 (when atmospheric CO_2 is expected to have doubled) are presented in Table 5. The change in mean annual temperature under Scenario 1 is +4.9°C, while under Scenario 2 it is +6.5°C. Temperatures are predicted to increase in all seasons, although both scenarios indicate that warming will be greatest in the fall and winter months. This lengthens the thaw season considerably, as it would begin 5 to 8 days earlier and end 6 to 18 days later. It currently lasts an average of 87 days, but this would increase to between 98 and 113 days. The number of thawing degree days would rise from the current average of 343 to 552 TDD under Scenario 1, and 856 TDD under Scenario

2. How these temperature increases will affect the thaw season is shown graphically in Figure 36a, while Figure 36b shows how the cumulative thawing degree days will change as a result of the warmer temperatures. The changing slope in Figure 36b represents an increase in the rate of thaw.

5.3 Predicted thaw

To estimate the ground surface temperatures for the abandoned Eureka airstrip and the Gemini wellsite that could be expected under global warming, the power laws developed in Section 4.4.1 using 1998 data are applied to the predicted air temperatures for the Eureka weather station. Once the predicted ground temperatures for each of the sites has been established, the number of thawing degree days can be calculated. Table 6 shows what the thaw seasons would be like at the abandoned airstrip and Gemini under the two different climate scenarios. The number of thawing degree days at the abandoned airstrip would be between 746 and 1271 TDD, a substantial increase from the 1998 value of 633 TDD. At Gemini, the number of thawing degree days would be between 686 and 1106, as compared to 597 TDD in 1998.

The predicted depths of thaw for the two climate warming scenarios were calculated using Stefan's solution. The estimated thawing degree days at the ground surface of the two primary sites constitute one input variable, and a soil thermal constant constitutes the other. The constants used range from 2 to 4.5; these are based on the calculated 1998 values and should represent the various soil conditions that can be expected in the Eureka area. Table 7 compares the resulting thaw depths for the two climate scenarios with the average values for the 1948-1997 period. At the abandoned airstrip, the thaw depth could increase by 15 to 70 cm, resulting in a maximum active layer thickness of 160 cm. At the Gemini wellsite, changes in thaw depth could range from 12 to 59 cm, for a maximum active layer of 150 cm. Although these values provide a bracketing indication of how a warming climate could affect the active layer, it must be remembered that site-specific factors will also influence how increased temperatures will affect the terrain. For example, areas with thicker vegetative or

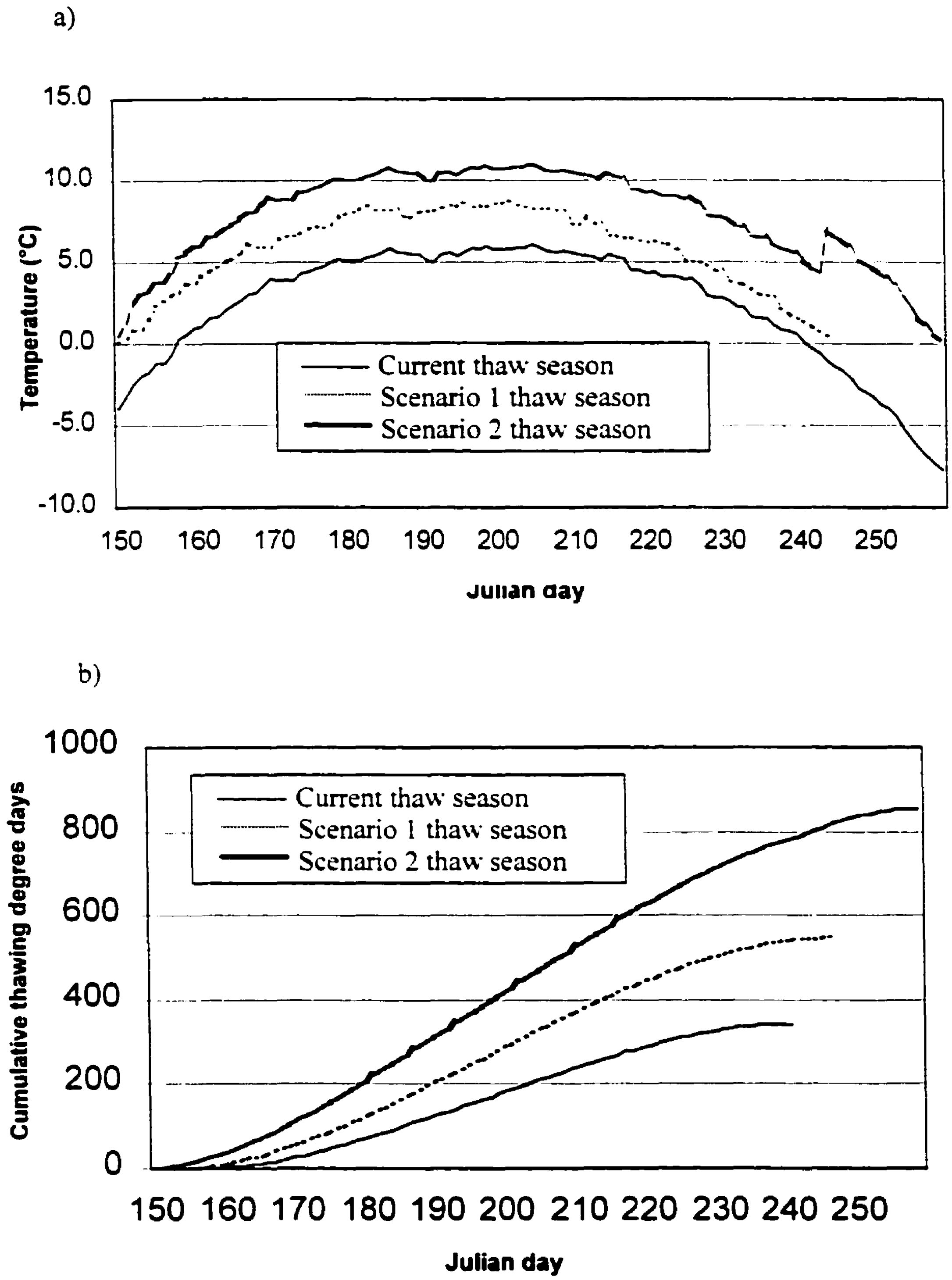

Figure 36. Changes to a) the length and magnitude of the thaw season and b) the number of cumulative thawing degree days under two different climate warming scenarios.

Table 6. Expected changes in the thaw season at the two study sites, based on two different climate warming scenarios.

	Abandoned air strip ground temperature		Gemini ground temperature	
	Scenario 1	Scenario 2	Scenario 1	Scenario 2
Thawing degree days	746	1271	686	1106
Length of thaw season	98	113	98	113
Start of thaw season	Julian day 153 (June 2)	Julian day 150 (May 30)	Julian day 153 (June 2)	Julian day 150 (May 30)
End of thaw season	Julian day 250 (Sept. 7)	Julian day 262 (Sept. 19)	Julian day 250 (Sept. 7)	Julian day 262 (Sept. 19)

Table 7. Predicted thaw depths (in cm) for the two primary study sites based on a range of thermal constants.

Thermal	Abandoned airstrip			Gemini		
Constant	Average 1948-97	Scenario 1	Scenario 2	Average 1948-97	Scenario 1	Scenario 2
2	40	55	71	40	52	67
2.5	50	68	89	50	65	83
3	60	82	107	61	79	100
3.5	70	96	125	71	92	116
4	80	109	143	81	105	133
4.5	90	123	160	91	118	150

spring snow cover will be insulated from the warmer temperatures and so thaw will not penetrate as deeply. Conversely, those with higher moisture contents will likely see greater thaw than what is predicted. Additionally, the thermal constants used here were derived from measurements in relatively similar soils, primarily fine-grained marine sediments. In coarser-grained soils or bedrock, the thermal constants would be higher and therefore so would thaw depths.

5.4 Predicted response

In the Eureka area, the geomorphic response of the different subsurface units to the increased thaw depths expected under global warming is largely dependent on the ground ice content and, more specifically, on the amount of excess ice. The only certain response to greater thaw depths that can be evaluated is the amount of ground subsidence due to the melting of this excess ice. Areas of bedrock mantle contain no excess ice, so no subsidence is expected there. Table 8 shows what the total subsidence would be in subsurface units with differing amounts of excess ice if the minimum and maximum predicted thaws were to occur over a period of 50 years. The initial thaw ranges from 12 cm to 70 cm. As the ground surface subsides each year, the permafrost table comes closer to the surface. In subsequent years, thaw can therefore once again penetrate into the permafrost. As a result, it can take a number of years for permafrost terrain to arrive at equilibrium with a new depth of seasonal thaw. The first three columns in Table 8 represent the excess ice contents for the subsurface units as calculated in Chapter 4. In areas of pore ice and thin segregated ice lenses where the density of ice wedges is low, the excess ice content is 31.5%. The total ground subsidence could range from 5 to 32 cm and stability would be achieved within 6 years. Where the density of wedges is high, the excess ice content is 33%. Subsidence would be slightly higher -- from 6 to 34 cm -- and the time frame for reaching stability would be the same. Where pore ice and segregated ice lenses are underlain by massive ice, the excess ice content rises to 61%. Here, subsidence would range from a low of 19 cm to a high of 109 cm, and it would take 14 years for the ground surface to stabilize. It must be remembered that these excess ice contents, however, are integrated throughout the entire subsurface unit and can only give an indication of the large-scale response that could be expected. The last three

Table 8. Predicted ground subsidence for different subsurface units, based on two possible thaw depths.

Terrain unit	P&S+low density wedges		P&S+high density wedges		P&S+ massive ice		P&S only		Wedge ice only		Massive ice only	
Excess ice volume (%)	31.5	31.5	33	33	61	61	29.9	30	99	99	86.8	86.8
Initial thaw (cm)	12	70	12	70	12	70	12	70	12	70	12	70
	Subsidence (cm)		Subsidence (cm)		Subsidence (cm)		Subsidence (cm)		Subsidence (cm)		Subsidence (cm)	
Year 1	3.8	22.1	4.0	23.1	7.3	42.7	3.6	20.9	11.9	69.3	10.4	60.8
2	1.2	6.9	1.3	7.6	4.5	26.0	1.1	6.3	11.8	68.6	9.0	52.7
3	0.4	2.2	0.4	2.5	2.7	15.9	0.3	1.9	11.6	67.9	7.8	45.8
4		0.7	0.1	0.8	1.7	9.7	0.1	0.6	11.5	67.2	6.8	39.7
5		0.2		0.3	1.0	5.9		0.2	11.4	66.6	5.9	34.5
6		0.1		0.1	0.6	3.6		0.1	11.3	65.9	5.1	29.9
7					0.4	2.2			11.2	65.2	4.5	26.0
8					0.2	1.3			11.1	64.6	3.9	22.6
9					0.1	0.8			11.0	63.9	3.4	19.6
10					0.1	0.5			10.9	63.3	2.9	17.0
11					0.1	0.3			10.7	62.7	2.5	14.8
12						0.2			10.6	62.0	2.2	12.8
13						0.1			10.5	61.4	1.9	11.1
14						0.1			10.4	60.8	1.7	9.6
15									10.3	60.2	1.4	8.4
16									10.2	59.6	1.2	7.3
17									10.1	59.0	1.1	6.3
18									10.0	58.4	0.9	5.5
19									9.9	57.8	0.8	4.8
20									9.8	57.3	0.7	4.1
21									9.7	56.7	0.6	3.6
22									9.6	56.1	0.5	3.1
23									9.5	55.6	0.5	2.7
24									9.4	55.0	0.4	2.3
25									9.3	54.4	0.3	2.0
26									9.2	53.9	0.3	1.8
27									9.1	53.4	0.3	1.5
28									9.1	52.8	0.2	1.3
29									9.0	52.3	0.2	1.2
30									8.9	51.8	0.2	1.0
31									8.8	51.3	0.1	0.9
32									8.7	50.7	0.1	0.8
33									8.6	50.2	0.1	0.7
34									8.5	49.7	0.1	0.6
35									8.4	49.2	0.1	0.5
36									8.4	48.7	0.1	0.4
37									8.3	48.3	0.1	0.4
38									8.2	47.8	0.1	0.3
39									8.1	47.3		0.3
40									8.0	46.8		0.2
41									7.9	46.4		0.2
42									7.9	45.9		0.2
43									7.8	45.4		0.2
44									7.7	45.0		0.1
45									7.6	44.5		0.1
46									7.6	44.1		0.1
47									7.5	43.6		0.1
48									7.4	43.2		0.1
49									7.3	42.8		0.1
50									7.3	42.4		0.1
Total subsidence (cm)	5	32	6	34	19	109	5	30	469	2737	79	460

columns in Table 8 are included to provide a better picture of what might happen at a smaller scale. For instance, the geomorphic response in a polygon centre would be due to the melting of pore ice and segregated lenses only. The volumetric ice content of this small area would be 48.6%, with an excess ice content of 29.9%. Total subsidence here would be similar to what it would be for the entire subsurface unit if ice wedges are included: 5 to 30 cm over a six year period. However, this is considerably different from what would occur directly above an ice wedge, which we have assumed to be virtually pure ice. Theoretically, ground subsidence could be over 27 m and it could take more than half a century for the surface to stabilize. Practically, this is unrealistic since ice wedges on the Fosheim Peninsula generally do not penetrate deeper than 8 m. Additionally, field studies have shown that the relief generated by the increased melt over an ice wedge results in re-working of the adjacent surface materials down into the ice wedge trough, so that the surface of the wedge becomes insulated from further thaw. The final column in Table 8 shows what the subsidence would be if a body of massive ice (with an excess ice content of 86.8%) were directly exposed. The ground surface could subside by over 4 m and would only stabilize after approximately 50 years. However, this assumes that the horizontal surface of the massive ice is directly exposed, while field experience indicates that such ice bodies on the Fosheim Peninsula usually have an overburden of from 1 to 6 m and exposure is usually in a vertical headwall. Nevertheless, these values do underline the importance of ground ice content in evaluating the terrain response to increased thaw.

CHAPTER 6 - DISCUSSION AND CONCLUSIONS

6.1 Discussion

Past investigations of how permafrost landscapes respond to climate change have either omitted the polar desert environment, or have only focussed on specific features within the landscape. This study is one of the few that examines overall landscape response to climate change in Nunavut. The investigation of ground ice volumes and past thermokarst activity allows for a more complete understanding of how different subsurface units within the landscape will evolve under a warmer climate.

In order to develop an understanding of how the landscape might change, the first objective of this thesis was to quantify the amount and types of ground ice in the Eureka area. The total percentage volume of ground ice in the region calculated by this study is 30.8% for all subsurface units. This is comparable to volumes determined for Richards Island (47.5%) (Pollard and French 1980), Alaska (46.6%) (Brown 1967), and Melville Island (30 to 70%) (French et al. 1986), but is less than a previous value reported for the Fosheim Peninsula (53%) (Hodgson and Nixon 1998). However, Hodgson and Nixon's work intentionally focussed on areas suspected of being ice-rich, whereas the present study incorporates data from all terrain types so the lower percentage obtained for ground ice volume is not surprising. The percentage of wedge ice estimated for the Eureka area is 3.5% in areas of high density wedges and 1.8% in areas where the density of wedges is low. This is much smaller than a value of 16% found in the western Arctic (Pollard and French 1980), but is similar to one found on Melville Island (French et al. 1986). In comparing ground ice volumes from the various studies (including this one), it must be remembered that such investigations, almost by their very nature, will tend to focus on regions where ground ice is prevalent. The standard errors for many of the values for ground ice volume in this study are indicative of the high natural spatial variability of ground ice and the limited size of the available database. Therefore, this study does not attempt to go beyond a first approximation of the volume of ground ice in the Eureka area. Additionally, the results of this study must be considered in light of the various assumptions made. The ice wedge dimensions used should be considered minimum values, since only the depth of wedge ice visible in exposures was considered, although wedges often appeared to extend to greater depths. A second assumption concerning ice wedges is that they all have a surface expression, which field observations show is not the case, so wedge ice may be more prevalent than indicated by this study. Another assumption is that massive ice underlies only raised marine terraces. However, small bodies of massive ice have been observed in areas where the topography is more irregular (Pollard in press). Because there was no way to systematically identify massive ice in these regions of irregular topography, such areas were not included in this study. It is therefore likely that the total volume of massive ice is underestimated. Given the high percentage of pore ice and thin segregated ice lenses in the permafrost, the most likely source of error in the estimate of total ice volume is the conclusion that the mean ice content can be applied to the entire thickness of frozen materials under consideration. However, some support for this contention is provided by a previous study in the region (Hodgson and Nixon 1998) which noted that mean ground ice content remains relatively constant with depth. Overall, these estimates of ground ice volume rely on conservative assumptions. Accordingly, the estimate for total ground ice (30.8%) should be considered a minimum estimate.

Of major importance in attempting to predict future terrain response to climate change is assessing how the terrain has responded to past disturbances. The results show that the degree of response is a function of the ground ice volume and especially of the volume of excess ice. At both of the primary study sites -- the abandoned airstrip at Eureka and the Gemini wellsite -- the main geomorphic response to disturbance involves ground subsidence due to the melting of pore ice and thin lenses of segregated ice. Above ice wedges, subsidence is greater than elsewhere in the disturbed areas since the wedges have a higher percentage of excess ice. The deeper depressions at the Gemini well site (>3m) are likely due to the presence of small bodies of massive ice, a supposition supported by the findings of Hodgson and Nixon (1998), who reported massive ice in the vicinity of the wellhead. Ground subsidence of almost 2 m in the old dumpsite near Eureka also suggests that small bodies of massive ice were present. Subsidence and changes to the active layer are not as evident at the Gemini airstrip as they are in the area surrounding the wellhead at Gemini, the abandoned airstrip at Eureka, and other disturbed sites; this may be accounted for by the sandier soil at the Gemini airstrip, which would limit the amount of pore ice and thin segregated ice lenses. Terrain underlain by massive ice has the highest volume of excess ice and shows the most dramatic response to disturbance, primarily in the form of retrogressive thaw slumping which can affect areas greater than 5000^2m. The headwall retreat of these slumps on the Fosheim Peninsula has been calculated to be 8-14 m/year for high angle slumps (Robinson in press), although in one case, a slump headwall retreated 25 m in 38 days (Edlund et al. 1989). The high ice content of ice wedges means that the troughs that form above them tend to act as natural conduits, as evidenced by the concentration of gullies along such troughs. Another significant form of thermokarst observed in the field is active layer detachment sliding, which has occurred regularly on slopes throughout the Fosheim Peninsula in the past. The mere existence of these slides is evidence of the presence of enough ice at the base of the active layer for pore water pressures to increase significantly when this ice melts. How the underlying permafrost responds to exposure at the surface once the active layer has been removed depends on the ground ice content in the subsurface unit in which the slides occur. The survey of the abandoned airstrip at Eureka demonstrates that the effects of a disturbance that ended in 1951 are still evident after almost 50 years. Most of the subsidence of the ground surface appears to have taken place in the first several years, however, re-working of surface materials in the vicinity of the ice wedges was not complete by the time of the 1973 survey, 22 years later. Deeper active layers and the accumulation of standing water in some of the troughs above ice wedges at the Eureka airstrip and in the large depressions at the Gemini site suggests that there will probably be further changes to the sites.

The ultimate goal of this study is to assess the sensitivity of permafrost terrain to disturbances at the ground surface resulting from global warming. The projected warming scenarios for the Eureka area show that the mean annual air temperature could increase by 4.9°C to 6.5°C. Predicted thaw depths as a result of these temperature increases could be as little as 12 cm, based on a conservative thermal constant, but could range as high as 70 cm.

Based on past thermokarst activity, the response of the terrain in the Eureka area to thaw is highly dependent on ground ice content. Of the subsurface units examined, only areas of bedrock mantle above marine limit are likely to remain unaffected. All other areas have a high enough ice content and, more specifically, a high enough excess ice content, so that at least some ground subsidence will occur. In subsurface units with pore ice, thin segregated lenses and wedge ice, maximum ground subsidence as a result of the predicted warming will be approximately 30 cm. This is very similar to the subsidence that was seen at the abandoned airstrip and at the Gemini wellsite. These study sites therefore serve as appropriate snapshots for how the terrain might look following global warming. Wedge ice and massive ice comprise only a small percentage of the total ice in the study area, but because of their high excess ice content, significant local subsidence is likely to occur and could continue for close to 50 years. Note that the predictions of thaw in areas of wedge ice in Table 8 are somewhat misleading for several reasons: Firstly, although we have made the assumption that wedge ice is virtually pure, the wedges generally contain some sediment. Secondly, the size of the ice wedges is limited and the wedges are more likely to melt out before all the subsidence indicated in Table 8 could take place. Finally, the geometry of the wedges is such that surrounding sediment will likely tumble on to the top of the wedge as it melts, insulating it from further thaw. Many of the predicted changes to the landscape can be expected to occur within 10 to 15 years of the initial disturbance. However, it is important to remember that the values of subsidence modelled in this study are based on the assumption that the temperature changes will occur in a step-like fashion over one season, rather than in a gradual fashion. Additionally, the initial geomorphic responses may be smoothed out over time by the re-working of sediment from areas of high to low topography. A final note to consider is that since the warming will be relatively uniform in any one area, ground subsidence will be widespread and relative changes in the ground surface will not be as dramatic as they are in the case of a limited disturbance.

Increased thaw in areas of massive ice will likely result in more exposures of the ice bodies themselves, leading to a rise in the number of retrogressive thaw slumps. Given warmer temperatures, it would be expected that headwall retreat rates would also rise. In fact, Robinson (1993) recorded good correlation between headwall retreat and thawing degree days. However, Lewkowicz notes that solar radiation plays a large role in retreat rates (Lewkowicz 1987). Since solar radiation budgets will not increase under global warming, it would be unwise to predict headwall retreat rates based on the expected number of thawing degree days. Woo at al. propose a 25% increase in the rate of headwall retreat (Woo et al. 1992). Using Robinson's current value for the Fosheim Peninsula of 8-14 m/year, this would mean that under global warming, retrogressive thaw slumps could progress at the rate of 10-17.5 m/year.

The number of active layer detachment slides on the Fosheim Peninsula is anamalously high compared to other regions in the Canadian high Arctic (Lewkowicz 1992). Since their initiation is based to a large degree on the buildup of pore water pressures at the base of the active layer, the rate at which the thaw season progresses would likely have a greater influence on their development than would the total thaw depth. As noted in Figure 36b, thaw rates are expected to increase under the two predicted climate warming scenarios. This, combined with the thaw of the ice-rich upper layers of permafrost, should lead to an even greater number of active layer detachment slides in the early stages of global warming. However, because slope recovery time between slides is on the order of 6 to 15 years, the increased frequency of slides would not be a sustained one.

Finally, a note on climate modelling. The predicted temperature increases for Eureka, based on data from the Canadian Centre for Climate Modelling and Analysis, are in line with those projected by the Intergovernmental Panel on Climate Change. In considering the climate model used in this study, however, a number of factors must be kept in mind. First is the high uncertainty associated with all modelling of temperatures in polar climates. Additionally, the current study only examines changes in temperature, but a number of other environmental variables need to be considered when assessing changes to ground temperatures under a climate warming scenario. For instance, current climate models suggest that soil moisture in the polar regions will increase in winter, but that there will be little difference in summer (IPCC 1996). Again, there is a high degree of uncertainty associated with these predictions (Fitzharris 1996). The dependence of the thermal constants used in this study on thermal conductivity and soil moisture underlines how important it is to assess soil moisture accurately. The timing and amount of snowfall can also significantly change the number of thawing degree days that can be expected at the ground surface, and predictions of change in this variable too, are still speculative.

6.2 Conclusions

The initial goal of this study was to assess how sensitive permafrost terrain in the Eureka area might be to changes in climate. The primary result of the research is that significant geomorphic changes can be expected, particularly in the immediate vicinity of ice wedges and bodies of massive ice. In addition to this conclusion, the following secondary ones can be drawn:

1. Ground ice is shown to be a significant component of the surficial materials near Eureka, comprising 30.8% of the top 5.9 m of permafrost. Pore ice and thin segregated ice lenses make up the bulk of ground ice and the excess ice content is sufficiently high for ground subsidence to occur. Although massive ground ice and wedge ice comprise a small percentage of the total ground ice, they may dominate ice content at specific sites and have a significant effect on terrain stability and response to thermal disturbance.

2. Investigations of past disturbance indicate that the level of disturbance is directly related to the amount of excess ice present. Thermokarst features include subsidence of the ground surface by up to 3.2 m, degradation of ice wedges, and the development of retrogressive thaw slumps, active layer detachment slides, and gullies.

3. Under a doubling of atmospheric CO_2, air temperatures in the Eureka area will increase by 4.9 to 6.5°C. This will lengthen the thaw season by 11 to 26 days and increase the number of thawing degree days at the ground surface.

4. The landscape response to predicted global warming will be a function of the ground ice

and excess ice contents. As a result, areas of weathered bedrock with no excess ice will show virtually no response to warming. In areas of pore ice and thin segregated ice lenses with a low density of ice wedges, excess ice contents are 31.5% and ground subsidence may be as much as 32 cm. In areas with a high density of ice wedges, excess ice is 33% and subsidence will be slightly higher at 34 cm. Where massive ice is present, excess ice accounts for 61% of the subsurface unit and subsidence will be greater than 1 m. The frequency and rate of retrogressive thaw slumping is expected to increase and active layer detachment slides will be more common in the initial stages of warming.

5. The geomorphic response to a change in the ground surface temperature can take a number of years. Although the model of ground subsidence indicates that the response occurs over a 3 to 14 year range, actual measured changes suggest that it can be longer.

6.3 Future research

There are a number of factors that could reduce the uncertainties associated with the results presented here. The first is a more extensive database of ground ice contents. Any drilling or sampling program should focus on whether the ice content at any one location shows variation with depth. The actual ice content of wedge ice should also be examined in greater detail. Given the importance of the larger ice bodies in assessing geomorphic changes, it is imperative to arrive at a better understanding of the density of ice wedges (perhaps through more effective remote sensing techniques) and the location of massive ice beds.

Climate modellers continue to refine the techniques they use to account for as many environmental variables and feedback mechanisms as possible. Hopefully, such improvements in the models will provide better results of air temperature, soil moisture and snowfall in the polar regions, which will allow us to refine our understanding of how landscapes in these parts of the globe will be affected by changing climate.

REFERENCES

ACGR (Associate Committee on Geotechnical Research), 1988. *Glossary of permafrost and related ground ice terms*. Permafrost Subcomittee, National Research Council of Canada, Technical Memorandum 142, 156 pp.

Andersland, O.B. and Anderson, D.M., 1978. *Geotechnical Engineering for Cold Regions*. New York, McGraw Hill, 566 pp.

Anisimov, O. A., and Nelson, F. E., 1997. Permafrost zonation and climate change in the northern hemisphere: Results from transient general circulation models. *Climatic Change*, 35, 241-258.

Barry, P. J., 1992. Ground ice characteristics in permafrost on the Fosheim Peninsula, Ellesmere Island, N.W.T.: A study utilizing ground probing radar and geomorphological techniques. Unpublished M. Sc. thesis, McGill University, Montreal, Quebec, 135 pp.

Bell, T., 1992. Glacial and sea level history of western Fosheim Peninsula, Ellesmere Island, Arctic Canada. Ph.D. thesis, University of Alberta, Edmonton,172 pp.

Bell, T., 1996. The last glaciation and sea level history of Fosheim Peninsula, Ellesmere Island, Canadian High Arctic. *Canadian Journal of Earth Sciences*, 33, 1075-1086.

Bockheim, J. G., and Tarnocai, C., 1998. Nature, occurrence and origin of dry permafrost. Proceedings of *Seventh International Permafrost Conference*, Yellowknife, N.W.T., 57-63.

Boer, G. J., Flato, G. M., Reader, M. C., and Ramsden, D., 2000. A transient climate change simulation with greenhouse gas and aerosol forcing: experimental design and comparison with the instrumental record for the twentieth century. *Climate Dynamics*, 16, 405-425.

Brown, J., 1967. An estimation of volume of ground ice, Coastal Plain, northern Alaska. *Memorandum*, Cold Regions Research and Engineering Laboratory, Hanover, N.H., 22 pp.

Brown, J., and Grave, N. A., 1979. Physical and thermal disturbance and protection of permafrost. *Special Report* 79-5, Cold Regions Research and Engineering Laboratory, Hanover, N.H., 43 pp.

Brown, R. J. E., 1974. Distribution and environmental relationships of permafrost. Proceedings of *Workshop Seminar on Permafrost-Hydrology and Geophysics*, Calgary, Alberta, 1-17.

Brown, R. J. E., 1978. Influence of climate and terrain on ground temperature in the continuous permafrost zone of northern Manitoba and Keewatin District, Canada. Proceedings of *Third International Conference on Permafrost*, Edmonton, 15-21.

Burn, C. R., 1990. Frost heave in lake-bottom sediments, Mackenzie Delta, Northwest Territories. *Permafrost Canada - Proceedings of the Fifth Canadian Permafrost Conference*, Québec City, 103-109.

Burn, C. R., 1992. Thermokarst lakes. *The Canadian Geographer*, 36, 81-85.

Burn, C. R., and Friele, P. A., 1989. Geomorphology, vegetation succession, soil characteristics and permafrost in retrogressive thaw slumps near Mayo, Yukon Territory. *Arctic*, 42, 31-40.

Burn, C. R., and Lewkowicz, A. G., 1990. Retrogressive thaw slumps. *Canadian Geographer*, 34, 273-276.

Caron, A., Rose, P., and Rose, I., 1995. Canada - Permafrost (map), 1:7,500,000. Natural Resources Canada.

de Krom, V., 1990. A geomorphic investigation of retrogressive thaw slumps and active layer slides on Herschel Island, Yukon Territory. Unpublished M.Sc. thesis, McGill University, Montreal, Quebec, 157 pp.

Edlund, S. A., and Alt, B. T., 1989. Regional congruence of vegetation and summer climate patterns in the Queen Elizabeth Islands, Northwest Territories, Canada. *Arctic*, 42, 3-23.

Edlund, S. A., Alt, B. T., and Young, K. L., 1989. Interaction of climate, vegetation, and soil hydrology at Hot Weather Creek, Fosheim Peninsula, Ellesmere Island, Northwest Territories. In: *Current Research, Part D*, Geological Survey of Canada, 125-133.

Emers, M., and Jorgenson, J. C., 1997. Effects of winter seismic exploration on tundra vegetation and the soil thermal regime in the Arctic National Wildlife Refuge, Alaska. In: *Disturbance and Recovery in Arctic Lands*, R. M. M. Crawford, ed., Kluwer Academic Publishers, 443-454.

Environment Canada, 1998. Canadian Climate Normals 1961-1990.

Farouki, O. T., 1981. Thermal properties of soils. *Monograph* 81-1, Cold Regions Research and Engineering Laboratory, Hanover, N.H., 136 pp.

Felix, N. A., and Raynolds, M. K., 1989. The role of snow cover in limiting surface disturbance caused by winter seismic exploration. *Arctic*, 42, 62-68.

Fitzharris, B. B., 1996. The cryosphere: changes and their impacts. In: *Climate Change 1995: Impacts, Adaptations and Mitigation of Climate Change: Scientific-Technical Analyses*, R. T. Watson, M. C. Zinyowera, R. H. Moss, and D. J. Dokken, eds., Cambridge University Press, Cambridge, 241-265.

Forbes, B. C., 1996. Plant communities of archaeological sites, abandoned dwellings, and trampled tundra in the eastern canadian Arctic: A multivariate analysis. *Arctic*, 49, 141-154.

French, H. M., 1975. Man-induced thermokarst, Sachs Harbour airstrip, Banks Island, Northwest Territories. *Canadian Journal of Earth Sciences*, 12, 132-144.

French, H. M., 1981. Sump studies IV: Permafrost terrain disturbances adjacent to exploratory wellsites, northern Yukon Territory. *Environmental Studies* No. 19, Arctic Land Use Research Program, Department of Indian and Northern Affairs, Ottawa, Ontario, 41 pp.

French, H. M., 1996. *The Periglacial Environment*. Longman, London, 341 pp.

French, H. M., Bennett, L., and Hayley, D. W., 1986. Ground ice conditions near Rea Point and on Sabine Peninsula, eastern Melville Island. *Canadian Journal of Earth Sciences*, 23, 1389-1400.

French, H. M., and Harry, D. G., 1990. Observations of buried glacier ice and massive segregated ice, western Arctic coast, Canada. *Permafrost and Periglacial Processes*, 1, 31-43.

Fujino, K., Sato, S., Matsuda, K., Sasa, G., Shimizu, O., and Kato, K., 1988. Characteristics of the massive ground ice body in the western canadian Arctic. Proceedings of *Fifth International Conference on Permafrost*, Trondheim, Norway, 143-147.

Gadja, R. T., 1949. Eureka, Slidre Fiord (Ellesmere Island): Geographical appreciation report (site and vicinity). *Unpublished report*.

Goodrich, L. E., 1982. The influence of snow cover on the ground thermal regime. *Canadian Geotechnical Journal*, 19, 421-432.

Halvorson, J. J., McCool, D. K., King, L. G., and Gatto, L. W., 1998. Ground freezing effects on soil erosion of army training lands. Part 2: Overwinter changes to tracked-vehicle ruts, Yakima Training Center, Washington. *Special Report* 98-8, Cold Regions Research and Engineering Laboratory, Hanover, N.H., 48 pp.

Harry, D. G., French, H. M., and Pollard, W. H., 1985. Ice wedges and permafrost conditions near King Point, Beaufort Sea coast, Yukon Territory. In: *Current Research, Part A*, Geological Survey of Canada, 111-116.

Harry, D. G., French, H. M., and Pollard, W. H., 1988. Massive ground ice and ice-cored terrain near Sabine Point, Yukon Coastal Plain. *Canadian Journal of Earth Sciences*, 25, 1846-1856.

Heginbottom, J. A., 1973. Some effects of surface disturbance on the permafrost active layer at Inuvik, N.W.T. *Environmental-Social Committee Northern Pipelines, Task Force on Northern Oil Development* 73-16, Geological Survey of Canada, 29 pp.

Hodgson, D. A., 1985. The last glaciation of west-central Ellesmere Island, Arctic Archipelago, Canada. *Canadian Journal of Earth Sciences*, 22, 347-368.

Hodgson, D. A., and Nixon, F. M., 1998. Ground ice volumes determined from shallow cores from western Fosheim Peninsula, Ellesmere Island, Northwest Territories. *Bulletin* 507, Geological Survey of Canada, 178 pp.

Hodgson, D. A., St-Onge, D. A., and Edlund, S. A., 1991. Surficial materials of Hot Weather Creek basin, Ellesmere Island, Northwest Territories. In: *Current Research, Part E*, Geological Survey of Canada, 157-163.

International Permafrost Association, 1998. *Multi-Language Glossary of Permafrost and Related Ground-Ice Terms*, R.O. van Everdingen, ed., The Arctic Institute of North America, University of Calgary, Calgary, Canada.

IPCC, 1996. *Climate Change 1995: The Science of Climate Change*. Cambridge University Press, Cambridge, UK, 572 pp.

Johnston, G. H., 1981. *Permafrost: Engineering Design and Construction*, John Wiley & Sons, Toronto, 540 pp.

Jorgenson, M. T., 1997. Patterns and rates of, and factors affecting natural recovery on land disturbed by oil development in arctic Alaska. In: *Disturbance and Recovery in Arctic Lands*, R. M. M. Crawford, ed., Kluwer Academic Publishers, 421-442.

Judge, A. S., Taylor, A. E., Burgess, M., and Allen, V. S., 1981. Canadian geothermal data collection - nothern wells 1978-80. *Geothermal Series* 12, Earth Physics Branch, Energy, Mines and Resources Canada, Ottawa, Ontario.

Kane, D. L., Hinzman, L. D., and Zarling, J. P., 1991. Thermal response of the active layer to climatic warming in a permafrost environment. *Cold Regions Science and Technology*, 19, 111-122.

Kurfurst, P. J., 1973. Terrain disturbance susceptibility, Norman Wells area, Mackenzie Valley. *Environmental-Social Committee Northern Pipelines, Task Force on Northern Oil Development* 73-24, Geological Survey of Canada, 36 pp.

Lachenbruch, A. H., 1962. Mechanics of thermal contraction cracks and ice-wedge polygons in permafrost. *Special Paper No. 70*, Geological Society of America, 69 pp.

Lamothe, C. and St-Onge, D.A., 1961. A note on a periglacial process in the Isaachsen area, N.W.T. *Geographical Bulletin*, 16, 104-113.

Lawson, D. E., 1986. Response of permafrost terrain to disturbance: A synthesis of observations from northern Alaska, U.S.A. *Arctic and Alpine Research*, 18, 1-17.

Lawson, D. E., Brown, J., Everett, K. R., Johnson, A. W., Komarkova, V., Murray, B. M., Murray, D. F., and P.J., W., 1978. Tundra disturbance and recovery following the 1949 exploratory drilling, Fish Creek, Northern Alaska. *Report* 78-28, Cold Regions Research and Engineering Laboratory, Hanover, N.H., 91 pp.

Leffingwell, E. d. K., 1915. Ground ice-wedges. The dominant form of ground ice on the north coast of Alaska. *Journal of Geology*, 23, 635-654.

Lewkowicz, A. G., 1987. Headwall retreat of ground-ice slumps, Banks Island, Northwest Territories. *Canadian Journal of Earth Sciences*, 24, 1077-1085.

Lewkowicz, A. G., 1990. Morphology, frequency and magnitude of active-layer detachment slides, Fosheim Peninsula, Ellesmere Island, N.W.T. *Permafrost Canada - Proceedings of the Fifth Canadian Permafrost Conference*, Québec City, 111-118.

Lewkowicz, A. G., 1992. Factors influencing the distribution and initiation of active-layer detachment slides on Ellesmere Island, Arctic Canada. *Periglacial Geomorphology, Proceedings of the 22nd annual Binghamton Symposium in Geomorphology*, Bignhamton, 223-250.

Lewkowicz, A. G., and Duguay, C. R., 1999. Detection of permafrost features using SPOT panchromatic imagery, Fosheim Peninsula, Ellesmere Island, N.W.T. *Canadian Journal of Remote Sensing*, 25, 34-44.

Lunardini, V. J., 1996. Climatic warming and the degradation of warm permafrost. *Permafrost and Periglacial Processes*, 7, 311-320.

Lunardini, V. J., 1998. Effect of convective heat transfer on thawing of frozen soil. Proceedings of *Seventh International Permafrost Conference*, Yellowknife, N.W.T., 689-695.

Mackay, J. R., 1963. The Mackenzie Delta area, N.W.T. *Memoir* 8, Geographical Branch, Department of Mines and Technical Surveys, Ottawa, Ontario, 202 pp.

Mackay, J. R., 1970. Disturbances to the tundra and forest tundra environment of the western Arctic. *Canadian Geotechnical Journal*, 7, 420-432.

Mackay, J. R., 1971. The origin of massive icy beds in permafrost, western Arctic coast, Canada. *Canadian Journal of Earth Sciences*, 8, 397-422.

Mackay, J. R., 1972. The world of underground ice. *Annals of the American Association of Geographers*, 62, 1-22.

Mackay, J. R., 1973. Problems in the origin of massive ice beds, western Arctic, Canada. Proceedings of *Second International Permafrost Conference*, Yakutsk, USSR, 223-228.

Mackay, J. R., 1974. Ice-wedge cracks, Garry Island, Northwest Territories. *Canadian Journal of Earth Sciences*, 11, 1366-1383.

Mackay, J. R., 1988. Ice wedge growth in newly aggrading permafrost, western Arctic Coast, Canada. Proceedings of *Fifth International Conference on Permafrost*, Trondheim, Norway, 809-814.

Mackay, J. R., 1990. Some observations on the growth and deformation of epigenetic, syngenetic and anti-syngenetic ice wedges. *Permafrost and Periglacial Processes*, 1, 15-29.

Mackay, J. R., 1992. The frequency of ice-wedge cracking (1967-1987) at Garry Island, western Arctic coast, Canada. *Canadian Journal of Earth Sciences*, 29, 236-248.

Mackay, J. R., 1995. Active layer changes (1968 to 1993) following the forest-tundra fire near Inuvik, N.W.T., Canada. *Arctic and Alpine Research*, 27, 323-336.

Mackay, J. R., and Dallimore, S. R., 1992. Massive ice of the Tuktoyaktuk area, western Arctic coast, Canada. *Canadian Journal of Earth Sciences*, 29, 1235-1249.

Maxwell, B., 1997. *Responding to Global Climate Change in Canada's Arctic*, Environmental Adaptation Research Group, Atmospheric Environment Service, Environment Canada, Downsview, Ontario, 82 pp.

McRoberts,E.C. and Morgenstern, N.R., 1974. The stability of thawing slopes. *Canadian Geotechnical Journal*, 11, 447-469.

Nicholson, F. H., and Granberg, H. B., 1973. Permafrost and snow cover relationships near Schefferville. Proceedings of *Second International Permafrost Conference*, Yakutsk, USSR, 151-158.

Nixon, J. F., 1975. The role of convective heat transport in the thawing of frozen soils. *Canadian Geotechnical Journal*, 12, 425-429.

Nixon, J. F., and McRoberts, E. C., 1973. A study of some factors affecting the thawing of frozen soils. *Canadian Geotechnical Journal*, 10, 439-452.

Panarctic Oils Ltd., 1973. Panarctic Gemini E-10. *Well history report*, 72 pp.

Pihlainen, J. A., and Johnston, G. H., 1963. Guide to a field description of permafrost. *Technical memorandum* 79, National Research Council, Ottawa, Ontario.

Pollard, W. H., 1990. The nature and origin of ground ice in the Herschel Island area, Yukon Territory. *Permafrost Canada - Proceedings of the Fifth Canadian Permafrost Conference*, Québec City, 23-30.

Pollard, W. H., 1991. Observations of massive ground ice on Fosheim Peninsula, Ellesmere Island, Northwest Territories. In: *Current Research, Part E*, Geological Survey of Canada, 223-231.

Pollard, W. H., in press. Ground ice distribution and characterization. In: *The High Arctic Global Change Observatory of the Geological Survey of Canada: 5 years of Multidisciplinary Research on the Climate Change Program*, M. Garneau, ed., Geological Survey of Canada Bulletin.

Pollard, W. H., and Bell, T., 1998. Massive ice formation in the Eureka Sound Lowlands: a landscape model. Proceedings of *Seventh International Permafrost Conference*, Yellowknife, N.W.T., 903-908.

Pollard, W. H., and Dallimore, S. R., 1988. Petrographic characteristics of massive ground ice, Yukon Coastal Plain, Canada. Proceedings of *Fifth International Conference on Permafrost*, Trondheim, Norway, 224-229.

Pollard, W. H., and French, H. M., 1980. A first approximation of the volume of ground ice, Richards Island, Pleistocene Mackenzie Delta, NWT. *Canadian Geotechnical Journal*, 17, 509-516.

Radforth, J. R., 1972. Immediate effrects of wheeled vehicle traffic on tundra during the summer. *ALUR* 72-73-12, Arctic Land Use Research Program, Department of Indian and Northern Affairs, Ottawa, Ontario, 32 pp.

Rampton, V. N., 1974. The influence of ground ice and thermokarst upon the geomorphology of the Mackenzie-Beaufort region. Proceedings of *3rd Guelph Symposium on Geomorphology*, Guelph, Ontario, 43-59.

Rampton, V. N., 1988. Origin of massive ground ice on Tuktokaktuk Peninsula, Northwest Territories, Canada: A reivew of stratigraphic and geomorphic evidence. Proceedings of *Fifth International Conference on Permafrost*. Trondheim, Norway, 850-855.

Ricketts, B. D., 1986. New formations in the Eureka Sound Group, Canadian Arctic Islands. In: *Current Research, Part B*. Geological Survey of Canada, 363-374.

Robinson, S. D., 1993. Geophysical and geomorphological investigations of massive ground ice, Fosheim Peninsula, Ellesmere Island, Northwest Territories. Unpublished M.Sc. thesis, Queen's University, Kingston, Ontario, 169 pp.

Robinson, S. D., 1994. Geophysical studies of massive ground ice, Fosheim Peninsula, Ellesmere Island, Northwest Territories. In: *Current Research, Part B*, Geological Survey of Canada, 11-18.

Robinson, S. D., in press. Ground ice and thermokarst in the vicinity of Hot Weather Creek, Fosheim Peninsula, Ellesmere Island, Canada. In: *The High Arctic Global Change Observatory of the Geological Survey of Canada: 5 years of Multidisciplinary Research on the Climate Change Program*, M. Garneau, ed., Geological Survey of Canada Bulletin.

Robinson, S. D., Moorman, B. J., Judge, A. S., and Dallimore, S. R., 1993. The characterization of massive ground ice at Yaya Lake, Northwest Territories using radar stratigraphy techniques. In: *Current Research, Part B*, Geological Survey of Canada, 23-32.

Robinson, S. D., and Pollard, W. H., 1998. Massive ground ice within Eureka Sound Bedrock, Ellesmere Island, Canada. Proceedings of *Seventh International Permafrost Conference*, Yellowknife, N.W.T., 949-954.

Scott, W. J., Sellman, P. V., and Hunter, J. A., 1990. Geophysics in the study of permafrost. In: *Geotechnical and Environmental Geophysics*, S. H. Ward, ed., Society of Exploration Geophysicists, 355-384.

Shumskiy, P. A., and Vtyurin, B. I., 1963. Underground ice. Proceedings of *First International Permafrost Conference*, Lafayette, Indiana, 108-113.

Slusarchuk, W. A., and Foulger, P. H., 1973. Development and calibration of a thermal conductivity probe apparatus for use in the field and laboratory. *Technical Paper No.*

388, Division of Building and Research, National Research Council of Canada, 28 pp.

Smith, M. W., 1975. Microclimatic influences on ground temperatures and permafrost distribution, Mackenzie Delta, Northwest Territories. *Canadian Journal of Earth Sciences*, 12, 1421-1438.

Smith, M. W., and Riseborough, D. W., 1996. Permafrost monitoring and detection of climate change. *Permafrost and Periglacial Processes*, 7, 301-309.

Smith, S. L., and Burgess, M. M., 1999. Mapping the sensitivity of Canadian permafrost to climate warming. In: *Interactions Between the Cryosphere, Climate and Greenhouse Gases (Proceedings of IUGG 99 Symposium HS2, Birmingham, July 1999)*, IAHS Publ. no. 256, 71-78.

van Everdingen, R. O., 1979. Potential interactions between pipelines and terrain in a northern environment. *NHRI Paper* 8, National Hydrology Research Institute, Inland Waters Directorate, Ottawa, Ontario, 7 pp.

Walker, D. A., Cate, D., Brown, J., and C., R., 1987. Disturbance and recovery of arctic Alaskan tundra terrain: A review of recent investigations. *Report* 87-11, Cold Regions Research and Engineering Laboratory, Hanover, N.H., 70 pp.

Walsh, J. E., 1995. Long-term observations for monitoring of the cryosphere. *Climatic Change*, 31, 369-394.

Walsh, J. E., and Crane, R. G., 1992. A comparison of GCM simulations of arctic climate. *Geophysical Research Letters*, 19, 29-32.

Washburn, A. L., 1973. *Periglacial processes and environments*, Edward Arnold, London, 320 pp.

Wechsler, A. E., 1966. Development of thermal conductivity probes for soils and insulations. *Technical Report* 182, Cold Regions Research and Engineering Laboratory, Hanover, N.H., 83 pp.

Woo, M.-K., Lewkowicz, A. G., and Rouse, W. R., 1992. Response of the canadian permafrost environment to climatic change. *Physical Geography*, 13, 287-317.

Woo, M.-k., and Young, K. L., 1997. Hydrology of a small drainage basin with polar oasis environment, Fosheim Peninsula, Ellesmere Island, Canada. *Permafrost and Periglacial Processes*, 8, 257-277.

Young, K. L., Woo, M. K., and Edlund, S. A., 1997. Influence of local topography, soils, and vegetation on microclimate and hydrology at a High Arctic site, Ellesemere Island, Canada. *Arctic and Alpine Research*, 29, 270-284.

APPENDIX – SURVEY RESULTS FOR THE PRIMARY STUDY SITES

Abandoned airstrip at Eureka - Profile 1				
	1973		1998	
Station	Distance from west end (m)	Relative elevation (cm)	Distance from west end (m)	Relative elevation (cm)
A1	0.00	1000.0	0.00	1000.0
A2	10.74	982.4	10.74	985.4
A3	15.74	961.6	15.74	969.1
A4	26.07	992.5	26.07	983.3
A5	32.80	991.6	32.80	993.5
A17	39.40	971.6	39.40	967.0
A18	42.80	965.4	42.80	951.6
A19	44.76	958.1	44.76	952.4
A20	46.95	942.2	46.95	947.6
A21	56.89	936.3	56.89	937.3
A22	68.35	930.1	68.35	909.6
A23	70.90	888.1	70.90	900.7
A24	74.80	925.4	74.80	924.0
A25	77.03	916.6	77.03	911.1
A26	86.03	921.1	86.03	915.5
A42	91.31	942.9	91.31	935.6
A43	94.10	954.5	94.10	947.9
A44	96.40	961.3	96.40	958.3
A45	106.83	957.6	106.83	958.4
A46	118.03	952.1	118.03	952.8

Abandoned airstrip at Eureka - Profile 2				
	1973		**1998**	
Station	Distance from west end (m)	Relative elevation (cm)	Distance from west end (m)	Relative elevation (cm)
B34	9.29	985.3	9.29	994.3
B33	18.94	990.7	18.94	977.8
B32	28.62	991.2	28.62	995.7
B31	39.82	984.3	39.82	989.8
B30	43.29	958.9	43.29	943.4
B29	46.08	926.3	46.08	930.5
B28	48.56	902.9	48.56	898.8
B13	49.81	933.7	49.81	911.4
B12	60.35	933.1	60.35	931.1
B11	71.45	923.2	71.45	910.2
B10	75.00	871.1	75.00	895.6
B9	78.32	918.1	77.00	906.1
B7a	82.80	860.6	78.32	913.1
B8	82.80	860.6	84.40	890.0
B7	90.22	917.6	90.22	908.0
B6	92.54	945.1	92.54	943.5
B5	94.42	957.0	94.42	957.0
B4	98.92	962.9	98.92	957.2
B3	108.70	969.3	108.70	972.3
B2	111.02	948.6	111.02	949.6
B1	120.00	949.6	120.00	950.0

Abandoned airstrip at Eureka - Profile 3				
	1973		1998	
Station	Distance from west end (m)	Relative elevation (cm)	Distance from west end (m)	Relative elevation (cm)
C1	0.00	970.1	0.00	970.0
C2	10.65	977.5	10.65	975.1
C4	18.08	972.6	18.08	967.8
C3	19.28	953.6	19.28	949.2
C5	23.91	968.1	23.91	960.6
C6	30.26	965.3	30.26	965.4
C7	32.08	961.4	32.08	962.5
C8	34.78	956.1	34.78	961.6
C9	43.16	948.2	43.16	941.5
C10	45.05	917.1	45.05	930.4
C11	46.77	950.1	46.77	945.5
C12	57.57	952.6	57.57	945.0
C33	67.44	937.5	67.44	942.1
C34	75.47	934.3	75.47	931.9
C35	78.1	911.4	78.10	919.7
C36	80.36	932.5	80.36	933.8
C37	81.88	967.1	81.00	951.0
C38	88.94	967.9	81.88	971.3
C39	96.86	967.5	96.86	966.5
C40	106.86	939.9	106.86	943.9
C41	107.91	949.1	107.91	954.2
C42	118.22	948.2	118.22	934.3
C43	129.24	928.9	129.24	928.7
C44	134.86	895.7	134.86	894.5
C45	135.66	905.0	135.66	907.5
C46	161.26	868.5	161.26	863.0

Gemini E-10 wellsite					
Airstrip Profile 1			Airstrip Profile 2		
Station	Distance from west end (m)	Relative elevation (cm)	Station	Distance from west end (m)	Relative elevation (cm)
1	0.00	971.5	1	0.00	1000.0
2	2.00	974.6	2	2.90	983.9
3	4.00	976.9	3	6.00	976.8
4	7.80	980.2	4	7.90	972.8
5	8.40	977.3	5	10.00	963.8
6	10.00	1000.0	6	11.70	943.5
7	12.30	1010.7	7	26.70	930.7
8	14.00	1018.8	8	27.80	939.0
9	16.20	1022.0	9	30.00	932.8
10	18.00	1016.9	10	31.50	940.1
11	20.00	1012.0	11	33.70	953.1
12	20.30	1007.8	12	35.40	945.4
13	22.00	1014.8	13	37.80	946.5
14	24.10	1018.7	14	38.30	933.1
15	26.00	1018.0	15	39.10	938.0
16	28.20	1029.8	16	40.20	925.3
17	29.90	1047.8	17	41.60	932.0
18	32.00	1052.6	18	43.70	933.2
19	34.00	1038.9	19	45.50	935.1
20	35.80	1052.7	20	48.00	941.5
21	38.00	1077.7	21	50.00	942.5
22	40.00	1072.0	22	51.50	931.1
23	41.80	1086.3	23	54.00	940.0
24	43.90	1087.8	24	55.80	941.2
25	46.00	1090.6	25	57.80	940.5
26	48.00	1091.7	26	59.80	944.5
27	49.80	1093.3	27	61.40	947.0
28	52.00	1095.8	28	64.00	948.8
29	54.00	1099.7	29	66.00	949.8
30	56.00	1101.0	30	67.80	949.3
31	58.00	1102.9	31	69.70	944.1
32	58.50	1108.5	32	72.00	946.8
33	62.20	1105.7	33	73.30	955.0

Gemini E-10 wellsite					
Airstrip Profile 3					
Station	Distance from west end (m)	Relative elevation (cm)	Station	Distance from west end (m)	Relative elevation (cm)
1	0.00	1000.0	28	50.00	1023.8
2	1.70	997.5	29	52.80	1026.4
3	4.00	979.3	30	54.00	1036.7
4	5.30	1001.3	31	56.00	1030.9
5	8.00	1009.7	32	58.00	1034.0
6	9.80	1013.0	33	59.80	1030.8
7	11.60	1013.7	34	62.00	1032.0
8	13.70	1014.8	35	64.00	1033.5
9	15.00	1014.2	36	66.00	1035.3
10	17.80	1011.0	37	68.00	1025.0
11	19.90	1022.6	38	70.00	1029.7
12	21.90	1021.7	39	71.60	1034.3
13	23.60	1019.2	40	73.50	1035.5
14	25.80	1018.6	41	75.30	1038.3
15	27.90	1018.4	42	77.70	1031.5
16	30.00	1019.7	43	80.00	1042.5
17	31.90	1017.7	44	81.70	1042.3
18	32.60	1009.7	45	83.60	1044.3
19	34.00	1018.1	46	85.50	1048.8
20	34.50	1009.5	47	87.70	1046.8
21	35.70	1017.0	48	89.70	1048.8
22	38.00	1017.6	49	91.70	1051.7
23	40.00	1017.8	50	93.60	1044.0
24	42.00	1020.6	51	95.70	1051.0
25	43.90	1031.7	52	97.60	1045.3
26	45.90	1031.1	53	100.00	1044.5
27	47.80	1038.4			

Gemini E-10 wellhead					
Profile 1 (to north of wellhead)			Profile 2 (to east of wellhead)		
Station	Distance from well head (m)	Relative elevation (cm)	Station	Distance from well head (m)	Relative elevation (cm)
1	0.00	1000.0	1	0.00	1000.0
2	3.20	1001.4	2	1.10	980.2
3	5.90	974.7	3	10.80	767.3
4	9.00	925.8	4	18.80	758.3
5	12.10	962.9	5	20.00	890.7
6	16.10	945.7	6	23.50	806.0
7	20.20	970.9	7	31.40	749.5
8	25.50	992.9	8	47.50	735.0
9	30.60	1000.2	9	58.10	712.3
10	35.50	1040.3	10	66.20	753.7
11	41.00	1027.1	11	69.40	940.6
12	42.80	1036.5	12	80.00	788.0
13	44.80	1031.8	13	86.00	884.0
14	49.00	1015.5	14	103.00	799.0
15	50.50	983.0	15	114.00	771.0
16	53.20	993.0	16	127.00	750.5
17	55.10	1047.5	17	147.50	643.5
18	59.60	1032.0	18	172.00	464.5
19	63.50	1055.0			
20	68.30	1032.7			
21	71.30	1069.6			
22	77.00	1060.6			
23	78.50	1036.2			
24	80.00	1048.0			
25	81.40	1083.2			
26	89.40	1104.1			
27	90.60	1075.5			
28	94.10	1088.1			
29	96.80	1117.3			
30	106.00	1119.5			
31	107.60	1093.8			
32	113.40	1143.5			

Gemini E-10 wellhead					
Profile 3 (to south of wellhead)			**Profile 4 (to west of wellhead)**		
Station	Distance from well head (m)	Relative elevation (cm)	Station	Distance from well head (m)	Relative elevation (cm)
1	0.00	1000.0	1	0.00	1000.0
2	3.60	1005.3	2	5.90	1008.8
3	10.20	999.2	3	10.10	981.7
4	21.50	997.1	4	15.60	1002.3
5	30.00	956.7	5	24.10	992.3
6	35.50	878.5	6	30.90	974.6
7	39.10	781.3	7	36.20	962.9
8	45.80	861.1	8	40.40	938.2
9	51.20	828.7	9	48.00	900.9
10	58.00	574.5	10	53.50	925.6
11	63.00	682.4	11	56.70	877.3
12	74.00	556.0	12	59.50	912.8
13	83.00	651.5	13	67.70	907.2
14	98.00	547.0	14	73.80	749.5
15	100.50	710.5	15	81.60	729.5
16	112.50	663.0	16	90.40	764.3
17	117.00	556.5	17	102.60	703.7
			18	116.60	700.9
			19	120.90	788.8
			20	124.60	809.0